esa estec

Keplerlaan 1
2201 AZ Noordwijk
The Netherlands

SPICA Mission Study Summary Report

Prepared by SPICA Study Team
Future Missions Department - Science Directorate
Reference ESA-SPI-EST-MIS-RP-001
Issue/Revision 1.1
Date of Issue 12/07/2021
Status Approved

European Space Agency
Agence spatiale européenne

This page intentionally left blank

Table of Contents

1 EXECUTIVE SUMMARY

The definition of the SPace Infrared telescope for Cosmology and Astrophysics (SPICA) is a collaboration between ESA and JAXA. The SPICA Observatory is a 2.5-m class infrared telescope to study and answer fundamental astrophysical questions ranging from the formation and evolution of galaxies to the physics of star formation in dusty environments, including the role of magnetic fields, and the origin of planetary systems. A scientific successor to the Herschel and Akari missions, SPICA was conceived to be used by international teams of astronomers to conduct imaging, polarimetric and spectroscopic observations in the wavelength range between 10 to 420 μm. The Observatory would be located in an orbit near the second Lagrange point (SEL2), approximately 1.5 million kilometres from Earth. The telescope and instruments would be actively cooled below 8K and shielded from the heat of the Sun by large Sunshields in order to achieve true background limited performance. As a result of the low background, the Observatory would achieve unprecedented sensitivity over its entire wavelength range and improve, by two orders of magnitude, the spectroscopic sensitivity as compared to previous space telescopes like Herschel and Spitzer.

The telescope is diffraction limited at 20 μm and capable to map wide fields of view, with a maximum angular scanning speed of 60.0 arcsec/sec. It delivers infrared light to the Fine Guidance Sensor (FGS) for fine pointing and to the three scientific instruments of the Observatory:

- A mid-infrared imager and spectrometer (SMI) providing spectrometric measurements over the entire band between 10 and 36 μm at low (R=60-160), medium (R=1400-2600), and high (R=29000) spectral resolving power in addition to imaging capability at 34 μm.

- A far-infrared spectrometer (SAFARI) providing continuous coverage spectroscopy between 34 and 230 μm with highly capable a Fourier Transform Spectrometer (FTS) for high spectral resolution.

- A far-infrared polarimeter (B-BOP) with imaging and polarimetric capabilities in discrete spectral bands at 70, 200 and 350 μm.

The SPICA design concept minimizes complexity and the selected vertical architecture with the infrared telescope boresight aligned with the Launch Vehicle longitudinal axis in conjunction with a silicon carbide telescope carries significant performance margins. The Observatory would use staged cooling provided by mechanical cryocoolers with very high reliability. In contrast to Herschel, which relied on stored liquid helium to provide cold gas to cool the focal plane units, SPICA Observatory has multiple long life cryocoolers that together produce cooling capability to maintain instruments below 4.8 K.

The far-infrared detectors, cryocoolers and mechanisms are the only technologies that are considered currently below Technology Readiness Level (TRL) 5. The technology development plans established in phase A outline a path leading to TRL 6 by 2024. Transition-edge sensor (TES) and polarization sensitive bolometers developments were both already initiated and detector technologies matured during the course of phase A. Ancillary development of cryogenic components for instruments such as cold read-out electronics and superconducting cryoharness were initiated.

The SPICA joint study team with support of the instrument and industrial partners developed a mission design concept, technical approach, technology maturation plan, risk management approach and master schedule which are compatible with ESA guidelines for selection of M5 mission launch opportunity, but exceeding significantly the science programme budgetary constraints for a Cosmic Vision M-class mission.

Performance/Resources Parameters	Unit		Requirement Capability
Sensitivity Parameters			
SMI Point Source Sensitivity at 34.0 μm (Tint=3600sec)	μJy	≤	15.0
SMI Point Source Line Sensitivity at 27.0 μm (R=1300, Tint=3600sec)	Wm^2	≤	2.80E-20
SAFARI Point Source Line Sensitivity at 45.0 μm (R=250, Tint=3600sec)	Wm^2	≤	9.50E-20
B-BOP Point Source Sensitivity in Stokes at 200.0 μm (Tint=5040sec)	mJy	≤	36.7
ITA Effective Collecting Area	m^2	≥	4.0
ITA Transmission at 35.0 μm	-	≥	0.97
ITA Rejection of Stray Light at 20.0 μm, Normalized Detector Irradiance (NDI)	-	≤	6.20E-03
ITA Rejection of Thermal Emission	-	≤	1.00E-04
Polarization Parameters			
Fractional Linear Polarization Error	-	≤	1.0%
Polarization Angle Error	deg	≤	1.0
Image Quality Parameters			
SMI RMS Wave Front Error at 20.0 μm (Strehl Ratio ≥ 0.8)	nm	≤	1400.0
SAFARI RMS Wave Front Error at 30.0 μm	nm	≤	2200.0
B-BOP RMS Wave Front Error at 200.0 μm	nm	≤	15000.0
80% Encircled Energy Radius at 20.0 μm	as	≤	6.00
80% Encircled Energy Radius Stability over 1.0 hour at 20.0 μm	-	≤	5.00%
Thermal Parameters			
SAFARI Heat Rejection Capacity at 0.05 K	μW	≤	0.7
Cryogenic Module Heat Rejection Capacity at 30.0 K	mW	≤	320.0
Cryogenic Module Heat Rejection Capacity at 4.8 K	mW	≤	30.0
Cryogenic Module Rejection Capacity at 1.8 K	mW	≤	10.0
Pointing Parameters			
Absolute Pointing Error (APE)	mas	≤	500.0
Relative Pointing Error (RPE)	mas	≤	150.0
Absolute Pointing Knowledge Error (AKE)	mas	≤	250.0
Observatory Resources			
Observatory Wet Mass	kg	≤	3750.0
Observatory Maximum Power Load	W	≤	3445.0
Observatory Decontamination and Cooldown Power Load	W	≤	1254.5
Operations Parameters			
Observatory Operational Efficiency	-	≥	50.0%
Observatory Slew Capability over 90 degrees Maneuvre	min	≤	15.0
Maximum Cooling Time (Delract 80 days for Performance Verification)	days	≤	100.0

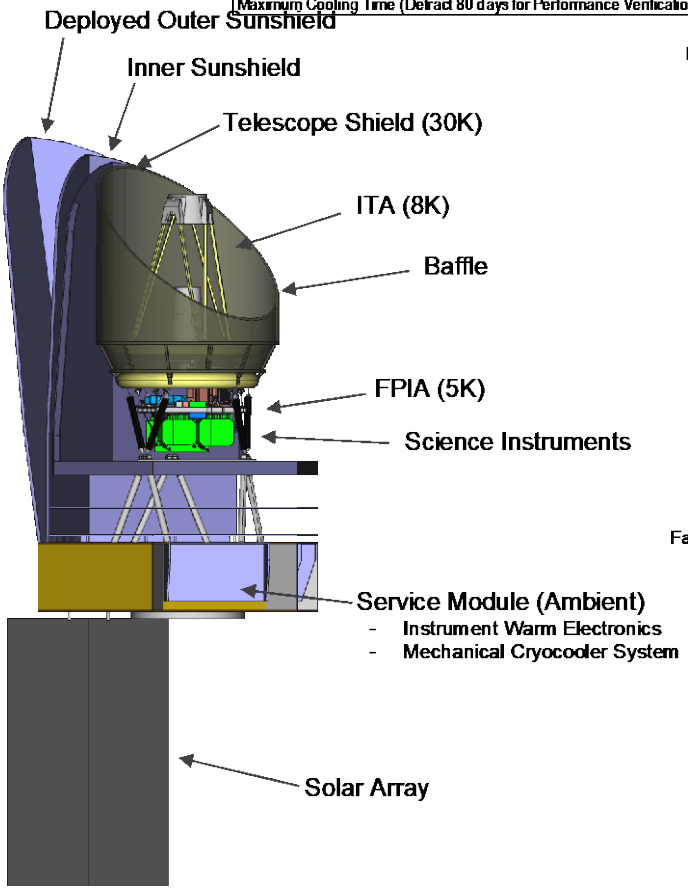

SMI
Mid-Infrared Imager and Spectrometer

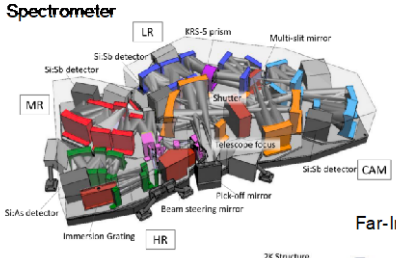

B-BOP
Far-Infrared Polarimeter

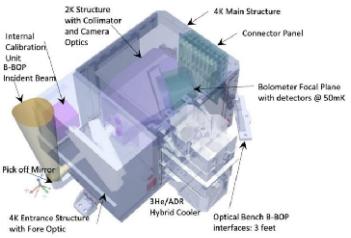

SAFARI
Far-Infrared Spectrometer

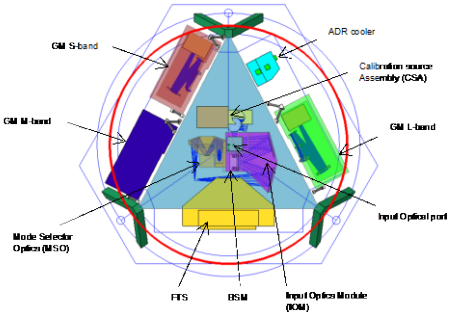

2 INTRODUCTION

The purpose of this document is to describe the mission concept for the Space Infrared telescope for Cosmology and Astrophysics (SPICA) established at the end of the definition phase in May 2021. It provides an overview of all the mission elements and operations, and describes the important features that affect the proposed baseline.

In complement to the identification of the key mission requirements and definition of the technical baseline, the document provides a summary of the development plan and schedule, including considerations on the enabling technologies and major development risks.

3 SCIENTIFIC OBJECTIVES AND REQUIREMENTS

The SPICA mission is designed to provide resolution for three major science topics:

Establishing the mechanisms that drive galaxy evolution over cosmic timescales
By taking spectra of *thousands* of galaxies out to high redshift, their evolution can be followed over cosmic timescales. SPICA is designed to readily detect atomic and molecular lines, as well as PAH emission likely even out to redshifts of 5 to 6. This would allow SPICA to determine how baryonic matter cycles through galaxies and how matter is enriched over time with metals. Also, it would allow to determine which of the different formation and evolution processes are dominant and how they influence the overall galaxy formation efficiency, as well as what the interrelation is between star formation and black hole matter accretion.

Understanding the physics of star formation in dusty environments and the role of magnetic fields in that process.
SPICA is designed to trace the gas, ice and dust evolution from statistically relevant surveys of a number of key star forming regions and to map the magnetic field in dense dust regions where stars are forming to determine how that field influences the formation process.

Unravelling the formation process of planetary systems
SPICA will have the sensitivity to study the transition of planet forming systems from protoplanetary to debris disks, a phase of prime importance for the understanding of the process of planet formation. SPICA will trace the gas masses of several hundred disks into the debris phase using HD, determine the position of the "snow line" and mass of the ice reservoir in planet forming disks, trace the main gas coolants and key chemical species (e.g. water, oxygen, organics), and follow the processing from primordial dust into planetesimals and asteroids.

For further details on the science capabilities of SPICA, see the list of references.

The Science Requirements Document [RD14] describes a set of observing programmes which allows SPICA to meet the scientific objectives above, and the detailed scientific justification of each individual programme is described in the corresponding Justification Document [RD15]. The specific observational implementation described in [RD14] is referred to as the SPICA Reference Mission Programme (RMP). The RMP is the observing programme from which the scientific requirements on the SPICA payload and satellite are extracted.

The RMP is subdivided into three large themes:
1. The evolution of galaxies across cosmic time
2. The physics of star formation and the interstellar medium
3. The formation of planetary systems

Within each theme, [RD14] defines specific observing programmes. Each of the programmes in the RMP requires observing capabilities in the following categories:
- Low-resolution (R~100) MIR spectroscopy
- High-resolution (R~1500) MIR spectroscopy
- Very-high-resolution (R~30000) MIR spectroscopy

- MIR imaging photometry (R~5)
- Medium-resolution (R~300) FIR spectroscopy
- High-resolution (R~10000) FIR spectroscopy
- FIR imaging photometry and polarimetry (R~2)

The required observational capabilities are summarized in Section 4.1 of [RD14]. The RMP consists of a number of surveys and maps of specific types of objects, each of which serves as a source of data for different scientific investigations in one or more themes. The RMP is summarized in Section 5.2 of [RD14].

Formal requirements extracted from the RMP are listed in Section 6 of [RD14], categorized into Observatory-level requirements (Section 6.1), payload-level requirements (Section 6.2), operational requirements (Section 6.3), and Sky Visibility requirements (Section 6.4).

At the highest level, SPICA is required to operate as a general-use observatory and to provide all the services expected by a wide community of observers from such a facility, from proposal handling all the way to provision of science-ready products. SPICA is designed to support a modestly fast response to Targets of Opportunity (of order 5 days).

The most fundamental requirement for SPICA is that it should allow the RMP to be completed within 1.5 years of routine science operations. Meeting this stringent requirement guarantees that the major objectives of SPICA can be achieved within a fraction of the lifetime of the observatory, leaving a substantial fraction of time to be spent on additional programmes to be proposed by the community. The minimum total amount of operational time guaranteed by SPICA is 2.5 years, but it is designed to achieve a goal of 4.5 years.

In order to complete the RMP within the required time, the instruments must achieve high levels of instantaneous sensitivity for spectroscopy, photometry, and polarimetry, typical levels of which are shown in Appendix B of [RD14]. The sensitivity of the SPICA instruments depends critically on the collecting area of the SPICA telescope, and at longer wavelengths on its temperature and emissivity. The huge improvement of SPICA with respect to its predecessors is due to the very low temperature of the SPICA telescope, which is required to be below 8 K, implying that observations will be limited by the thermal background at wavelengths longer than $\lambda \sim 200$ μm. Instead, at the shortest wavelengths, observations will be limited by astrophysical backgrounds, mainly zodiacal light.

The faintness of the lines which SPICA seeks to observe implies that "typical" spectroscopic observations will be long, of order one hour per source. Long observation times per source imply that some of the observing programmes in the RMP will require weeks if not months to complete. For this reason, SPICA also requires a high level of observing efficiency, taking into account all factors at instrument and system level that combine to reduce the time spent by the observatory integrating on an astrophysical source. The visibility of the sky is also an important factor in the overall observing efficiency. Some of the fields included in the RMP must be observed for periods up to months. Very long maps (e.g. cosmological deep fields) must be built over more than one observing season.

Considering the variety and complexity of factors contributing to its observing capabilities, the ability of SPICA to complete the RMP as required can only really be assessed via realistic simulations which include all performance aspects at payload and system level.

4 BASELINE MISSION OVERVIEW

4.1 Mission Requirements

The SPICA main mission objective is to perform 10-420 μm mid and far-infrared science observations with unprecedented sensitivity. The SPICA mission requirements and rationale are documented in [RD16]. These requirements are in part derived from the science and observation requirements specified in [RD14]. Table 4-1 illustrates the rationale for the SPICA, main mission requirements, and their flow-down to the flight and ground elements.

Mission Requirement		Rationale	Observatory Requirement	Ground System Requirement	Operation Requirement
MR2000	Entrance Pupil Diameter ≥ 2500 mm	Meet driving angular resolution requirement			
MR2010	Effective Collecting Area ≥ 4.0 m2	Meet driving sensitivity requirement in a total of 10654 hours of effective exposure within 1.5 year	2500 mm diameter circular primary mirror		
MR2310	Telescope mirror temperature ≤ 8 K	Meet driving sensitivity requirements	▪ Telescope baseline at 8 K ▪ Cryocoolers, sunshield, thermal decoupling and insulation		Telemetry monitoring
MR0400 MR0430 MR0460	SPICA payload suit comprised of SMI, SAFARI and B-BOP instruments	Enable observations that meet SPICA mission science requirements	Fully accommodate telescope and three instruments meeting all interface requirements	Receive downlink data, and process and archive data	▪ Spacecraft and instrument operation planning and execution ▪ Monitoring health and safety telemetry ▪ Uplink command/data
MR1070	Track and scan rate ≥ 60 arcsec/sec	Efficient scan mapping of wide survey areas by B-BOP	AOCS design		
MR1140 MR1160	Pointing jitter (RPE) ≤ 150 mas Pointing drift (PDE) ≤ 400 mas up to 10000 sec	Ensure location of targets within SMI mid-infrared spectrometer slits	AOCS design		
MR1130	Pointing knowledge (AKE) after ground processing ≤ 250 mas	Enable target matching and spectral offset correction	AOCS design		
MR0120 MR0140	Full celestial sphere coverage over one sidereal year, and any location for 15 consecutive days in any period of 6 months		Field of Regard (FoR) ≥ 25% - Pitch: -25° to +5° - Roll: -5° to +5° - Yaw: -180° to 180°		Observation planning and execution
MR0030 MR5070 MR1770 MR2280	Minimize background heat and light				Orbit maintenance manoeuvres planning and execution
MR0220 MR0310 MR3600 MR5200	3-year nominal mission life plus 2-year extended mission (5 year lifetime consumables), and 3 year post-operation ground system support to users of SPICA data		▪ Reliability ▪ Radiation protection ▪ Micrometeoroid protection ▪ Contamination protection ▪ 5-year lifetime propellant ▪ 5-year lifetime solar array and coolers	▪ 5-year ground system support, plus 3-year post-operation support to users ▪ 5-year worth of data processing and archiving	▪ 5-year spacecraft and instrument operation ▪ 5 year of data operation, plus 3-year post-operation support to users
MR0760	450 Gbits/day science data downlink (instruments not operating simultaneously)	Accommodate driving observation scenario	▪ Power subsystem ▪ Onboard data storage ▪ Downlink capability	▪ Ground stations availability ▪ Data transfer from ground stations to Science Operations Centre	Observation planning and execution
MR0960 MR4220	Observing efficiency ≥ 50%	Design goal: Achieve all core scientific objectives within 1.5-year mission	▪ AOCS design ▪ Minimise momentum offload, orbit maintenance and downlink overheads ▪ Design robustness ▪ Fault detection and recovery		Efficient observation planning and execution

Table 4-1: SPICA mission requirements, rationale and flowdown

4.2 Observatory Architecture

During the first phase of the study, the different teams conducted extensive trade studies to establish the preferred Observatory configuration. From this effort, it was concluded that an infrared telescope boresight perpendicular the Launch Vehicle longitudinal axis, similar to Planck or Ariel spacecraft, would have been marginally compliant. In particular the primary mirror mass coupled with instrumented optical bench led to a large transverse offset of the Observatory centre of mass of about 0.65 metre. The different structures to transfer the launch loads from the focal plane to the launcher interface could not be optimized without more detailed coupled analyses and resulted into further increase of the Observatory structural mass. Moreover, this configuration limits the available area for solar cells to the bottom side of the SC and the power budget was already considered marginally compliant and power generation was extremely limited by both the fairing accommodation and avoidance of complicated deployments to reduce mission risk. It was therefore concluded that a vertical configuration with the infrared telescope boresight aligned with the Launch Vehicle longitudinal axis offered more conservative system margins. During the second phase of the study, the vertical configuration was baselined.

The Observatory uses staged cooling provided by passive cooling and mechanical cryocoolers with very high reliability. In contrast to Herschel, which relied on stored liquid helium to provide cold gas to cool the focal plane units, SPICA has multiple long life cryocoolers that together produce cooling capability to provide the necessary interface temperatures for the telescope and the instruments. As a result of the cryogenic payload and the low background emission, the Observatory would achieve unprecedented sensitivity over its entire wavelength range. A simple heat flow budget to the cryocooler stages is provided in Table 4-2. This represents the heat flow at the worst-case attitude of the spacecraft with the worst-case End-of-Life (EoL) emissive properties.

T (K)	Total Heat Load Allocation[1]	Requirement toward the Cooler	Rationale
30	320 mW at 30 K	480 mW at 26 K EOL	Capability of 2x2ST EOL running at 60% assuming 50% system margin and 4K gradient between the cold finger and the shield.
4.8	30 mW at 4.8 K	40 mW at 4.5 K EOL	Capability of 2x4K JT Coolers EOL running at 50% assuming 33% system margin, 0.3K gradient between the cold tip and the application.
1.8	10 mW at 1.8 K	13.3 mW at 1.7 K EOL	Based on instruments CBE and 20% bulk margin, 0.1K gradient between the cold tip and the application.

[1] From application side

Table 4-2: Heat flow to the three cryocooler stages

The Observatory is to be located in an orbit near the second Sun-Earth Lagrange point (SEL2), approximately 1.5 million kilometres from Earth in the direction opposite the Sun, and it is to orbit around the SEL2 point in a large halo orbit. SEL2 is advantageous from a passive cooling perspective as Earth heating is negligible and the telescope and instruments can be shaded from the sun while simultaneously allowing for a large view of the sky and continuous illumination of the solar arrays. The payload will be protected from Sun/Earth and spacecraft radiations by multiple thermal shields maximizing the radiation to deep space. The telescope shield temperature is fixed at 30K thanks to the active cooling and corresponds to the radiative boundary for SIA assembly, protecting colder surfaces within from higher temperature radiation. The telescope and instruments will be cold and shielded from the heat of the Sun by a large Sunshield. The science instruments are clustered in a zone below 8 K near the focal plane, immediately behind the primary mirror structure.

The SPICA Observatory consists of a Payload Module (PLM) and Service Module (SVM). The PLM is composed of two assemblies: The Science Instrument Assembly (SIA) and the Cryogenic Assembly (CRYO). The SIA assembly includes the Infrared Telescope Assembly (ITA), a telescope of 2.5-meter diameter cooled to below 8 Kelvin, the Focal Plane

Instrument Assembly (FPIA) which contains the instrument Focal Plane Units (FPUs): a far-infrared spectrometer (SAFARI), a far-infrared polarimeter (B-BOP) and a mid-infrared imager and spectrometer (SMI). The FPIA includes also two redundant Fine Guidance Systems used for attitude determination during Science observations. In order to achieve the required background limited sensitivity, the CRYO module consisting of the Mechanical Cooler System (MCS) and Thermal Insulation and Radiative Cooling System (TIRCS), maintains the three instruments FPUs at cryogenic temperature. The MCS system consists of three types of coolers: double-stage Stirling coolers (2ST), 4K-class Joule-Thomson coolers (4K-JT), and 1K-class Joule-Thomson coolers (1K-JT). The service module (SVM) consists of the typical spacecraft subsystems, as well as warm electronics for the science instruments and the mechanical cryocoolers. The observatory configuration is fully driven by the optimisation of the thermal environment provided to the SIA assembly.

The spacecraft bus provides the required attitude control, power, thermal control, command and data handling, propulsion, and communication. The Observatory attitude is three-axis controlled with a chemical propulsion system to enable highly efficient orbit control and station keeping manoeuvres while minimising the generation of unpredictable parasitic impulse. The Observatory is powered by a Direct Energy Transfer (DET) electrical power system with a solar array deployed below the SVM benefiting from direct cold space view on its rear side which decreases its temperature and ensures optimum power with minimal surface. The mission lifetime is five years. Propellant is the lifetime limiting expendable, and sufficient propellant is carried to allow operation until the end of the decommissioning phase, including the extended science mission lifetime. The SPICA Observatory could be launched on H3 Launch Vehicle with 8.0-meter long fairing and maximum diameter of 4.6 metres.

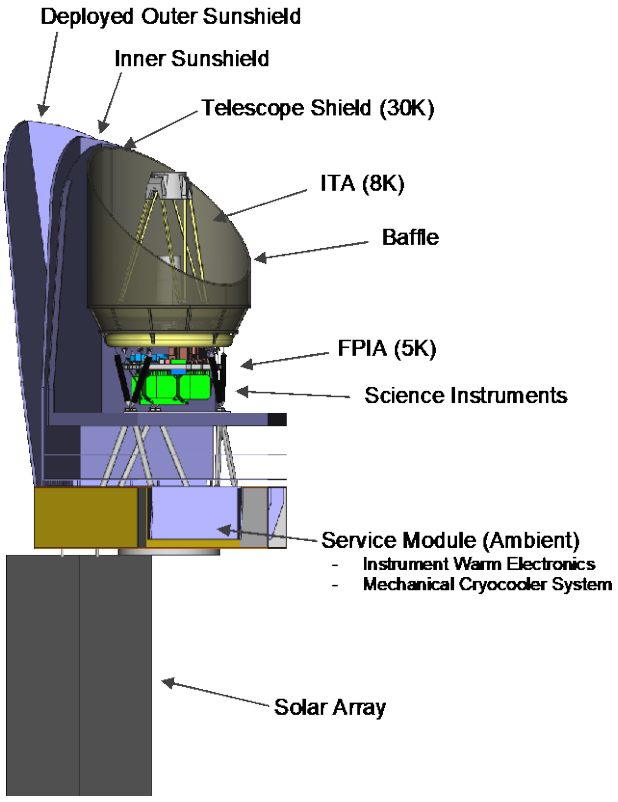

Figure 4-1: Observatory architecture

4.3 Infrared Telescope

The complete SIA is cooled down below 8K thanks to a combination of passive cooling, via dedicated Sun and thermal radiative shields, and active cooling, including mechanical coolers of two thermal stages with base temperatures of 4.5K and 1.7K. The SIA assembly is conductively insulated from warm bus by the CRYO truss separation mechanisms

(TSM). The outer telescope baffle is black coated inside, and VDA coated outside in order to limit the radiative heat load with the 30 K active thermal shield. It implements 40 degrees cut-angle to avoid earth illumination of the inner black part.

The telescope optical components are made of silicon carbide (SiC). The selection of this technology is driven by the stringent performances requested for SPICA: the material must be highly stable, reproducible and have a strong homogeneity (isotropy of the material itself) to be insensitive when submitted to large temperature changes from ambient down to cryogenic conditions. The mass allocated budget to the Science Instrument Assembly was also early identified as a critical driver for the mission, and the low density offered by the material is clearly a great advantage. This technology has good heritage for large size of mirror and structure up to 3.5m diameter through Herschel and Gaia programs [RD20][RD21].

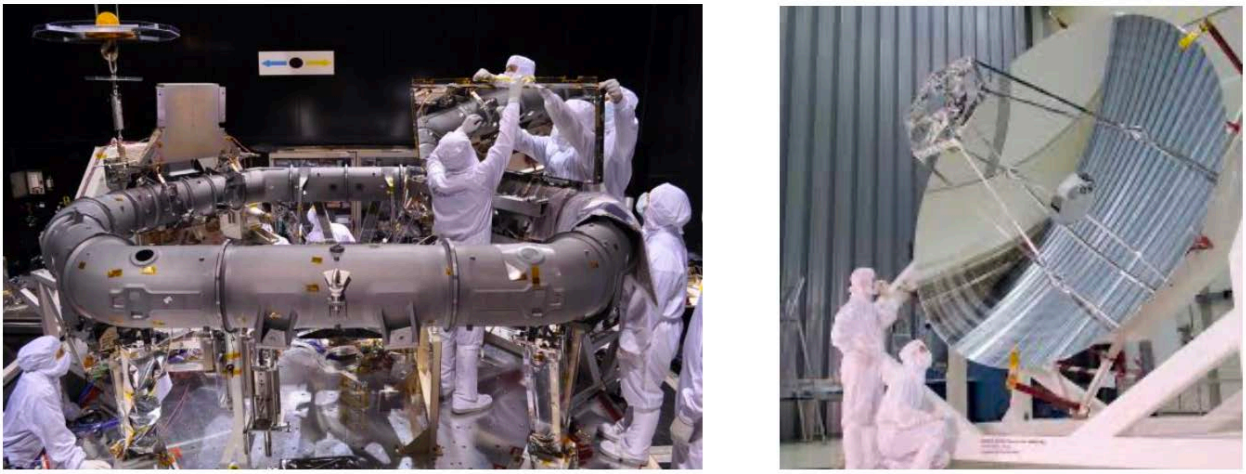

Figure 4-2: SiC Heritage from GAIA and HERSCHEL 3.5 meters telescope

The extension of the qualification domain down to 8K is still to be performed but is deemed achievable. The proposed telescope architecture has been driven by the mechanical constraints: the SPICA secondary reflector structure is fixed at two thirds of the primary mirror diameter, similar to Herschel telescope, which offers the best mechanical performances in term of mass and eigenfrequency. The resulting occultation in the telescope aperture, occurring within the beam before and after primary mirror reflection, diffraction and straylight have all been carefully assessed during the study and remain compatible with the scientific needs.

The Focal Plane Instruments (FPI) and Fine Guidance Sensor (FGS) are mounted and aligned on both sides of an aluminium sandwich panel (IMS) which is supported by the ITA optical bench through a set of bipods.
The scientific instruments of SPICA are:

- SPICA Mid-infrared Instrument (SMI), from 17 to 36 µm
- SPICA Far-Infrared Instrument (SAFARI) from 34 to 210 µm
- B-field Bolometric Polarimeter (B-BOP) at 70, 200 and 300 µm

With these three instruments, the mid to far-infrared range of the spectrum is completely covered from 12 to 420 µm. The SMI instrument may include also the function of a Fine Guidance System (FGS).

4.3.1 Optical Baseline

The telescope is a Ritchey-Chretien design, which offers a quite large Field of View (FoV) of 18 arcmin radius with a curved focal surface. As shown in Figure 4-3, the telescope is composed of two mirrors. The primary mirror design is close to a parabola while the secondary mirror is a hyperbola. The collecting area of 4.0 m2 includes the obscuration loss due to the secondary mirror baffle and supporting structure.

The F-number of the primary mirror has been selected to keep a reasonable overall telescope length while limiting primary mirror manufacturing and testing complexity (surface form errors) and secondary mirror tolerance sensitivity to acceptable values. On the curved image surface, the only uncorrected telescope aberration is only astigmatism and this varies as the square of field distance from the optical axis: The design WFE is then 1.53 µm RMS at 18 arcmin from axis (extreme field edge).

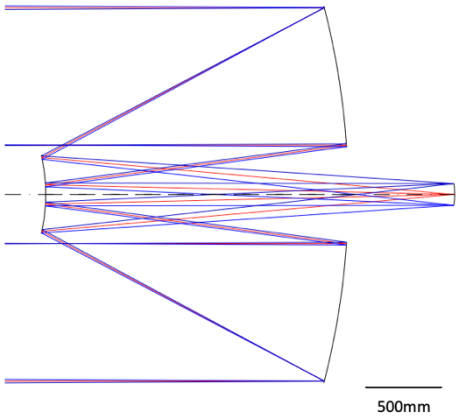

Parameter	Requirement	Baseline
Entrance Pupil Diameter	≥ 2500 mm	2500 mm
Effective Collecting Area	≥ 4.0 m^2	4.0 m^2
Focal Length		13900 mm
Focal Ratio	≥ 5.0	5.56
Half Field	≥ 18 arcmin	18 arcmin
Obscuration Ratio		17.0%
Distance between Mirrors	2000 mm	2000 mm
Nominal Back Focal Length	600 to 800 mm	705 mm
Nominal Distance Between Exit Pupil and Focus	≥ 2400 mm	3160 mm
Field Curvature	≥ 500 mm	512 mm

Figure 4-3: Infrared telescope configuration and parameters

The requirement on the Strehl ratio for the Science Instrument Assembly (SIA) is 0.8 at 20 µm wavelength, which corresponds to a global WFE allocation of 1.4 µm rms for the most demanding instrument [RD22]. This specification can only be achieved with a compensation of telescope astigmatism aberration within the SMI fore-optics. An average correction of astigmatism within SMI field-of-view is implemented such as the end-to-end SIA design WFE on SMI critical channel is below 820 nm rms. No astigmatism compensation is considered for SAFARI and B-BOP channels.

An extensive common work has been performed with all the stakeholders to define the FoV for each instrument and their pick-off mirrors accommodation in accordance with the ITA optical design. The selected accommodation is based on the implementation of SMI, B-BOP and FGS on the upper side of the Instrument Mounting structure (IMS), with pick-off mirrors located before the telescope focus. Figure 4-4 shows the pick-off mirror accommodation associated to the FoV definition. SMI-LR and HR (in light blue) will be collected with a common mirror. SAFARI beam (in dark blue) goes through the IMS before being collected, which leads to large but achievable fore-optics.

The individual (pick-off) mirror internal margins as well as the proximity margins between them have been carefully managed with tight, but achievable values. SAFARI is mounted on the lower side of the IMS and then collects the beam after the telescope focus. This concept offers more flexibility in term of pick-off mirror accommodation and improves significantly the mechanical performances.

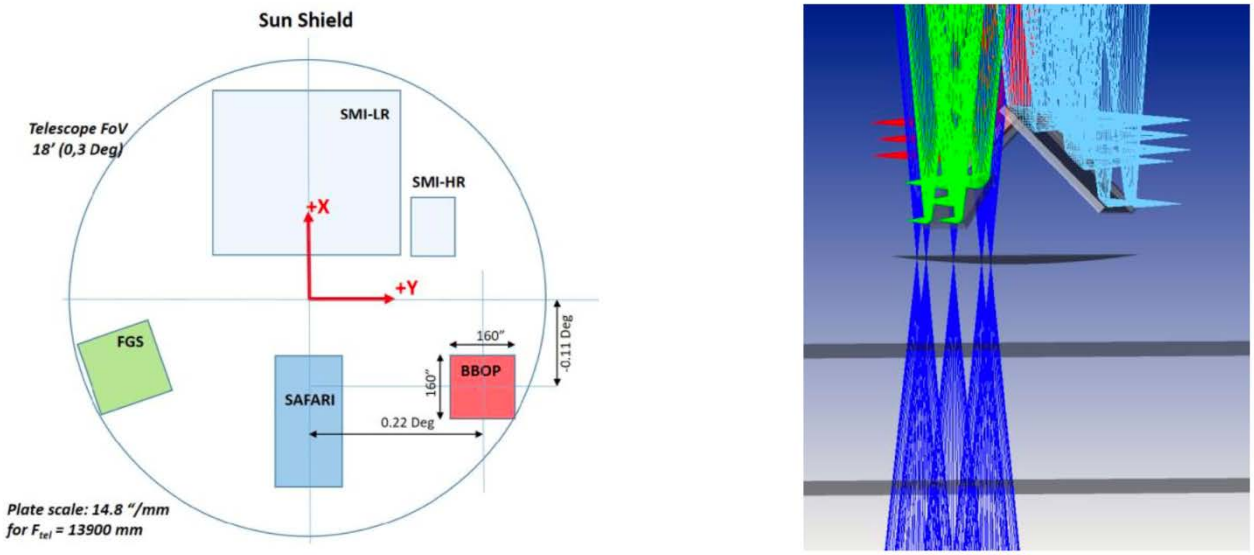

Figure 4-4: The Science Instrument and FGS FoVs definition and accommodation

The calculated spectral transmission performance based on previous Herschel mission is foreseen to be as described in Table 1. The primary mirror will be coated with protected aluminium coating. A protected silver coating is foreseen for the secondary mirror and better performance is expected. Light scattering by polished and coated raw SiC (roughness and porous micro-structures), as well as contamination, are also considered in the budgets. The polarization performance of the ITA itself has a low contribution to the polarization budget required at B-BOP level.

Wavelength (µm)	Transmission
5.0	0.91
10.0	0.94
35.0	0.97
230.0	0.99
420.0	0.99

Table 4-3: Predicted ITA spectral transmission predicted performance

4.3.2 Optical Performance

The major contributors to the ITA WFE budget are the primary mirror polishing and coating (530 nm rms), the secondary mirror polishing and coating (220 nm rms), the AIT tolerances, the gravity release and the cool down impact. A total allocation for the ITA WFE including all contributions is set at 695 nm rms, excluding the design aberrations.

The cool-down covers the effect of the variation from ambient to operational temperature (8 K), and the local effects coming from the different materials behaviour. The main effect of cool-down will be a change in telescope focus. This change is quantified by analysis, and translated into an equivalent M2 shimming compensation during AIT. Once at 8 K, the telescope will be in focus and the residual error, due to inaccuracy in M2 offset prediction, will be compensated by the Secondary Mirror Mechanism. The thermal gradient effects are very low, due to the very low ratio between Coefficient of thermal expansion and thermal conductivity of the SiC, even at 8K. The cool-down effect contribution is mainly driven by the precise design of the bipods/M1 connections, and the very low deviation in the thermal expansion coefficients (CTE) between segments (monophase and isotropic material). A Structural Thermal Optical Performance (STOP) analysis has been run and confirmed that a global allocation of 135 nm rms can be met.

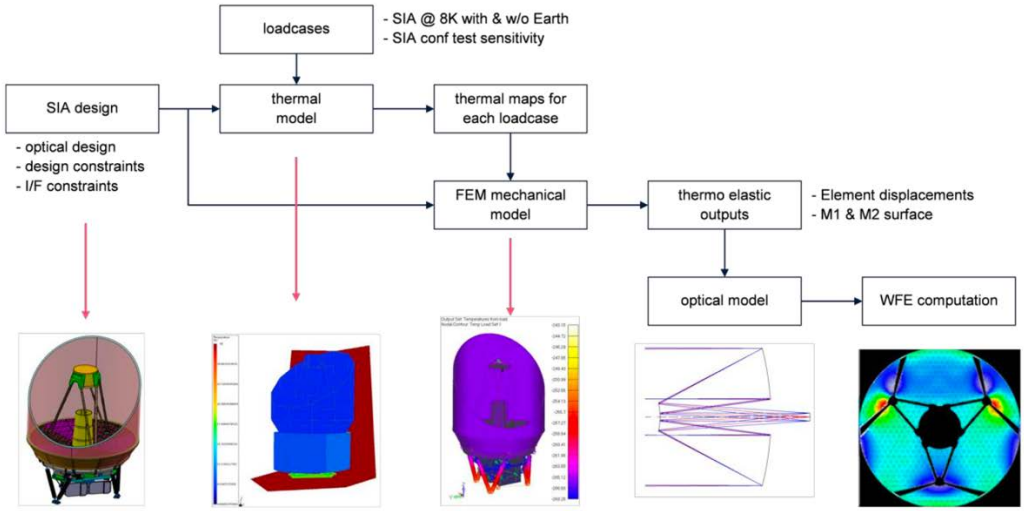

Figure 4-5: SPICA STOP analysis methodology

The Ritchey-Chretien configuration has a strongly curved focal surface, and this curvature leads to some defocus effect through the field for each instrument. An astigmatism compensation is implemented within the most sensitive instrument (SMI) fore optics to minimize the residual aberration effect of the end-to-end optical combination (below 820 nm rms). A Monte Carlo coupled analysis at ITA-SMI level was required to quantify the impact of the M2 and FPIA residual misalignment (after in-orbit correction) on the overall WFE. Indeed, residual misalignment will cause low order optical aberrations that will sum linearly with the ITA-SMI design aberrations. Misalignments can be due to residual errors during on-ground alignment (including gravity impact), residual error on cool-down predictions, and launch effect. Once in flight, a 3 DoF M2 correction (focus/tip/tilt) is then actuated in order to minimize the WFE on the SMI critical path. A global allocation of 1020 nm rms is considered for the ITA-SMI coupling WFE performance, considering end-to-end design aberrations and residual misalignment after in-flight correction.

Finally, a 700 nm rms is allocated to the SMI manufacturing and stability WFE. The global SIA WFE budget for SMI critical path is then lower than 1415 nm rms, compliant with the diffraction limit requirement. The two others instruments, because they operate at longer wavelengths are much less critical in term of WFE, even without astigmatism compensation in their fore-optics.

Contributor	WFE (nm rms)
Infrared Telescope, without aberrations	695.0
SMI instrument, without aberrations	700.0
Optical SIA – SMI, with design aberration and residual in flight misalignments after in-flight correction	1015.0
SIA SMI Total WFE	**1415.0**

Table 4-4: SIA SMI WFE budget

The point spread function (PSF) performance is clearly driven by the occultation pattern (Table 4-5). Indeed, the M2 supporting structure interfaced at two thirds of primary mirror diameter leads to double-path occultation which has an impact on the diffraction pattern and to the encircled energy performance.

Parameters		Value	Unit
Exit Pupil Diameter		2500.0	mm
Optical Area without Occultation		4.91	m^2
Occultation	M2 Baffle	0.4	m^2
	Hexapod Fittings	0.05	m^2
	Bars	0.13	m^2
	Return Path	0.255	m^2
Total Optical Area		4.08	m^2
Total Aeral Obscuration		17.0	%

Table 4-5: Telescope obscuration ratio

This architecture was selected as a mass optimum design, and the impacts on the performance were carefully assessed. The PSF 80% encircled energy radius at 20 µm wavelength is lower than 6.0 arcseconds, and 1.0 arcsecond at 40% encircled energy, which is compliant with the scientific needs. This includes contributions of the total SIA WFE with representative power spectral distribution of polishing errors, (cryo-)quilting impact, tolerances and occultation pattern.

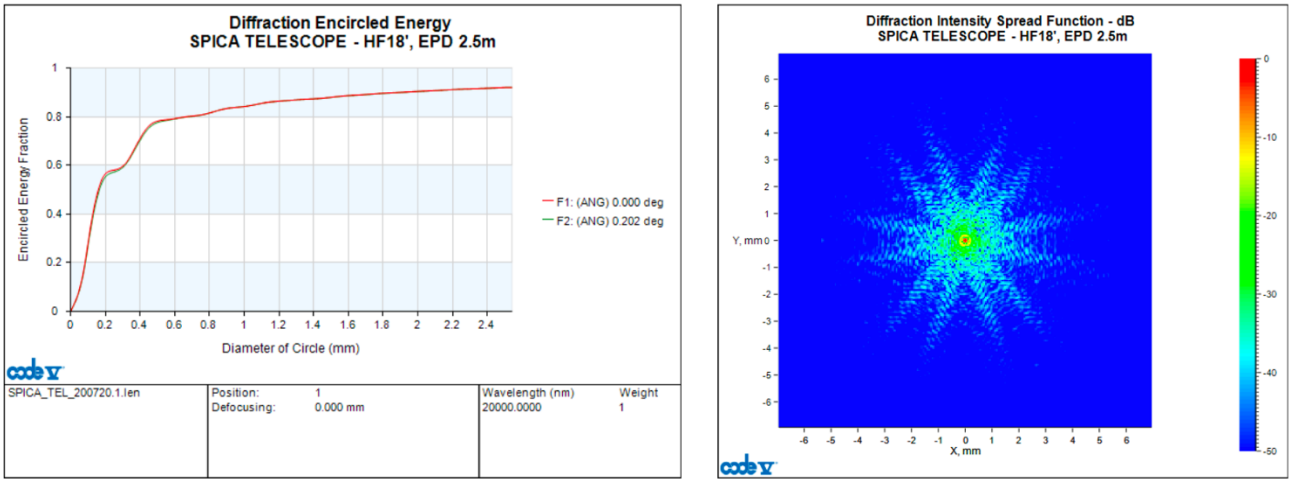

Figure 4-6: Infrared telescope Encircled Energy (EE) diameter and PSF at 20.0 micrometres

Straylight is specified at telescope level through a Normalized Detector Irradiance (NDI) template. The Straylight analyses have been performed with FRED software, and the 2D results are shown in Figure 4-7. The hexapod scattering starts to be significant around 7°, which is noticeable on the left map as a pattern with branches. The map on the left corresponds to the half space in front of the telescope entrance. The high part of the baffle is on the left, which explains the null NDI value on the left part of the picture. The specular direction is in (0°,0°). The map on the right corresponds to the half-space opposite to the telescope entrance aperture. The highest part of the baffle is on the right (after rotation of 180° around Y angle axis), which explains the null NDI value on the right part of the picture. The direction opposite to the specular is in (0°,0°).

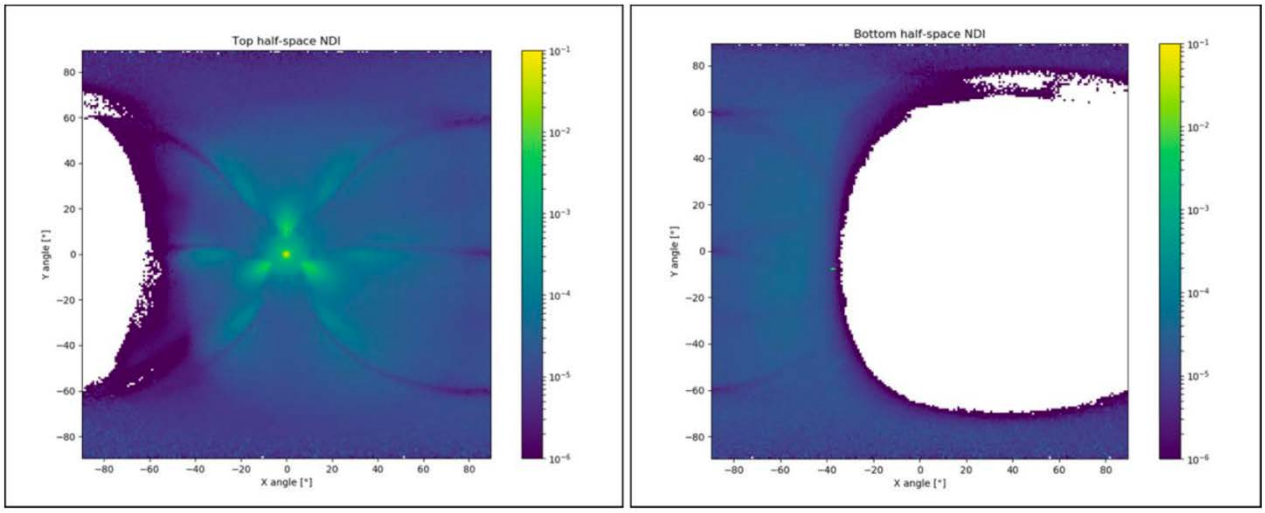

Figure 4-7: Infrared telescope Normalized Detector Irradiance (NDI)

It has been demonstrated with a very conservative approach, that the ITA straylight will never generate more than 14% of the zodiacal background noise, which is compliant with the scientific need. However, bright sources like Jupiter) that could be located in the same direction as the NDI bumps linked to hexapod concept (i.e. 3 bumps around 7° angle from the optical axis), should be avoided and operational constraints implemented during observations.

4.3.3 Mechanical and Thermal Design

The proposed telescope mechanical architecture is mainly driven by the mass and the operational temperature (8 K). The exploded view of the complete Science Instrument Assembly is shown on Figure 4-8.

The telescope assembly is made of following parts:

- 2,5 m parabolic raw SiC primary mirror (M1): As for Herschel, the primary mirror M1 is manufactured in 6 petals like pieces, later brazed together, ground and polished then coated. A reflective coating deposited by evaporation was developed for the Herschel telescope and is proposed as the baseline for M1. The backside of each segment is optimized as an open back structure for minimum deformation under gravity, under grinding and polishing constraints and for meeting the SPICA mass and stiffness specifications. As for Herschel, three equally spaced bipods ensure the iso-static mounting of the primary reflector on the optical bench (TOB).
- secondary mirror supporting structure made of 6 SiC struts linked together by the M2 top structure. As for Herschel, the M2 supporting structure is interfaced on 3 points symmetrically spaced at 120° and located at two thirds of M1 mechanical diameter. Mirror assembly iso-static mountings are located directly in front of those 3 hexapod structure points allowing loads to directly transit through these points, limiting by the same way residual stress across the M1 mirror.
- 620 mm diameter convex hyperbolic SiC secondary reflector (M2), mounted on a barrel by means of three invar bipods.
- secondary mirror mechanism (SMM) allowing the in-flight adjustment of the M2 mirror with three degrees of freedom (DoF) mechanism (Tip/Tilt/Piston).
- internal baffling system made up of two baffles: one around M2 and one located above the M1 hole.

The Secondary Mirror mechanism is a challenging topic for SPICA due to specific constraints. First, cryogenic operating temperature (8 K) constrains the material choices, increases the thermo-elastic deformation impacts, and increases the validation complexity. Then, a large and heavy M2 mirror (576 mm diameter, 8.4 kg mobile mass), compared to similar projects, has to be supported by the mechanism which needs to be designed to withstand mechanical launch loads. Finally, a large range (+/- 500 µm) and low-resolution requirements (i.e. < 2 µm) are required. Candidate technologies in Europe have been confirmed as promising, with respect to these challenging specifications. No locking device is

foreseen to survive the launch. However, technological roadmaps and breadboarding are identified to improve the Technological Readiness Level up to 6 before B2/CD phases as summarized in 4.6.3.1.

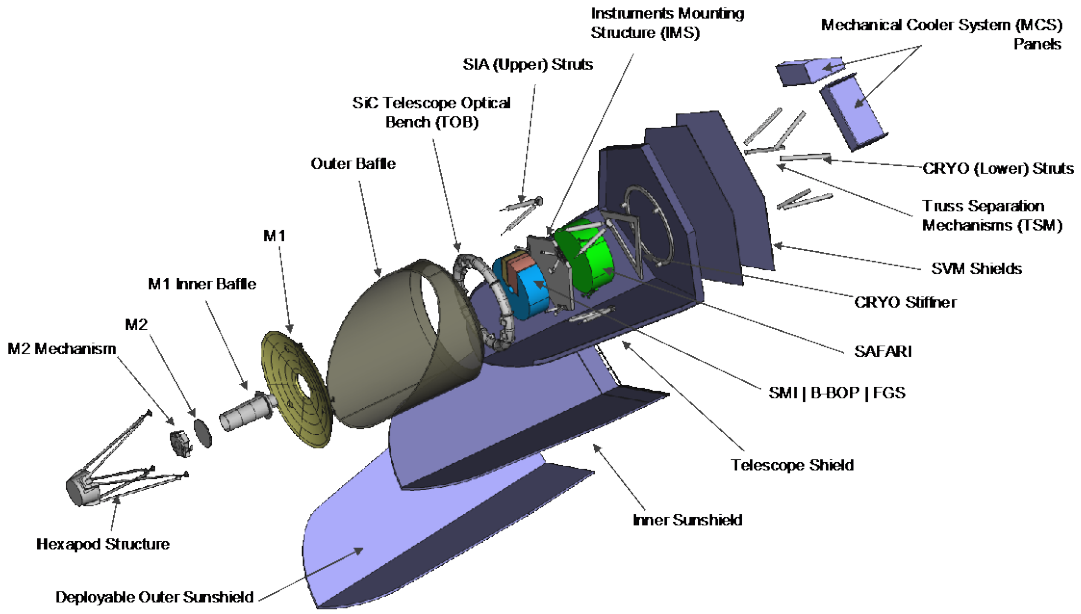

Figure 4-8: Exploded view of SPICA PLM

The Telescope Optical Bench (TOB) is also made of SiC and has a neutral fibre diameter of 1850 mm. This GAIA legacy design uses the same brazed torus segment approach even if only 9 segments are used, instead of the 17 used in GAIA. The choice of a torus design for the baseline is mainly due to the stringent mass versus stringent stiffness allocations. Besides its high stiffness to mass ratio, the toroidal shape has also the advantage of an empty central space between M1 mirror and IMS, allowing thus, the current very favourable instruments distribution on both sides of the IMS. The TOB is fixed on the CRYO stiffener through six CFRP tubes and supports the telescope assembly, the telescope baffle and the FPIA.

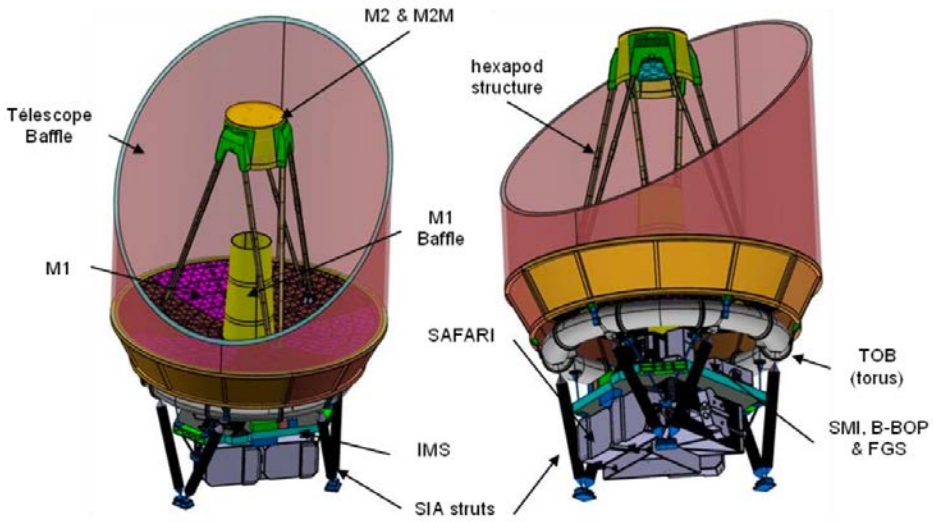

Figure 4-9: Mechanical design overview of the Science Instrument Assembly

The telescope baffle is made of aluminium for thermal and light weighting reasons. The bottom part of the baffle is made of a conic section to increase its stiffness. The overall telescope baffle is then fit directly to the SiC TOB through flexural blades to allow a good thermo-elastic behaviour during the cooling phase from 293 to 8 K. An aperture stop at M1 level is implemented and supported by the telescope baffle.

The FPIA consists in a baseplate supporting the scientific instruments, mounted on the TOB through bipods. The instrument Mounting structure (IMS) is a classical aluminium sandwich panel in order to limit the thermo-elastic effects with the instruments which structure is also made of aluminium. Its overall thickness is 80 mm to allow a good modal behaviour.

Two instruments (SMI and B-BOP) are implemented on the top side of the IMS and collect the beam before the telescope focus. The SAFARI instrument is mounted on the bottom side of the IMS and collects the beam after the telescope focus. SAFARI is the biggest and heaviest instrument, which has led to locate its interface in front of the IMS bipods interface. This allows to transfer the loads directly to the TOB which has a great impact on the mechanical performance of the Focal Plane Instrument Assembly.

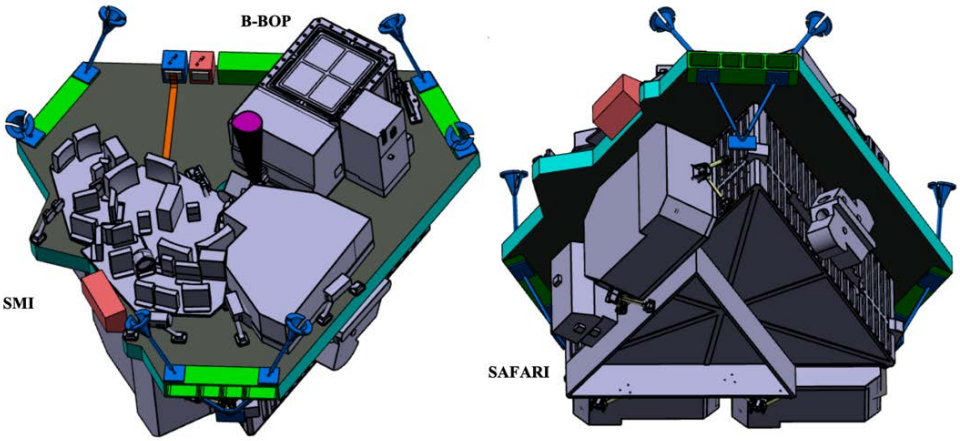

Figure 4-10: Science Instruments accommodation

The SIA total nominal mass (including design margins) is 768 kilograms, including 259 kilograms for Science instruments and fine guidance sensor. The first lateral mode frequency of 15.5 Hz is due to the SIA struts which design geometry is driven by the complete PLM mechanical design. It is 30% above the specification at 12 Hz. The first axial mode frequency of 50 Hz, mainly due to the bending mode of IMS, is well above the specification at 40Hz. The quasi-static limit loads that SIA can withstand are 10 g in lateral and longitudinal directions. Per contrary, the M2 can be submitted to 10 g in longitudinal, and 20 g in lateral.

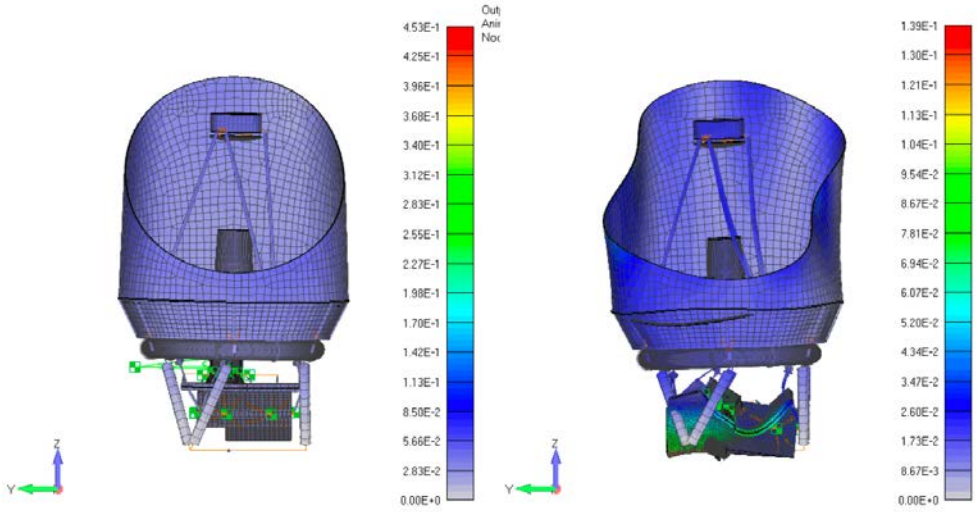

Figure 4-11: SIA first lateral and longitudinal mode at 15.5 and 50.1 Hz

The targeted thermal architecture aims at providing a telescope below 8 K and a FPIA at 5 K to provide the coldest environment to the instruments. This target is achieved by coupling directly the IMS to the 4 K stage, which optimizes thermal straps length, and thus their mass and efficiency.

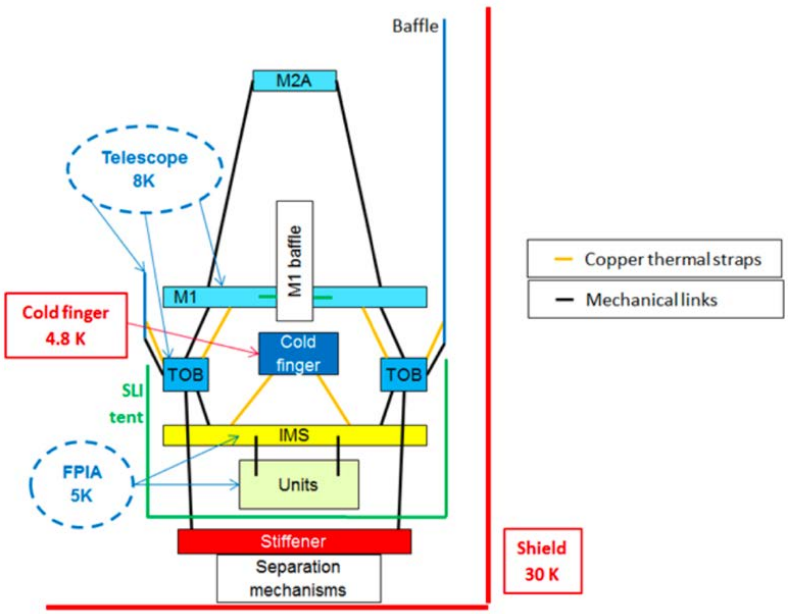

Figure 4-12: Overview of SIA thermal architecture

At the SIA conductive interface, the conductive coupling between the TOB and the stiffener plate has to be minimized in order to reduce the heat load coming from the CRYO module. This is achieved thanks to efficient CFRP struts with invar fittings that have been optimized regarding both thermal and mechanical constraints. Moreover, the separation mechanisms (part of the CRYO module) allow to conductively decouple the stiffener plate from the thermal shield (30 K). This allows getting an intermediate 18 K conductive interface at the stiffener plate.

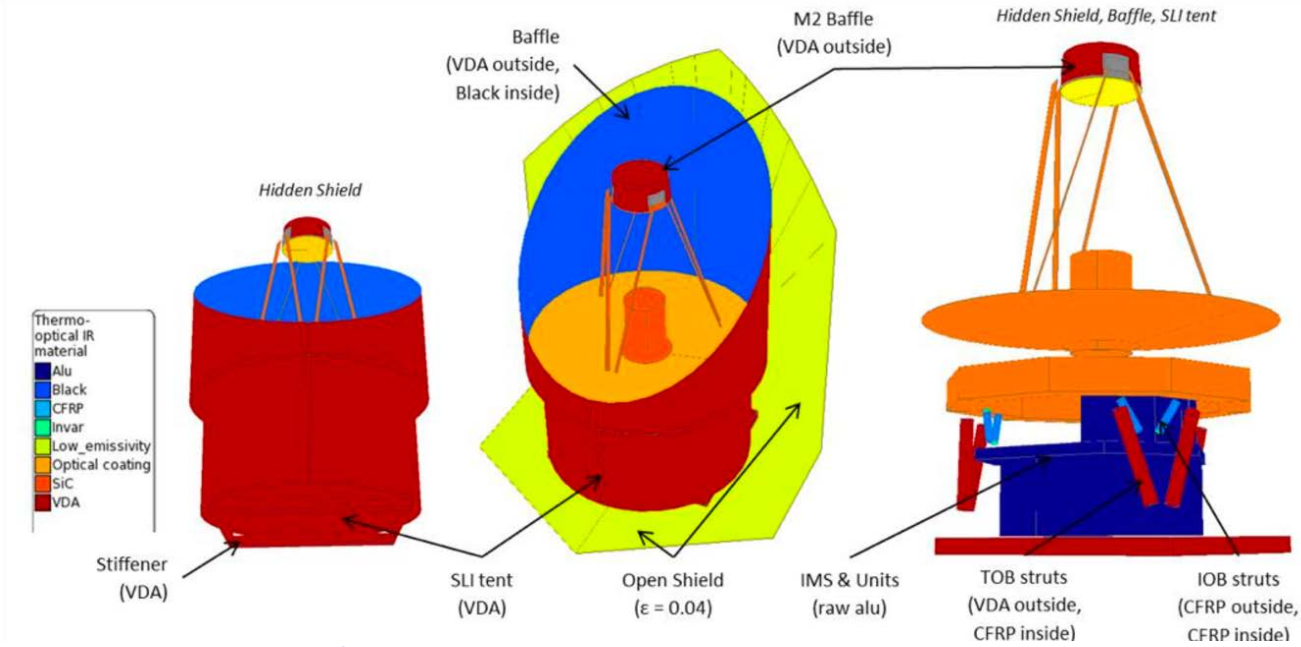

Figure 4-13: Thermal model of the SIA and coating description

To manage the radiative interface of the SIA, a low emissive coating is used on the external side of the baffle in order to limit radiative heat exchange with the shield. A SLI tent allows to protect the FPIA from the environment (shield, stiffener plate, amongst others) and to provide a homogeneous radiative cavity to the instruments.

In-orbit thermal performances are assessed in terms of SIA heat load to the 4 K stage power budget necessary to reach 8 K maximum on the whole ITA, and 5 K on the IMS. The Table 4-1 sums up the SIA contribution for different configurations analysed with detailed thermal model. The SIA heat load allocation includes a 2 mW of uncertainty and a maturity margin.

Configuration	ITA temp. range (K)	IMS temp. (K)	Stiffener temp. (K)	SIA alloc. (mW)	SIA load to 4K stage	Margin (mW)
Baseline (ITA at 8 K and IMS at 5 K)	7.6-7.64	4.91	17.8	8.2	7.4	0.8
Baseline without Earth flux	7.19-7.21	4.90	17.7	8.2	7.1	1.1

Table 4-6: SIA heat load to 4 K stage power budget

4.4 Cryogenic Assembly Thermal Architecture

CRYO employs the combination of effective radiative cooling (TIRCS) and mechanical cryocoolers (MCS) to meet the thermal requirements for SPICA. Figure 4-14 shows the active and passive cooling components of the Observatory. The main conductive heat paths to SIA include truss structure, cryoharness, and cooler pipes, which are heat exchanger

pipes in Joule-Thomson coolers. The heat conductance through ITA can become the dominant heat path, and TSM mechanism is introduce in order to reduce the heat flow.

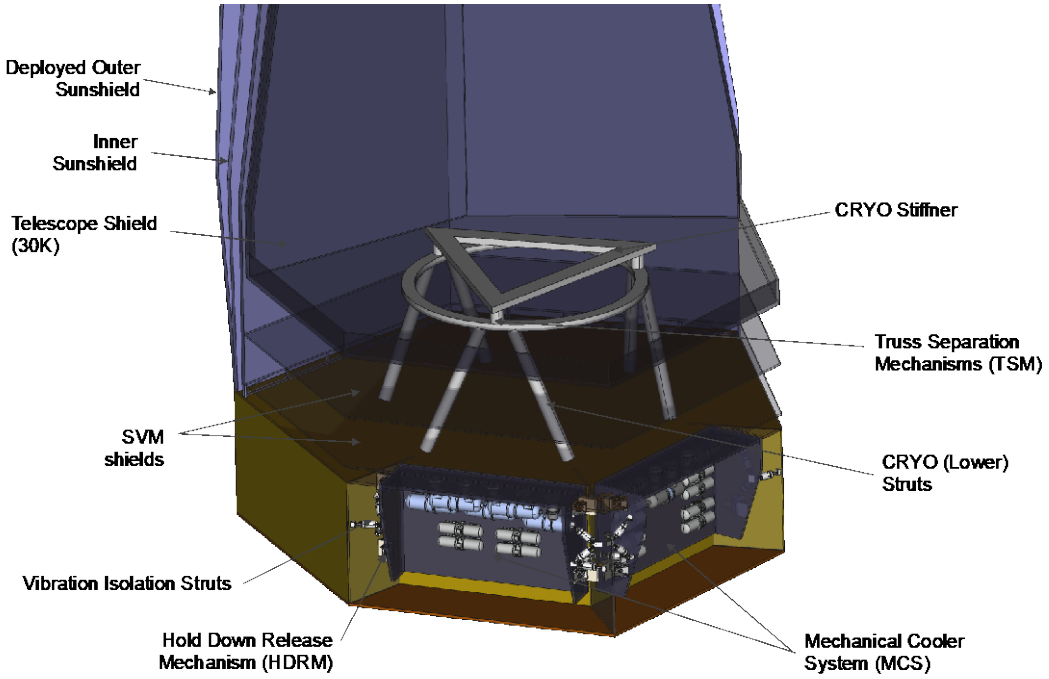

Figure 4-14: CRYO module overview

Figure 4-15 shows the cooling chain in CRYO together with SIA components to be cooled to below 8 K. CRYO is a hybrid system of effective passive (radiative) cooling (via the SVM shields and sunshields) and active cooling by MCS. The SPICA MCS uses three types of cryocoolers: double-stage Stirling coolers8, 9 (2ST), 4 K class Joule-Thomson coolers (4K-JT), and 1 K class Joule-Thomson coolers10 (1K-JT). A 4K-class Joule-Thomson cooler (4K-JT) in the mechanical cooler system cools the SIA directly through a thermal strap, while the thermal conductance needed for a thermal strap between the 4K-JT cold tip and the telescope assemblies are determined in order to cool the entire SIA to below 8 K by taking into account the SIA temperature distribution. The cooling power of 4K-JT is 40 mW with 4.5 K at EOL (End of Life) as a specification. A 1K-class Joule-Thomson cooler (1K-JT) is also used in the mechanical cooler system to provide the precooling stage of 1.8 K for scientific instruments. Particularly, the 1.8K precooling temperature is important for the 50mK hybrid coolers developed by CNES / the French Alternative Energies and Atomic Energy Commission (CEA) in the framework of SPICA SAFARI instruments project. The double stage Stirling cooler (2ST) is used as a pre-cooler of the 4K-JT as well as the 1K-JT, and another 2ST is also used to actively cool the telescope shield.

The 2ST cool the Telescope Shield (TS) to below 30 K and also work as precoolers for the Joule-Thomson coolers. 4K-JT cool the telescope below 8 K and provide the focal plane instruments (FPIs) with the 4.8 K stage. 1K-JT provide FPIs with the 1.8 K temperature stage. Two FPIs (SAFARI and B-BOP), which require lower temperature for their detectors, have dedicated sub-K coolers. The proposed MCS cooling capability requires the heat load budget at the 30 K TS to be below 320 mW, at the 4.8 K stage to be below 30 mW, and at the 1.8 K stage to be below 10 mW.

The mechanical cooler system (MCS) consists of three types of coolers: double-stage Stirling coolers (2ST), 4K-class Joule-Thomson coolers (4K-JT), and 1K- class Joule-Thomson coolers (1K-JT). Green lines indicate the thermal connection to the 4.8 K stage, blue lines show the connection to the 1.8 K stage, and the yellow line shows the connection to the 30 K stage. Since most of the SIA components are connected (through thick green lines in Figure

4-15) to the 4K-JT stage, the most critical part of the design is the feasibility of the thermal budget at the 4K-JT stage. The thermal balance of the system is discussed below with particular attention to consolidating the heat budget at the 4K-JT stage in the current analysis.

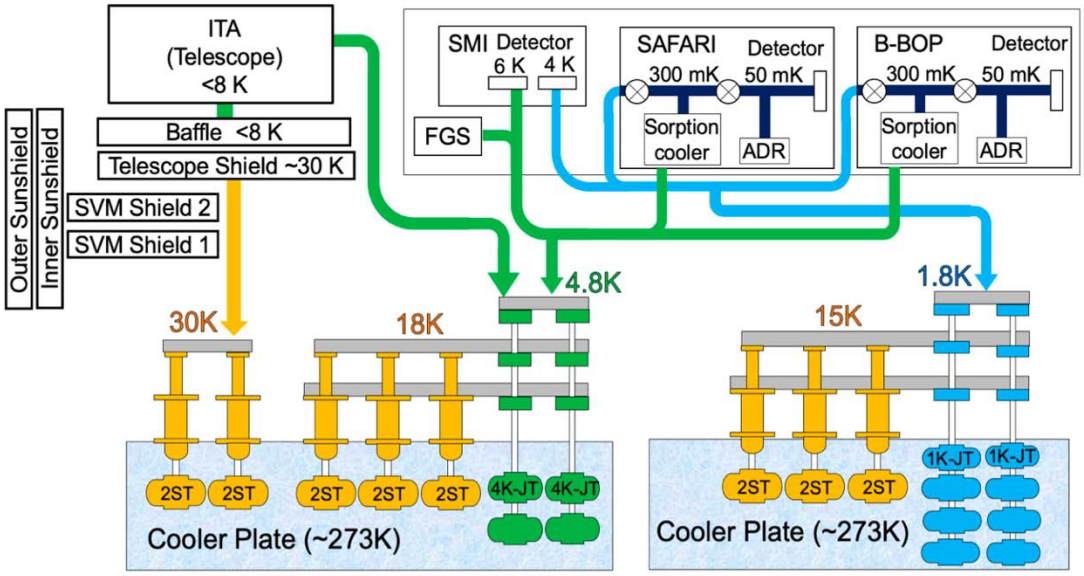

Figure 4-15: Cooling chain of the SPICA cryogenic system

MCS Redundancy Approach

In SPICA, because of the strong requirement, the redundancy of the cooler system is one of most important issues for the mission. Hence, two 1K-JT as well as 4K-JT coolers are used for a redundancy. Then, three 2ST coolers are used as pre-coolers for 4K-JT and 1K-JT coolers respectively. Additionally, two 2ST coolers are proposed to cool the telescope shield for the redundancy. The pre-coolers for 1K-JT should be separated from 4K-JT because of the influence of the pre-cooler's failure as well as a required pre- cooling temperature for 1K-JT lower than that for 4K-JT. In nominal operation, the cooling power of the 4K-JT stage (thermal interface with two 4K-JT cold tips) and 1K-JT stage (thermal interface with two 1K-JT cold tips) is 40mW at 4.8 K and 10mW at 1.8 K as interface requirements respectively, and all JT coolers are operated to satisfy these (hot redundancy), while all 2ST pre-coolers are also operated with almost half of the full driving power. The cooling power of 4K-JT stage can be maintained if one of 4K-JT cooler cannot be operated, while same operation can be done for the 1K-JT stage.

When one of three 2ST coolers is non-operated, pre-cooling temperature (2ST 1st stage and 2nd stage) can be maintained by operating two remaining 2ST coolers with full driving power. A significant heat load through the SUS cylinder of the failed 2ST must be rejected by the other 2STs. Since the heat load is typically 200 mW, which is comparable with the cooling power of the 2ST 2nd stage, three units of 2ST are therefore needed as pre-coolers.

In nominal operation, as the payload module requirement, the cooling power to cool the telescope shield is 480 mW at 26 K, which can be provided by two 2ST coolers with reduced driving power (60W). When one of these 2ST coolers is non-operated, the temperature of the telescope shield becomes higher even with full driving power of another 2ST cooler. Even in this higher telescope shield temperature case, nominal operation can be maintained because total heat load to the 4K-JT stage can be rejected by two 4K-JT coolers. In this phase, 33 % margin is proposed for the cooling power of the 4K-JT stage, the 1K-JT stage and the telescope shield. Hence, the heat load must be lower than 30 mW, 7.5 mW and 320 mW for each temperature stage respectively.

MCS Requirements and Heat Load Allocations

Table 4-7 shows the requirements used for the development of the coolers baselined for SPICA M5.

	20K Two Stage Stirling Cooler (2ST)	4K Joule-Thomson Cooler (4K-JT)	1K Joule-Thomson Cooler (1K-JT)
Working gas	4He	4He	3He
Cooling objectives	JT precooling	ITA + FPIA	FPIA (SAFARI+SMI)
Cooling power	200mW@20K, 1000mW@100K	40mW@4.5K	10mW@1.7K
Input power	< 90W	< 90W	< 75W
Life time	> 3 years (5 years goal)	> 3 years (5 years goal)	> 5 years (10 years goal)
Mechanical environment	Based on ASTRO-H	Based on ASTRO-H	Based on ASTRO-H
Quantity	3 for 4K-JT systems 3 for 1K-JT systems 2 for shield coolers	2	2
Heritage	AKARI(2006), JEM/SMILES(2009), ASTRO-H(2016)	JEM/SMILES(2009) ASTRO-H(2016)	ASTRO-H(2016)
R&D status	EM verification test PM and FM verification test (for ASTRO-H)	EM verification test PM and FM verification test (for ASTRO-H)	EM verification test

- Cooling performance and reliability have been improved based on the technologies of the AKARI and SMILES cryocoolers, which include flexure bearings to support the piston and displacer, internal gas contamination control, and microphonics control by optimizing the bearing clearance.
- Cooling power is defined as EoL performance with max power input for one unit.
- Design lifetime of the 1K-JT has been improved based on technologies of the ASTRO-H 4K-JT cooler with addition of enhanced contamination control and investigation. These technologies are reflected in the 2ST and 4K-JT coolers.
- Input power for the drive electronics is not included. Additional input power of 4W for one 4K-JT and 5W for one 1K-JT is also needed to operate pressure gauges in the JT circulation line.

Table 4-7: Specifications of the cryocoolers baselined for SPICA MCS

JAXA recommends the following system margins at cooler level:
- 50% system margin for the Shield Coolers.
- 33% system margin for the JT Coolers (4K and 1K Stage).

Provided system margin is applied and considering realistic thermal gradients between the cold tips and the applications, it leads to the following resources available at each stage:
- 320mW at 30K
- 30mW at 4.8K
- 7.5mW at1.8K

In the frame of the Mission Consolidation Review, a bottom up allocation exercise was performed for the 4.8K and 1.8K stages taking into account current best estimates and suitable uncertainties and maturity margins.

Table 4-8 summarizes the heat budget allocation for heat sources at 4.8 K during science observation. The dominant heat source is the heat dissipation of FPIs, as shown in the table's first row. The budget is the allocation for the maximum heat load, and the entire FPI is required to be operated below the allocation in every operation mode. Other rows in the table show the heat budget allocation for other sources assumed in the current analysis. This allocation is compatible with the 4K coolers requirements.

Parameter	**Heat budget (mW)**

FPI heat dissipation	15.1
Harness parasitic heat load	4.9
Radiative heat from Earth and Moon	1.5
JT pipes parasitic heat load	1.0
Off JT coolers parasitic heat load	2.3
Heat load leak to 1.8K stage	2.7

Table 4-8: Thermal budget allocations assumed for heat sources at the 4.8 K stage

Table 4-9 shows the heat budget allocation at the 1.8 K stage during science observation. The 1K-JT stage cooling chain (blue lines in Figure 4) is mostly independent of the whole thermal budget. Moreover, most of the heat loads are assumed as allocation (e.g. heat dissipation of FPIs) and can be controlled separately. All other heat loads should be kept negligible compared to those listed in the table.

Parameter	Heat budget (mW)
FPI heat dissipation	4.10
Heat load leak from upper temperature stages	4.30
JT pipes parasitic heat load	0.75
Off JT coolers parasitic heat load	0.85

Table 4-9: Thermal budget allocations assumed for heat sources at the 1.8 K stage

The bottom-up allocation exercise led to a number (10mW) which is higher than the cooling capability of the machine derived from the requirements and assuming the 33% system margin (7.5mW). In order to be compatible with the 1.8K stage allocation while conserving the required system margin, a solution to increase the cooling power of the 3He JT Coolers to 13.3mW EOL has been identified and is addressed in section 4.6.3.2.

Static Thermal Analysis

The current thermal design has two layers of sunshields: outer and inner sunshields. The preliminary thermal design also has two layers of SVM shields between TS and SVM. TS is actively cooled to 30 K by 2ST. The design goal of the sun and SVM shields is to guarantee 30 K for TS while remaining in the capability of 2ST. SVM temperature has been fixed at 273 K. SVM is covered by a Multi-Layer Insulator (MLI) so that SVM is thermally isolated from the thermal shields.

The two sunshields are stored in parallel in the rocket fairing during the launch phase, and the outer sunshield is to be tilted in orbit to secure enough view factors from the sunshields to deep space. One of the critical parameters is the tilt angle of the outer sunshield. A significant fraction of the heat from the sun is radiated into space, and the heat flow from the outer sunshield to the inner sunshield is thereby reduced. Increasing the outer sunshield tilt angle is expected to be effective for this reduction of the heat flow from the outer sunshield. The sensitivity analysis of the outer sunshield tilt angle has been carried out with a simplified thermal model.

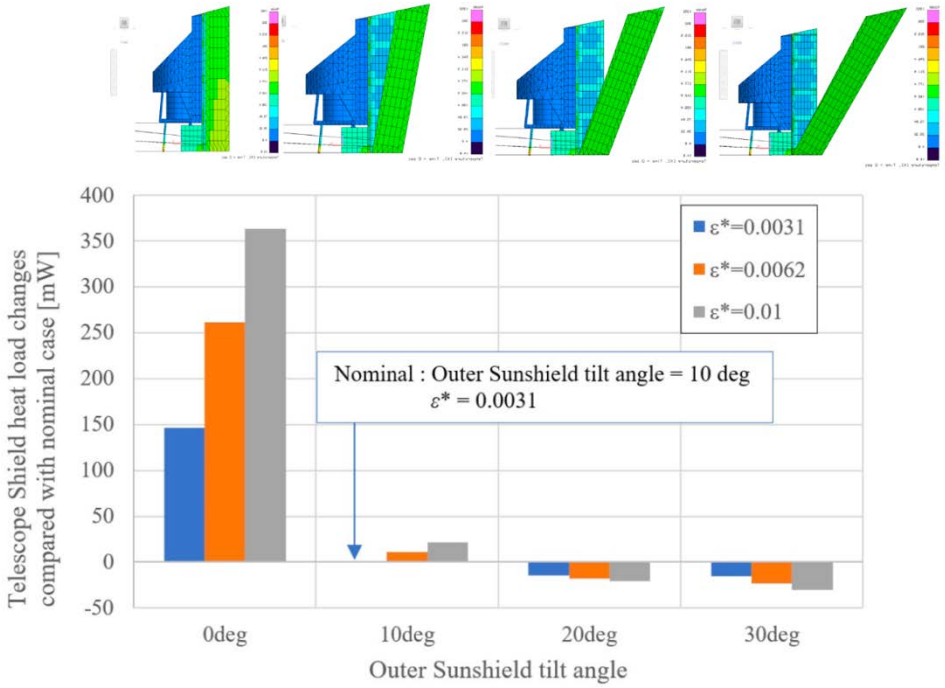

Figure 4-16: Telescope Shield heat load relative to sunshield tilt angle

The TS heat load dependence on the change of the outer sunshield tilt angle has been evaluated. Figure 4-16 shows the results of sensitivity analysis. The results show that the TS heat load is lower for the larger tilt angle of the outer sunshield. We do not have a feasible solution for the null tilt angle, but the tilt angle sensitivity beyond 10 degrees is not significant. It was therefore decided to adopt 10 degree as the baseline for the tilt angle of the outer sunshield.

The results depend on the MLI performance, which was used on the solar side of the inner sunshield, and sensitivity relative to MLI performance was characterised by analysis. Figure 4-16 also shows the heat load dependence on the effective emissivity of inner sunshield MLI, which is changed from the reference value of 0.0031 to 0.0062 and 0.01, respectively. The results show that the TS heat load is not sensitive to the effective emissivity when the outer sunshield tilt angle is larger than 10 degrees. It was concluded that the configuration with the outer sunshield tilted more than 10 degrees has feasible solutions even for the more conservative MLI performances.

Figure 4-17 shows thermal flows results obtained with the preliminary thermal model and the outer sunshield tilt angle of 10 degrees. The three stage temperatures were fixed: SIA at 8 K, telescope shield at 30 K, and SVM interface at 273 K. Although SIA is assumed to be at 8 K following the requirements in the previous section, all the heat loads to SIA are assumed to be transferred to the 4.8 K temperature stage via a thermal strap connecting SIA and 4K-JT. The net heat input at the SIA and the telescope shield stages was estimated and compared to the cooling capability of cryocoolers at the 4.8 K and 30 K stages.

Figure 4-17 shows that the heat flow to the 4K-JT coolers is 28.9 mW, compatible with the cooling capability allocation of 30 mW at the 4K-JT stage (Table 4-8). In particular it illustrates that the heat flow from TS to the 2ST coolers is 310 mW, which is compatible with the cooling capability allocation of 320 mW for the TS temperature of 30 K.

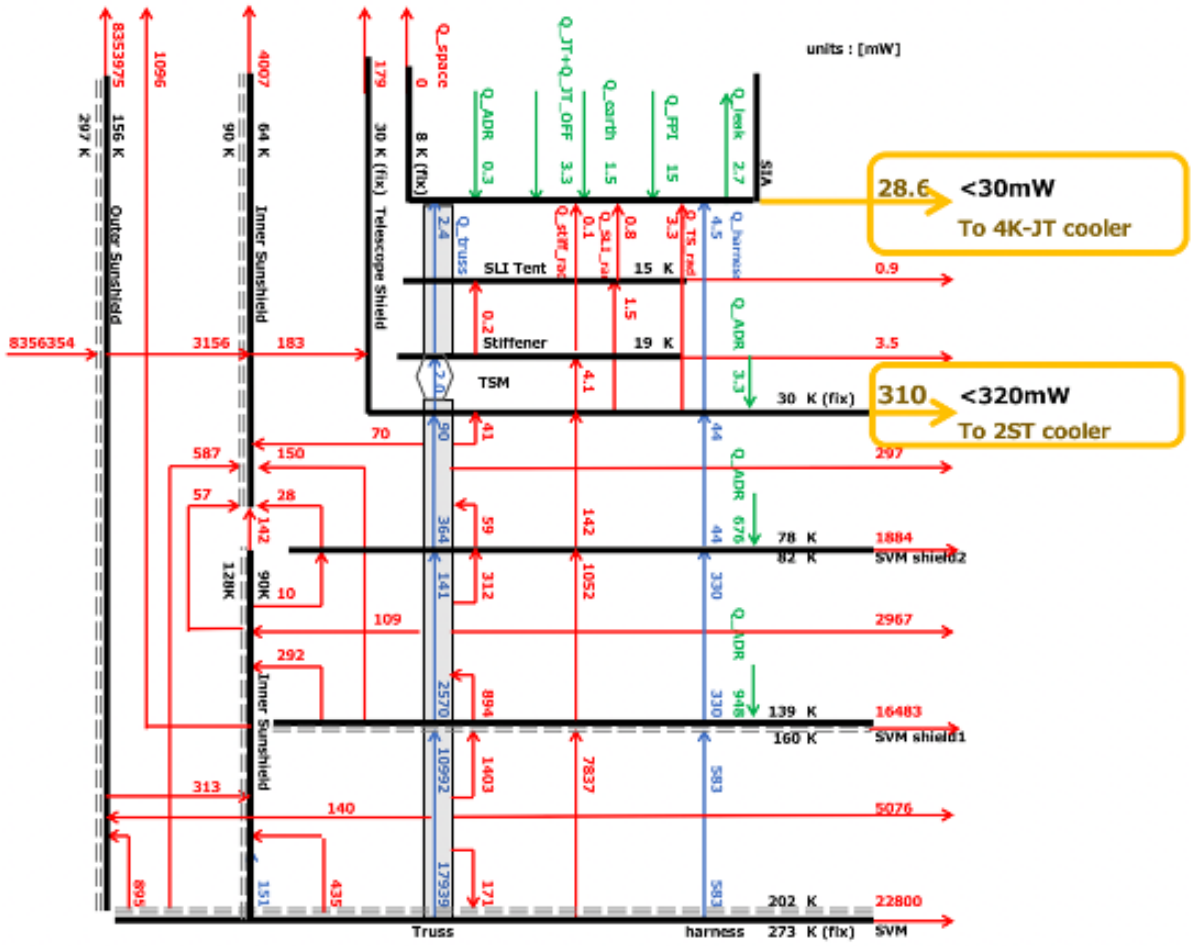

Figure 4-17: Heat-flow diagram

Table 4-10 summarizes the thermal requirements and the heat load at each temperature stage estimated with the thermal model. The heat loads at the stages shown in Table 4-10 are well below those of the thermal requirements. It was concluded that the current thermal model meets the heat budget requirements both at the 4K-JT stage and at TS.

Parameter	Heat load to 2ST for Telescope Shield (mW)	Heat load to 4K-JT (mW)
Requirements	≤ 320.0	≤ 30.0
Model results	310.0	28.6
Margin	10.0	1.4

Table 4-10: Thermal control performances

Transient Thermal Analysis

Another critical point of the thermal design of PLM/CRYO is the cooling time in orbit. A preliminary transient thermal analysis was conducted to estimate the cooling time in orbit. It was assumed that FPI is made of Al with 334 kg and ITA is made of SiC and weighs 457 kg. The transient thermal analysis permitted to establish that SIA can reach 4.8 K in about 105 days. Note that the current analysis is still preliminary, and SIA, whose detailed design affects the cooling time significantly, is treated as a single-node component for simplicity. To estimate a more realistic cooling time, one must take the operational procedures into account. One critical operation is the decontamination operation to avoid telescope contamination by water vapor outgas. We estimated that the operation takes a few weeks and the total cooling time is about 120 days.

4.5 Instruments Overview and Accommodation

The three science instruments, with a spectral coverage that extends from 10 to 420 micrometres, enable all the science objectives described in section 1. The instrument main capabilities (Table 4-11) are derived from the science requirements. The Mid-infrared Imager and Spectrometer (SMI, Section 5.1), Far-Infrared Spectrometer (SAFARI, Section 5.2) and Far-infrared Polarimeter (B-BOP, Section 5.3) are described in detail in later subsections.

Observing Mode	Band (μm)	Field of View (arcsec^2)	Spectral Resolution (R=λ/Δλ)	Saturation Limits	Sensitivity, 5σ in 1 hr
SMI, Mid-Infrared Imager and Spectrometer					
Dispersive Prism	17-36	600x3.7 (4 slits)	60 - 160	20.0 Jy at 27 μm	5.0 10^{-20} W/m^2 at 27 μm
Imaging	34	600x720	5	1.0 Jy at 34 μm	13.0 μJ at 34 μm
Grating	18-36	60x3.7 (1 slit)	1400 - 2600	1000.0 Jy at 27 μm	2.3 10^{-20} W/m^2 at 27 μm
Immersion Grating	10-18	4x1.7(1 slit)	29000	20000.0 Jy at 15 μm	0.8 10^{-21} W/m^2 at 15 μm
SAFARI, Far-Infrared Spectrometer					
Grating	34-230	120x120	250 (SAFARI 3.0) 200 (SAFARI 4.2)	90.0 Jy at 85 μm	8.8 10^{-20} W/m^2 at 85 μm (SAFARI 4.2)
High Resolution Fourier Transform Spectrometer	34-230	120x120	11000 - 1500	90.0 Jy at 85 μm	19.0 10^{-20} W/m^2 at 85 μm (SAFARI 4.2)
B-BOP, Far-Infrared Polarimeter					
Polarimetry	52-88 135-225 280-420	160x160	3	-	1.0% in linear polarization ±1.0° in polarization angle

Table 4-11: Summary of Science Instrument capabilities

SMI is a spectrometer that covers the entire band between 10 and 36 μm at low (LR, R=60-160), medium (MR, R=1400-2600), and high (HR, R=29000) spectral resolving power. SMI provides in addition imaging measurements at 34 μm (CAM). SMI/LR channel is a multi-slit prism spectrometer of a wide field-of-view with 4 long slits of 10′ in length, which is operated in combination with SMI/CAM, a 10′ ×12′ slit viewer. SMI/MR is a grating spectrometer with a long slit of 1′ in length and high line sensitivity. SMI/HR is an immersion grating spectrometer with high line sensitivity. SMI/MR and HR are operated in combination with a beam-steering mirror and shared fore-optics to perform spectral mapping (or dithering) of a relatively small area of about 1′x1′. On the other hand, the design of SMI/LR with CAM is based on wide-area surveys in a telescope step-scan mode to produce a spectral map of 10′ ×12′ area as a minimum field unit.

SAFARI is a highly capable a Fourier Transform Spectrometer (FTS), providing continuous coverage in both photometry and in spectroscopy over the desired wavelength range and over a 2'×2' field of view with a spectral resolution of R~2000. In order to cover the full 34 to 210 μm wavelength range with adequate spatial and wavelength resolution the instrument integrates three wavelength sub-bands each optimised to cover a single octave.

B-BOP provides imaging and polarimetric measurement capabilities in three spectral bands at 70, 200 and 350 μm. B-BOP has a common entrance optics for the three bands. Two dichroic filters define the three optical paths that correspond to the three different bands. The Field of Views are almost identical for the three channels varying between 3.2′ x 3.2′ and 3.7′ x 3.7′. B-BOP utilizes observatory mapping speed from 10 to 60 arcsec per second to map one to thousands of square arcminutes.
Figure 4-10 shows the location of each instrument mounted on IMS structure below the telescope primary mirror subassembly. This location is effective for maintaining the three instruments below 4.8 K in the payload module.

Table 4-12 summarizes the nominal mass for all three instruments. In order to determine the mass required for each instrument, the team applied an average 20.0% Design Maturity Margin (DMM) over the Current Best Estimate (CBE) to arrive at the maximum possible value. Table 4-13 and Table 4-14 lists the power and data rate for all three instruments. The power demand is based on the average power consumption during observation, which is the mode with higher power requirement. Peak power is considered 10% above the average.

	CBE mass (kg)	DMM (%)	Nominal mass (kg)
SMI, Mid-Infrared Imager and Spectrometer	65.4	22	79.9
SMI Units in SIA	36.4	24	45.1
SMI Units in CRYO	2.0	20	2.4
SMI Units in SVM	27.0	20	32.4
SAFARI, Far-Infrared Spectrometer	180.6	20	216.8
SAFARI Units in SIA	147.7	20	177.2
SAFARI Units in SVM	33.0	20	39.6
B-BOP, Far-Infrared Polarimeter	52.8	20	63.4
B-BOP Units in SIA	21.9	20	26.3
B-BOP Units in CRYO	3.4	20	4.1
B-BOP Units in SVM	27.5	20	33.0
Total	298.9	20	360.1

Table 4-12: Nominal mass for the Science Instruments

At system level it is considered that, once the instruments are switched on, they remain powered on for the rest of the mission with no difference between observation and stand-by modes. For the power subsystem sizing, the total nominal power consumption, i.e. including DMM, of all three instruments together is considered without additional payload margin but then, at system level like for any other units, associated power losses plus 30% system margin is added.

	CBE power (W)	DMM (%)	Nominal power (W)
SMI, Mid-Infrared Imager and Spectrometer	35.0	20	42.0
SMI DPU	8.0	20	9.6
SMI DCU	27.0	20	32.4
SAFARI, Far-Infrared Spectrometer	201.2	22	246.1
SAFARI DCU	113.8	21	137.6
SAFARI WFEE	22.0	30	28.6
SAFARI ICU	65.4	22	79.9
B-BOP, Far-Infrared Polarimeter	60.3	20	72.3
B-BOP SSCU	13.2	20	15.8
B-BOP WFEE	26.3	20	31.6
B-BOP DPU	20.8	20	24.9

Table 4-13: Power demand estimates

The science and housekeeping nominal data rate of the instruments is presented in Table 4-14. This nominal data rate has been calculated for the different observation modes, considering the CBE estimation and the required margin (i.e. 20% for SMI) or compression factor for noise dominated signals (i.e. 35% for SAFARI). Since science data will be compressed by a lossless compression algorithm before recording and downlink, all science data volumes are calculated for the compressed form. Table 4-14 shows the compressed data volume for each SI. In the case of SMI instrument, the average data rate represents the nominal scenario with equal mode sharing between HR, MR and LR/CAM channels.

	SAFARI 4.0	B-BOP	SMI		
			HR	MR	LR/CAM
Pixels	2200	2688	1048576	1048576	1048576
Sampling	120	40	1	0.5	0.5
Nbit	16	24	16	16	16
Background Port			1.25	1.25	1.25
Science Data Rate (Mbps)	4.22	2.58	20.97	10.49	10.49
Compression	0.5	1	0.5	0.5	0.1
FTS (Mbps)	0.12				
Compressed Date Rate CBE (Mbps)	2.23	2.58	10.00	5.00	2.00
Margin (compression)	35%	0%	20%	20%	20%
Nominal Compressed Data Rate (Mbps)	2.95	2.58	12.0	6.0	2.4
House Keeping (kbps)	64	60.9	15	15	15

Table 4-14: Science Instrument data rate estimates

No detailed operational model was defined for science observation. However, considering the mission operational share, observation efficiency and instruments compressed science data generation, the nominal and total data volume generation per day is calculated, as shown in Table 4-15.

	SAFARI	B-BOP	SMI	Total
Utilization	48%	17%	35%	
Observation efficiency	50%	50%	50%	
Data rate (Mbps)	2.95	2.58	12.0	
Combined Data Volume, Average				
Nominal Compressed Data Volume (Gbit/day)				261.5
Compressed Data Volume, including 30% margin (Gbit/day)				340.0
Combined Data Volume, Worst Case				
Nominal Compressed Data Volume (Gbit/day)				518.5
Compressed Data Volume, including 30% margin (Gbit/day)				675.0

Table 4-15: Science data volume generation

The nominal interface heat loads of the instruments, including maturity margins, for each science instrument observational modes identified are presented in Table 4-16. The heat loads for FGS integration within SMI instrument are listed in bracket. This configuration assumes the Si:Sb CAM detectors are moved to the 4K-JT stage and the Beam Steering Mirror (BSM) is exchanged by a dichroic mirror for the possible implementation of a MR/HR parallel mode observation. Details of this configuration are presented in section 5.1.

Mode	1K-JT Stage (mW)		4K-JT Stage (mW)	
SMI, Mid-Infrared Imager and Spectrometer				
Power Off	0.588	(0.396)	0.300	(0.300)
Standby	0.948	(0.636)	0.420	(0.540)
Flat	3.780	(2.520)	4.250	(5.510)
Annealing	4.200	(4.032)	11.856	(11.856)
Calibration	3.780	(2.520)	3.002	(4.276)
Observation LR and CAM	3.780	(2.520)	3.002	(4.276)
Observation LR	3.780	(2.520)	3.002	(4.276)
Observation MR	3.780	(2.520)	3.002	(4.276)
Observation MR Mapping	3.780	(2.520)	6.270	(4.276)
Observation HR	3.780	(2.520)	3.002	(4.276)
FGS		(0.636)		(1.644)
SAFARI, Far-Infrared Spectrometer				
Power Off	3.750		2.171	
Standby	3.750		2.171	
Recycling	6.750		16.671	
Calibration LR	5.560		11.441	
Chop LR	5.560		10.891	
Scan LR	5.560		10.981	
Calibration LR	5.560		12.191	
Observation HR	5.560		12.191	
B-BOP, Far-Infrared Polarimeter				
Power Off	0.577		1.140	
Standby Cold	1.014		2.367	
Standby Warm	0.577		1.140	
Test	1.014		2.367	
Recycling	3.577		13.429	
Calibration	1.014		5.208	
Observation	1.014		2.367	

Table 4-16: Instruments SIA/SVM nominal interface heat loads

For sizing of the thermal control subsystem, the status of each instrument during a given operational mode and associated heat loads as per Table 4-16 are considered. The nominal (i.e. including DMM) parasitic and dissipated heat loads to the 1K-JT and 4K-JT stages per sizing mode are summarized in Table 4-17 considering the allocations for an external FGS, and Table 4-18 considering the SMI/CAM as the FGS. The colour code represents the comparison with respect to the allocation (green means compliant, red means above the allocation).

Allocation as per Heat Rejection Capacity EoL MRD v1.4	1K-JT Stage [mW]			4K-JT Stage [mW]			
	Parasitic w/ Margin	Dissipation w/ Margin	Total w/ Margin EOL	Parasitic w/ Margin	Dissipation w/ Margin	Total w/ Margin EOL	Heat leak to 1K
	≤ 4.30	≤ 4.10	≤ 8.40	≤ 6.10	≤ 15.10	≤ 21.20	> 2.60
SMI Observation	4.83	3.28	**8.11**	3.86	4.50	**8.36**	3.77
SAFARI Observation (Sizing Case: HR)	4.92	2.17	**7.09**	3.86	11.94	**15.80**	3.84
B-BOP Observation	4.92	0.80	**5.71**	3.94	3.07	**7.01**	3.84
SMI Annealing	4.83	3.70	**8.53**	3.86	11.56	**15.42**	3.77
SAFARI Recycling	4.92	3.36	**8.28**	3.86	14.62	**18.48**	3.84
B-BOP Recycling	4.92	3.36	**8.28**	4.15	12.12	**16.27**	3.84

Table 4-17: Instruments thermal budget per observing mode (external FGS)

Allocation as per Heat Rejection Capacity EoL MRD v1.4	1K-JT Stage [mW]			4K-JT Stage [mW]			
	Parasitic w/ Margin	Dissipation w/ Margin	Total w/ Margin EOL	Parasitic w/ Margin	Dissipation w/ Margin	Total w/ Margin EOL	Heat leak to 1K
	≤ 4.30	≤ 4.10	≤ 8.40	≤ 6.10	≤ 15.10	≤ 21.20	> 2.60
SMI Observation	4.66	2.18	**6.85**	3.61	3.98	**7.59**	3.63
SAFARI Observation (Sizing Case: HR)	4.72	2.05	**6.77**	3.61	11.36	**14.97**	3.68
B-BOP Observation	4.72	0.68	**5.40**	3.69	2.49	**6.18**	3.68
SMI Annealing	4.66	3.70	**8.36**	3.61	11.56	**15.17**	3.63
SAFARI Recycling	4.72	3.24	**7.96**	3.61	14.74	**18.35**	3.68
B-BOP Recycling	4.72	3.24	**7.96**	3.90	12.24	**16.14**	3.68

Table 4-18: Instruments thermal budget per observing mode (SMI/CAM as FGS)

4.6 Observatory Summary

4.6.1 Budgets

The nominal dry mass of the Observatory without the science instruments is 2285 kilograms, including an average design maturity margin of respectively 16% for SVM, 17% for CRYO module and 19% for SIA assembly. Adding a system margin of 25% and the science instrument mass allocation of 445.5 kilograms (i.e. 305 kilograms for SIA, 8.5 kilograms for CRYO and 132 kilograms for SVM) to this gives an Observatory total dry mass of 3311 kilograms. The Propellant has been calculated for 5 years mission. The wet mass is then 3553 kilograms, including propellant, residuals and pressurant mass and adding the balance mass allocation. The launch vehicle capability predicted by JAXA, without the launch vehicle adapter, is 3750 kilograms. A summary of the system mass budget is shown in Table 4-19.

An Observatory mass reserve of about 200.0 kilograms has been achieved thanks to:

- The decision to adopt a vertical configuration with the infrared telescope boresight aligned with the Launch Vehicle longitudinal axis, which in conjunction with the optimisation of the different telescope optical components and structure led to an SIA nominal mass below 510 kilograms, excluding FPIs and FGS.
- The accommodation of instruments in two layers on the Instrument Mounting Structure (IMS) and optimisation of the instrument interface and attachment points.
- The optimisation of the PLM thermal shields structure and shape.

The assumptions made when compiling the mass budgets are as follows:

- The instrument nominal mass as 354.3 kilograms, including design maturity margin. Applying 25% system margin gives the total allocation of 445.5 kilograms, as specified by [RD16].
- The cryoharness mass are obtained from a bottom up approach, based on unit interconnection schemes consolidated and harness length measured from a detailed routing exercise performed on the CAD model. The value of 27 kilograms corresponds to a worst case, including the thermal anchoring of the harness. It has been verified that the calculated values for harness and cryoharness are at least 5% of the nominal dry mass at launch.
- The delta velocity and propellant budgets have been calculated using preliminary mission analysis and requirements in conjunction with analysis of the propellant consumed during AOCS manoeuvres. The propellant has been calculated using the maximum separated mass for the spacecraft and a conservative specific impulse of the thrusters.
- The LVA is not included in the present mass budget, in line with the launch vehicle performance assumptions.
- The ITA mass includes a nominal mass of 4.5 kilograms to account for additional aluminium baffle skin thickness and stiffening of the stand-off structures, which are required to cope with Sun illumination during the ascent phase.
- The balance mass allocation of 10 kilograms has been provisioned at Observatory level.
- There is a mass allocation for the FGS accounted separately.

In accordance with standard guidelines in phase A, conservative design maturity and system margins have been applied to the Observatory structure and units. The baseline design is able to cope with changes in payload mass and provides contingency for mitigating potential technical risks.

Observatory Item	Estimated Mass [kg]	Margin [%]	Margin [kg]	Nominal Mass [kg]	Responsible
Service Module (SVM)					
Structure	245.3	20%	48.7	294.0	System
Thermal Control	51.7	15%	7.4	59.1	System
Propulsion	47.1	7%	3.4	50.5	System
Communication	46.8	9%	4.3	51.1	System
Data Handling	26.0	8%	2.0	28.1	System
Attitude Control	68.4	6%	3.9	72.3	System
Electrical and Power	131.6	15%	21.9	153.5	System
Fine Guidance Sensor	4.7	50%	2.3	7.0	System
Secondary Mirror Mechanism	2.5	20%	0.5	3.0	SIA
Mechanical Cooler System	106.9	11%	11.3	118.2	PLM
Science Instruments	87.5	20%	17.5	105.0	Instruments
Harness Assembly	104.0	19%	19.9	123.9	System
SVM	922.5	16%	143.2	1065.7	System
Payload Module (PLM)					
CRYO	689.7	17%	115.5	805.3	PLM
Structure	282.1	20%	56.4	338.5	PLM
Thermal Control	58.3	20%	11.7	70.0	PLM
Mechanical Cooler System	324.3	12%	39.1	363.4	PLM
Science Instruments	5.4	20%	1.1	6.5	PLM
Harness Assembly	19.7	37%	7.3	27.0	PLM
SIA	643.9	19%	124.0	767.9	SIA
ITA	361.6	18%	66.2	427.8	SIA
Structure	98.0	20%	19.6	117.6	SIA
Mirror Assembly	180.9	17%	30.1	211.0	SIA
Thermal Control	13.2	20%	2.6	15.8	SIA
Equipment	69.5	20%	13.9	83.4	SIA
FPIA	282.3	20%	57.8	340.1	SIA
Structure	55.5	20%	11.1	66.6	SIA
Thermal Control	3.7	20%	0.7	4.4	SIA
Equipment	8.6	20%	1.7	10.3	SIA
Fine Guidance Sensor	13.3	20%	2.7	16.0	System
Science Instruments	201.2	21%	41.6	242.8	Instruments
PLM	1333.6	18%	239.6	1573.2	PLM
Observatory	2256.1	17%	382.8	2638.9	System

Observatory System Margin Mass			571.2	
SVM System Margin Mass		25%	213.9	System
PLM System Margin Mass			357.3	PLM
CRYO System Margin Mass		25%	229.2	PLM
SIA System Margin Mass		25%	128.0	SIA
ITA System Margin Mass		25%	107.7	SIA
FPIA System Margin Mass		25%	20.3	SIA
Observatory Balancing Mass			10.0	

Observatory Total Dry Mass		3311.3	System
Observatory System Margin Mass		571.2	System
Observatory Balancing Mass		10.0	System
Propellant Mass incl. Residuals		240.0	System
Pressurant Mass		2.0	System
Observatory Wet Mass		3553.3	System
Wet Mass Allocation for Observatory		3550.0	ESA
Mass Margin for Observatory		-3.3	System
Observatory Wet Mass incl. Reserve		3753.3	System

Table 4-19: SPICA Observatory mass budget summary

The power budgets have been established in line with the margin philosophy as defined in [RD16]. The power consumption figures for the Mechanical Cryocoolers System and the Science Instruments, which represent respectively 55% and 15% of the total Observatory load, have been calculated from the best available current data including maturity margin. The budget has then been established with a maximum load around SEL2 orbit of about 3500 watts and 30% system margin corresponding to the data downlink operations. The details are presented in the power budget summary in Table 4-20. The solar arrays and batteries have been sized to provide required power at EoL (5 years mission), and taking into account one string failure for SA and one cell failure for the batteries.

From analysis of the power requirements in the different phases of spacecraft operations, the battery sizing case has been determined to be the sequence of events from pre-launch through launch, to a nominal Sun acquisition followed by a backup Sun acquisition process. Other operational sequences were analysed, but these were found to be less demanding.

Observatory Item	SAM Nominal Power [W]	COOL Nominal Power [W]	OBS (EoL) Nominal Power [W]	OBS+COM (EoL) Nominal Power [W]
Science Instruments (SI)				
SMI	0.00	0.00	42.00	42.00
SAFARI	0.00	0.00	246.11	246.11
B-BOP	0.00	0.00	72.36	72.36
SI Units in SVM	0.00	0.00	360.47	360.47
SI Units in SVM with P/L Margin	0.00	0.00	360.47	360.47
Science Instrument Assembly (SIA)				
Thermal Control	0.00	209.00	0.00	0.00
ITA	0.00	0.00	0.00	0.00
SIA Units in SIA	0.00	209.00	0.00	0.00
SIA Units in SVM	0.00	0.00	0.00	0.00
Cryogenic Assembly (CRYO)				
Thermal Control	0.00	311.30	17.30	17.30
MCS+TIRCS	0.00	897.72	1442.20	1442.20
CRYO Units in CRYO	0.00	751.63	876.20	876.20
CRYO Units in SVM	0.00	457.39	583.30	583.30
Service Module (SVM)				
Thermal Control	748.88	609.08	163.27	103.13
Propulsion	63.27	14.88	14.88	14.88
Communication	106.66	126.88	41.45	253.51
Data Handling	61.00	61.00	61.00	61.00
Attitude Control	82.25	88.80	139.80	139.80
Electrical and Power	103.84	198.09	197.59	208.98
Conditioning and distribution losses	81.34	175.59	170.09	181.48
SVM Units in SVM	1165.90	1098.72	617.99	781.31
Observatory	1165.90	2516.74	2437.96	2601.28
PLM Power Demand	0.00	960.63	876.20	876.20
SVM Power Demand	1165.90	1556.11	1561.76	1725.08
Observatory Total Power	1515.67	3271.76	3169.35	3381.66

Table 4-20: SPICA Observatory power budget

The communication link budget is based on the architecture described in section 4.6.2. This is based on a dual-band system with K-band communication for science data downlink and X-band for telecommand uplink and housekeeping downlink. The K-band link budget is calculated for minimum local elevation of 20 degrees with Observatory in orbit around SEL2. The considered data rate is 72 Mbps which corresponds to the capability of heritage European

transmitters. A 5.0 dB margin is verified in nominal case, and positive margins are verified in adverse and favour cases which is as needed. During a normal operations contact, the Observatory is therefore capable of downlinking 450 Gigabits of science data. The possibility to reduce the pass duration to less than 2 hours could be envisaged, if required. The X-band link budget is calculated for minimum local elevation of 5 degrees. X-Band downlink margins are greater than 3.0 dB for all the cases computed at the maximum distance. The margins for LEOP and transfer phase have not been calculated but are not considered critical.

Downlink Data Rate (kbps)	SC Antenna	Band	SC EIRP (dBW)	Distance (km)	Ground Station	El (deg)	Mod.	Coding	TM Recovery Margin (dB)	Range Recovery Margin (dB)	Uplink Data Rate (kbps)	TC Recovery Margin (dB)
73850	HGA	K	54.1	1.78E+06	Cebreros	20.0	OQPSK	LDPC 1/2	5.3	-	-	-
2	LGA	X	3.54	1.78E+06	New Norcia	5.0	NRZ-L	Rate 1/2	5.4	8.2	4	4.4
26	LGA	X	11.49	1.78E+06	Cebreros	5.0	NRZ-L	Rate 1/2	4.3	15.9	16	7.2
26	MGA	X	12.9	1.78E+06	Cebreros	5.0	NRZ-L	Rate 1/2	5.7	10.6	16	8.6

Table 4-21: SPICA Observatory link budget margin summary

The pointing accuracy and stability requirements are intrinsically related to spatial resolution and sensitivity. The Observatory shall be capable to place selected observation targets on the entrance slits of the spectrometers with pointing accuracy of 0.5 arcsec. Based on required image quality performances, the full width at half maximum (FWHM) of a point source is about 1.4 arcsec at diffraction limit of 20 micrometres and the width of SMI HR slit is 1.7 arcsec. The pointing performances are defined as half cone angle errors of and around the telescope line of sight. The APE comprises the attitude estimation and control errors during the science observations, the change in telescope boresight due to thermo-elastic distortion and micro-vibration effects presented as structural errors and the residual calibration between the attitude control sensor (i.e. FGS system or star tracker) and the instrument boresight. The different contributions have been analysed and the pointing budget in Table 4-21 have been generated based on statistical interpretation and summation rules defined in ECSS standard and guidelines. The SPICA science operation profiles impose some challenging requirements on the AOCS subsystem. In particular the APE and AKE requirement drive the need for an FGS system accommodated with the science instruments on the FPIA optical bench and a high-accuracy inertial measurement unit.

The thermal effects vary over much longer time scales than those specified in the requirements, so only the attitude control errors and microvibrations are considered when computing the RPE. The attitude control errors are a combination of sensor noise and actuator noise. A preliminary AOCS simulator has been developed for SPICA using these inputs to evaluate performance against the various pointing error requirements, including the RPE. Cumulative distribution functions are produced, from which the 95% confidence level value can be extracted. To assess the contribution of reaction wheel and mechanical cooler microvibration to the RPE, a preliminary assessment has been performed. The microvibration preliminary prediction is a combination of analytical and FEM numerical simulation results, which are have been compared to previous mission performances. The truss separation mechanism (TSM) between SVM and PLM module, when deployed, acts as a suspension with attenuation factor about 100 at 15 Hz. The attenuation factor is then more or less constant after 40 Hz with no longer the typical slope of a suspension. The preliminary conclusion is that attenuation factor between 20 and 100 from the TSM can be expected for frequency above 15 Hz. Both the reaction wheel and cooler plate isolators permit to reject the mechanical disturbances further. Moreover, it has been established that the mechanical disturbance levels generated by the reaction wheels and coolers are comparable. Considering the cryocooler and reaction wheels, and accounting for uncertainties, an error of about 50 mas have been provisioned for microvibration in the pointing budget.

However, the effect of cryogenic temperatures on the higher-frequency resonance modes on the PLM side have not been considered at this point. It is understood that the Q factor considered might have to be increased above the conventional value of 100, although it is also expected that the modes excited by the RW disturbances will also have some of their path on the warm side, and thus will benefit from non-cryogenics damping ratios. Most materials except titanium have damping ratios 2 to 3 times lower. Aluminium exhibits extremely low damping ratio at 40K, up to 60 times lower than at ambient and the trend around 40 K shows increasing drop which makes extrapolation at 8 K

difficult. In complement, it has been verified that the microgravity levels at instrument interface meet the preliminary specification (i.e. 30.0 μg/Hz$^{0.5}$ between 0.1 and 400 Hz).

The preliminary analysis shows that all the Observatory pointing requirements (APE, RPE, PDE and AKE) are met with sufficient margin.

Error Source	Error Class	Half Cone Error (mas)	Error around LoS (as)	Comment
Attitude Knowledge Error (AKE)				
AOCS errors				
AOCS estimation noise	random	120.0	5.00	
Residual thermo-elastic distortion (FGS interface to FGS boresight)	bias	0.0	-	
Residual thermo-elastic distortion (STR interface to STR boresight)	bias	-	10.00	
FGS bias, spatial and systematic errors	random	100.0	-	
STR bias	random	-	5.00	
Structural errors				
Microvibration RWs	random	35.4	0.04	
Microvibration cryocoolers	random	35.4	0.04	
Microvibration HGA	random	0.0	0.00	
Residual calibration error between SI LoS and FGS/STR	bias	0.0	0.00	
Observatory errors		**206.2**	**16.18**	
Random	random	156.2	5.00	
Bias	bias	50.0	11.18	
Requirement		**250.0**	**40.00**	**Probability 99.7%, Ensemble Statistical Interpretation**
Margin		21%	147%	
Attitude Pointing Error (APE)				
AOCS errors				
AOCS control error	random	150.0	5.00	
Residual thermo-elastic distortion (FGS interface to FGS boresight)	bias	0.0	-	
Residual thermo-elastic distortion (STR interface to STR boresight)	bias	-	10.00	
FGS bias, spatial and systematic errors	bias	100.0	-	
STR bias	bias		5.00	
Structural errors				
Microvibration RWs	random	35.4	0.04	
Microvibration cryocoolers	random	35.4	0.04	
Microvibration HGA	random	0.0	0.00	
Residual calibration error between SI LoS and FGS/STR	bias	0.0	0.00	
Thermo-elastic distortion (FGS/STR interface to SI interface)	bias	0.0	0.00	
Observatory errors		**258.1**	**16.18**	
Random	random	158.1	5.00	
Bias	bias	100.0	11.18	
Requirement		**500.0**	**85.00**	**Probability 99.7%, Ensemble Statistical Interpretation**
Margin		94%	425%	
Relative Pointing Error (RPE over 20 seconds)				
AOCS errors				
AOCS control error	random	55.0	0.07	
Structural errors				
Microvibration RWs	random	35.4	0.04	
Microvibration cryocoolers	random	35.4	0.04	
Microvibration HGA	random	0.0	0.00	
Thermo-elastic distortion (FGS/STR interface to SI interface)	bias	0.0	0.00	
Observatory errors		**105.0**	**0.12**	
Random	random	55.0	0.07	
Bias	bias	50.0	0.05	
Requirement		**150.0**	**30.00**	**Probability 99.7%, Temporal Statistical Interpretation**
Margin		43%	-	

Table 4-22: SPICA Observatory pointing budget

4.6.2 Spacecraft Subsystems Overview

AOCS System

The AOCS architecture has been derived from the mission needs and constraints taking into account redundancy and FDIR considerations. The equipment used for SPICA benefits from a long heritage for such mission class, using reaction wheels, star trackers and high accuracy gyros for nominal modes. A robust initial acquisition and safe mode is ensured by a set of sun sensors and an additional coarse gyro. The Fine Guidance System (FGS) provides accurate attitude measurements, once combined with the high accuracy gyro and standard star tracker (STR), for the science observation phase. The high-accuracy gyro is also used in combination with STR, used both in LEOP and during regular operations like slews between observation targets and station-keeping manoeuvres. The star trackers are used to determine attitude information around telescope line of sight and support FGS acquisition during the science observations.

A set of four reaction wheels (RW) are used for slews and for attitude control, including during science observations. Disturbance from reaction wheels are counteracted by having a high bandwidth control law, enabled by the use of the gyro providing high frequency measurements and by limiting the reaction wheel speed excursions. In addition, the impact of micro-vibrations is minimised by using reaction wheels isolators. The reaction wheels are sized such as to allow monthly off-loading at the same time as station-keeping manoeuvres. Finally, a four axes accelerometer is used during orbit control manoeuvres to achieve both accurate delta-V realisation and a-posteriori delta-V knowledge. It should be pointed out that the accelerometer is required to achieve the level of accuracy specified, but previous missions have been operated on similar orbit at a Lagrange point without making use of accelerometers.

The Fine Guidance System (FGS) is a fine attitude determination system, which delivers at low frequency and delay a three-axis attitude measurement relative to an inertial frame by identifying the stars in the field of view, by measuring these stars locations, and by determining the corresponding attitude using an on-board reference star catalogue. The FGS would however not be capable to acquire its attitude autonomously, and information from the AOCS subsystem will be required by FGS to initiate and maintain star tracking operations. In addition to support science observation, the SMI instrument mid-infrared cameras has an FGS function, providing high performance measurement of the spacecraft pointing typically every10 seconds, as part of the AOCS system. The FGS shall be comprised of two independent channels with the necessary processing, interface, and power converter electronics packages as a single system. Each FGS channel shall be comprised at least of single detector, and its dedicated electronics and harness. In order to enable attitude determination by SMI instrument in parallel of the science operation, the camera wavelength had to be reduced from 34 to 28 micrometres, without significant impact of the science observations (TBC). The FGS shall be able to perform attitude determination over 95% of the celestial sphere and boresight angular rate lower than 0.15 arcsec/s as specified in Table 4-23.

Parameter	Across LoS (mas)	Around LoS (arsec)	Probability
FGS Noise Equivalent Angle (NEA)	110.0	30.0	99.7%
FGS Random Bias Error	50.0	7.0	99.7%

Table 4-23: FGS performance requirements

In order to produce a reference star catalogue in a mid-infrared band, a cross-match between the Gaia DR2 and allWISE catalogues is required. It permits to combine precise photometric data of allWISE in the mid-infrared with Gaia astrometric accuracy. However, the cross-match significantly reduces the number of available stars for attitude determination, as well as the removal of stars with too high astrometric accuracy errors, after the propagation of the catalogue at the correct epoch as illustrated in Figure 4-18.

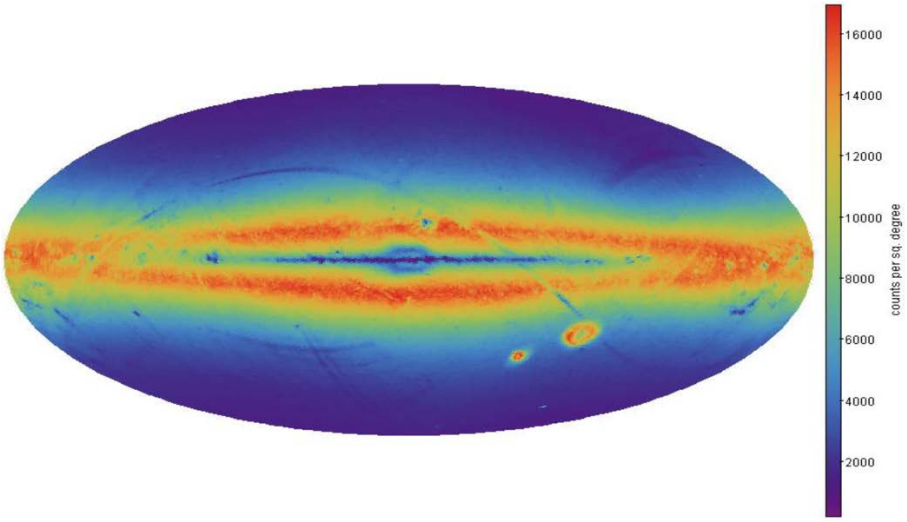

Figure 4-18: Star density map for Gaia-AllWISE cross-matched catalogue

The minimum and maximum detection magnitudes for integration time of 10 seconds and different celestial regions are obtained from the preliminary estimates of the sensitivity for the FGS. It permits to establish the cumulative star density of sources that could be tracked by the instrument around the North Galactic Pole (NGP) region. Assuming the stars distribution follows a Poisson distribution (with the average number of stars per FOV deduced from the density), the sky coverages presented in Figure 4-19 can be achieved at NGP depending on the minimum number of stars required per FoV.

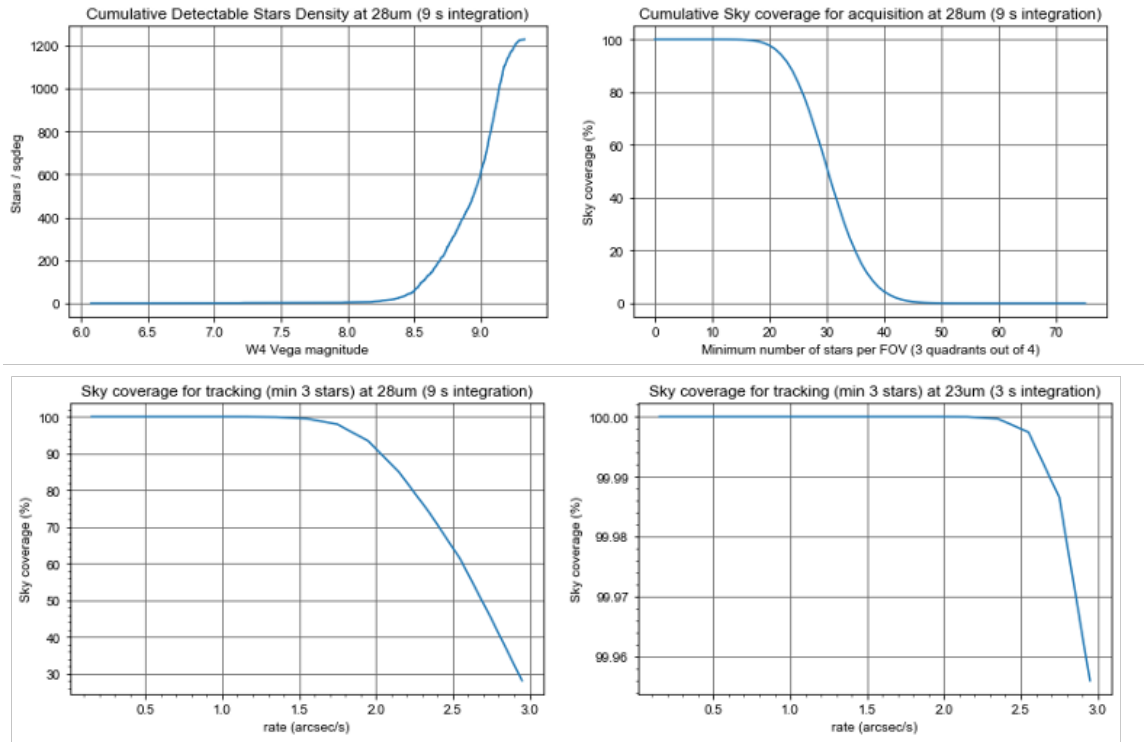

Figure 4-19: Cumulative star density relative to AllWISE W4 magnitude and sky coverage at NGP

The FGS centroid error has been calculated for the inertial pointing and when the PSFs are moved across the detector. The minimum number of stars over the FOV is derived to ensure the specified 95% sky coverage performance. It corresponds to an average of 7 tracked stars at NGP region. The background noise is considered as the mean value of the noise per pixel. The detector non-uniformity parameters are derived from the Si:Sb detector technology baseline for SMI instrument camera and have been considered negligible for the preliminary analysis. The standard deviation of the time-random part of the centroid error is calculated in Figure 4-20.

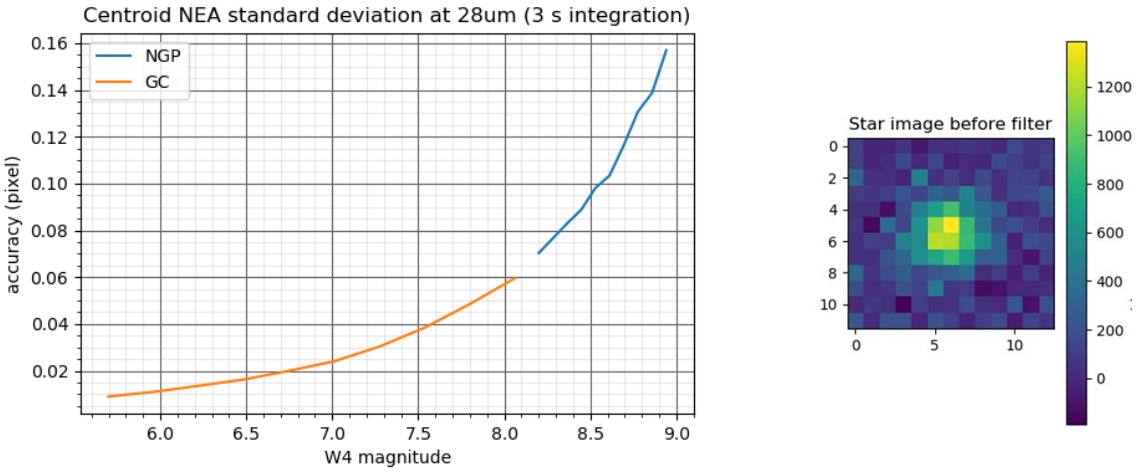

Figure 4-20: FGS centroid error and point source detector image

The preliminary analyses established the design feasibility of the FGS and its capability to meet the performance requirements, in particular in terms of sky coverage and attitude measurement accuracy. These analyses lead to a minimum integration time of 3.0 seconds for the FGS baseline configuration with a wavelength band at 28 µm, enabling to satisfy both the sky coverage and attitude AKE performances with a total transverse error of 150 mas total error, at 99.7% confidence level. However, in order to ensure comfortable performance margins, the FGS is operated by AOCS with a sampling period of 10 seconds, which lead to an attitude total accuracy of 60 mas. It corresponds to more than 150% margin relative to the transverse error specification. In order to be conservative, the maximum angular rate that can be tolerated from sky coverage performance perspective, with at least 3 stars tracked at NGP, is based on the estimated minimum achievable integration time, leading to a maximum angular rate of 0.4 arcsec/s for the baseline at 28 µm.

Propulsion System

The propulsion architecture has been derived from the mission needs and constraints taking into account redundancy and FDIR considerations. The equipment used for SPICA depends very much on the implementation solution.

In parallel, two alternative solutions have been explored: a) a hydrazine mono-propellant system, or b) an MMH/MON bi-propellant system. The mono-propellant system uses dedicated thrusters for orbit and attitude control, and two equatorial-mounted tanks. The orbit control is provided by a torque-free 2+2 20N redundant thrusters configuration, and the attitude control is provided by a force-free 6+6 5N redundant thrusters configuration. The bi-propellant system provides both, orbit and attitude control, with one single 6+6 10N redundant thrusters configuration and four polar-mounted tanks.

Both configurations have been defined such that thrust direction is always away from PLM, to minimise risk of contamination, while allowing thrusting in Sun and anti-Sun directions and ensuring all delta-V manoeuvres could be executed without any additional delta-V bias penalty. But in consequence, neither of them achieves fully spherical thrust capabilities.

Propellant estimate accounts for full mission, i.e. nominal plus extended, lifetime needs and the following efficiency factors: a) bias penalty in case anti-Sun thrust needs to be limited, b) geometry penalty due to non-spherical thrust capabilities, and c) thrust level transient penalty due to non-ideal thrusting profiles.

Electrical Power System

The electrical power architecture has been derived from the Observatory power demand through all mission phases derived from mission needs and constraints, and taking into account redundancy and FDIR considerations. The equipment used for SPICA benefits from a long heritage using for the deployable solar array, the battery, and conditioning and distribution units well established technologies including AZUR 3G30C solar cells and ABSL 18650 NL battery cells.

The solar array is locked after deployment at a position optimised for the full Observatory pointing range required during the operational life, and has been sized to cover all power needs up to EoL under the assumption of 1 string failure. Therefore, no operational constraints are derived from the solar array design. Due to this, the battery is used only during the early phases of the mission, from umbilical disconnections through launch and separation until end of Sun acquisition manoeuvre and solar array deployment. Since solar array is permanently Sun illuminated under very stable conditions, Direct Energy Transfer (DET) topology at 28V has been baselined for SPICA. Two alternative solutions have been explored to achieve bus voltage stability: a) to regulate the bus using directly the battery tapering voltage at a given state of charge, or b) to use a Battery Charge and Discharge Regulator to fully regulate the bus independently of the battery state of charge.

Communications System

The communication architecture has been derived from the mission needs and constraints taking into account redundancy and FDIR considerations, and it is based on a conventional dual band solution comparable to that of similar missions. X-band has been baselined for telecommands uplink and housekeeping telemetry downlink, allowing respectively from 4 up to 16 kbps and from 2 up to 26 kbps. Ka-band has been baselined for science data downlink, allowing up to 72 Mbps. The equipment selected for SPICA include two sets of redundant X-band transponders, amplifiers and hemispherical low gain antennas, all cross coupled providing fully redundant omnidirectional coverage, and two redundant K-band modulators and amplifiers cross coupled with one steerable high gain antenna (39.2 dB, and up to 0.7 m diameter), covering maximum Earth excursions from L2 orbit for any spacecraft attitude, therefore not requiring any slew for downlink slots.

Both bands are used during operational modes of the spacecraft, while X-band is also used during LEOP and contingency situations.

In parallel, two alternative solutions have been explored to ensure the maximum required housekeeping telemetry rate: a) the addition to the X-band channel of a steerable medium gain antenna, co-located with the high gain antenna, or b) the use of the Ka-band channel to downlink housekeeping telemetry during operational modes with the X-band channel performance limited to 4 kbps during contingency situations.

4.6.3 Observatory Development

The SPICA baseline mission design emphasized use of high TRL technologies wherever possible. As a result, the enabling technology requirements can be very simply stated as cryogenic mechanism used for the in-orbit alignment and focus of the telescope, mechanical cryocoolers and detectors (Table 4-24). The enabling technologies for instrument detector are addressed in section 5.

	Elements	Status	2020	2021	2022 TRL5	2023 EM	2024 TRL6	Comments and Recommendations
Cryogenic System	Extended Heat Exchanger	TRL5	Cooling performance verified by BBM test	→	Characterization elements in relevant environment	Integration element model	Demonstration element performances in relevant environment	- JT cold tip and compressor separated by straight heat exchanger of 4.5 m. Exchanger protected by JT pipe shield. - Parameters dependence will be verified by EM test
	Electronics 1K JT Cooler	TRL3	BBM Electronics manufactured	BBM Env. Testing				- Concept equivalent for 1K electronics but higher number of boards. - Electronics 4K and ST coolers flight qualified (Hitomi).
	2ST Cooler Compressor	TRL4	BBM compressor with flexure bearing evaluated	→				- Increase lifetime to 5 years - It requires change of supports in the compressor from linear ball-bearing to flexure bearing. - ST upgrade to be implemented under JAXA "Technology Front-Loading Program" (TBC)
Mechanisms	PLM Truss Separation Mechanism	TRL4	- Stiffness and modal performances verified by BBM mechanical test - Thermal insulation performance to be verified by TM test	→				Conceptual design study completed by selection of separation spring and CFRP pipe for thermal insulation
	MCS Vibrations Control System	TRL4	- Isolator BBM manufactured - Damping performance to be verified by isolator EM test	- Modal performance and damping of cooler plate with passive damping verified by EM test - Hold-down and Release Mechanism (HDRM) EM manufactured and tested				- Passive vibration isolation systems to reduce the MCS microvibration transmissibility from cooler plate to PLM and SVM - Isolation system with metal-type isolators (XRISM)
	PLM Sunshield Deployment Mechanism	TRL3	TBD →	→				- Shield material and structure development TBD
	PLM Flexible Blades Shields Attachment	TRL3	TBD →	→				- Ensure conductance and structural attachment between PLM main truss and SVM shields - Mechanism to be operated in cryogenic conditions
	ITA Secondary Mirror Mechanism	TRL5	- Performances verified by EQM test and to evaluated at 20K in 09/20 - Predevelopment effort identified: Cryo performance by BBM test, including representative cryoharness	→				- Refocus mechanism for a relatively large secondary mirror (more than 9kg), large range (+/- 500 µm) and low-resolution requirements (less than 2µm) - Mechanism to be operated in cryogenic conditions - HDRM to withstand loads at launch (TBC)

Table 4-24: SPICA technologies developments

4.6.3.1 Enabling technologies for cryogenic refocus mechanism

The M2M mechanism development activities have been put in place to de-risk procurement and specific requirements have been derived from the SPICA baseline mission:

- The mechanism shall be operated at cryogenic temperature below typically 8K, which constrains the material choices, increase the thermos-elastic deformation impacts, and inherently would increase the validation complexity.
- The mechanism shall translate and rotate a relatively large and heavy secondary mirror (i.e. 576 mm diameter, 8.4 kg mobile mass) when compared to precedent project like Euclid telescope with a secondary mirror of about 3.0 kilograms.
- The large range of motion (i.e. +/- 500 µm) and rather low-resolution requirements (< 2µm).

Due to the large diameter of the mirror of about 600mm the mirror is mounted on a barrel. An isostatic mount between the M2 mirror and the barrel is ensured using bipods. The M2MM interfaces with the barrel. This configuration leads to a detrimental distance between the M2 mirror centre of mass and the mechanism interface plane at barrel level. This leads to a distance from mechanism interface to mirror CoM of about 120 mm. Combined with the lateral acceleration, it has been identified that this configuration generates high radial and bending loads in the actuators plus some axial load. Potential use of locking devices could be foreseen which would add a lot of complexity. Different solutions were

trade in phase A and it was established following preliminary tolerance analysis that a 3 degree-of-freedom mechanism was the preferred architecture for SPICA mission.

Two potential European suppliers have an important heritage on M2M mechanisms in cold environment. They both propose a linear actuator concept, which can be adapted for SPICA requirements. They would support the major re-definition needed to cope with the colder temperature, the increased actuation range and the much larger mirror to support. The output of this activity is, for each potential supplier, a proposal for the TDA allowing reaching TRL6 by the end of Phase B1. One supplier has developed concepts and technologies based on the generic cryogenic M2M mechanism, originally targeted to the Echo, and then modified to ARIEL requirements. The design seems close to satisfy SPICA requirements with small modifications. Indeed the "Nano-strut" actuator already satisfies the stroke requirement and its design was made to be operational under a 5K environment. The other potential supplier has also developed for Gaia and Euclid telescopes, a M2M able to operate in cryogenic condition at around 100 K. The proposed approach would be to adapt the actuators by upscaling it to satisfy the requirements (heavier mirror and larger stroke), and to identify the material and elements that must be changed to satisfy the 8K environment.

4.6.3.2 Enabling technologies for mechanical coolers

The 4K-JT and 2ST cooler reached TRL 8 after the launch of the Japanese X-ray observatory Hitomi flight model. Then, the 1K-JT obtained TRL 5 after the environmental test using an engineering model. The 4K-JT lifetime test model achieved more than 5-year continuous operation in 2019. The result is helpful to investigate the aging effect, and the effect is represented as an incrementation of the power input from the beginning of the life state to keep a constant cooling power. The lifetime test of 1K-JT engineering model also began at May 2015. In this section, the critical items to satisfy the MCS requirements are described.

The thermal interface between JT coolers and the 50mK hybrid cooler

The thermal interface between the 50mK hybrid cooler (a combination of 300 mK sorption cooler and 50 mK single stage adiabatic demagnetization refrigerator) and 4K-JT and 1K-JT coolers is one of most critical point in the cooler system. In particular, the additional heat load from the sorption cooler must be rejected into JT coolers during the hybrid cooler recycling phase.

The detector cooling demonstration campaign from 300 K to 50 mK was started in 2016, under the framework of the ESA's Core Technology Program (CTP) for the X-ray Integral Field Unit (X-IFU) of the ESA X-ray astronomical mission ATHENA. As the intermediated step in the CTP, a 300K – 50mK cooling chain demonstration called "cryostat1" with the dedicated cryostat in France (CEA Grenoble) was planned and space-qualified mechanical coolers were coupled. The cryostat1 test was originally for Athena X-IFU, but this demonstration was also good opportunity to verify the SPICA thermal interface between the JT coolers and the hybrid cooler. In the cryostat1 test, the engineering models of the 4K-JT with the 2ST precooler and the 1K-JT were integrated with the 50 mK hybrid cooler and the 15K-class pulse tube cooler (PT15K) developed by ESA / CEA / Air Liquide / Thales Alenia Space. The cooling performance with the same interface condition to that for SPICA between the JT coolers and the hybrid cooler was demonstrated. Figure 2 shows the typical temperature behaviours of the 4K-JT and 1K-JT thermal interface during the hybrid cooler recycling. Both JT coolers were successfully operated with the proposed interface conditions and the temperature of 50 mK was successfully achieved. Any piston collisions in the compressors or dry-out of the working gas at the JT cold tip were not detected. This is a big milestone to demonstrate the high feasibility of SPICA MCS.

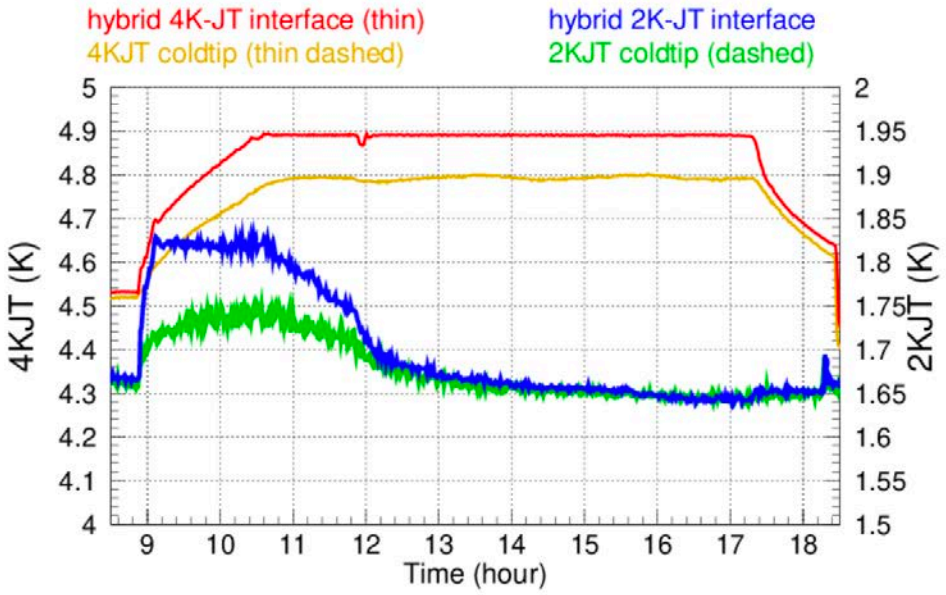

Figure 4-21: Interface temperature during the hybrid cooler recycling test in the cryostat1

A straight and longer heat exchanger

In SPICA, the cold tips of 4K-JT and 1K-JT are located on FPIA to cool the SIA, while compressors and coldheads are mounted on the cooler plate of the SVM. The heat exchangers of these JT coolers are divided into three temperature regions, the 1st heat exchanger (HEX1) between the compressors and 2ST 1st stage interface at around 100K, the 2nd heat exchanger (HEX2) between 2ST 1st stage and 2nd stage at around 18K, and the 3rd heat exchanger (HEX3) between the 2ST 2nd stage and the cold tip as shown in Figure 4-22 left. In SPICA, new HEX3 design for straight and longer length must be considered, while HEX1, HEX2 and 2ST coldhead design should be the same as the original design. In the payload module study, it is found that the required length of the HEX3 is 4.5 m at maximum, while the length is 1.65 m in the original design. Hence, the performance verification of the unique HEX3 design is needed.

Figure 4-22 right shows the schematic drawing of the JT coolers with the straight HEX3 and the thermal environment to be studied around the heat exchangers. As the baseline design, the straight HEX3 is surrounded by the JT pipe shield and the shield temperature is designed to be about 30 ~ 40 K by connecting the telescope shield to reduce the thermal radiation from the intermediated temperature stage (30 ~ 273 K). The thermally insulated mechanical supports are needed between the JT pipe shield and HEX3 in the mechanical design, and these head loads from the JT pipe shield must be managed in the total heat load budget of each JT stage. The pipeline routing of the HEX3 depends on the location of the JT cold tip and the 2ST cold head, the thermal and mechanical design of the JT pipe shield and the assembly sequence.

The use of the high purity metal thermal strap with the original HEX3 design is proposed for each JT stage interface in FPIA as the fallback design. However, higher mass (a few kg instead of a few hundred g for HEX3) is needed to provide the thermal conductance for satisfying the required temperature at the cold tips. This brings a larger parasitic heat from the JT pipe shield supports, since more mechanical supports are needed. Hence, the straight and longer HEX3 is one of most critical items in the mechanical cooler development for SPICA.

In the straight HEX3 demonstration test, three different length of the HEX3 test models (1.65 m, 3 m and 4.5 m) were fabricated to measure the dependence of the heat exchanger length in the cooling performance. The original design (1.65 m length and toroidal shaped HEX3) was also measured as a reference. Table 4-25 shows the performance test results of the HEX3 demonstration test model for both 4K-JT and 1K-JT. As expected, the cooling performance with the 1.65 m length could not satisfy the specification, because the heat-exchange efficiency obtained by 1.65 m is low in a straight shape. The specified cooling power of 40 mW was successfully obtained with the length of 3 m and 4.5 m, and

the measured outlet pressure and the flow rate were acceptable since both parameters can be obtained by the 4K-JT lifetime test model after 5 years operation. In the 1K-JT case, the cooling power of 12.5 mW at 2.5 K with 4He was verified, because the cooling power of 12.5 mW at 2.5 K with 4He corresponds to 10 mW at 1.7 K with 3He in the compressor design. The test model satisfied the cooling power of 12.5 mW and the measured outlet pressure was almost consistent with the 1K-JT lifetime model after 3 years operation. On the basis of the results, it is needed to perform the detailed study of the location of the cold tips, the HEX3 pipeline routing, and the JT pipe shield and supports prior to the development of the payload module structural thermal model.

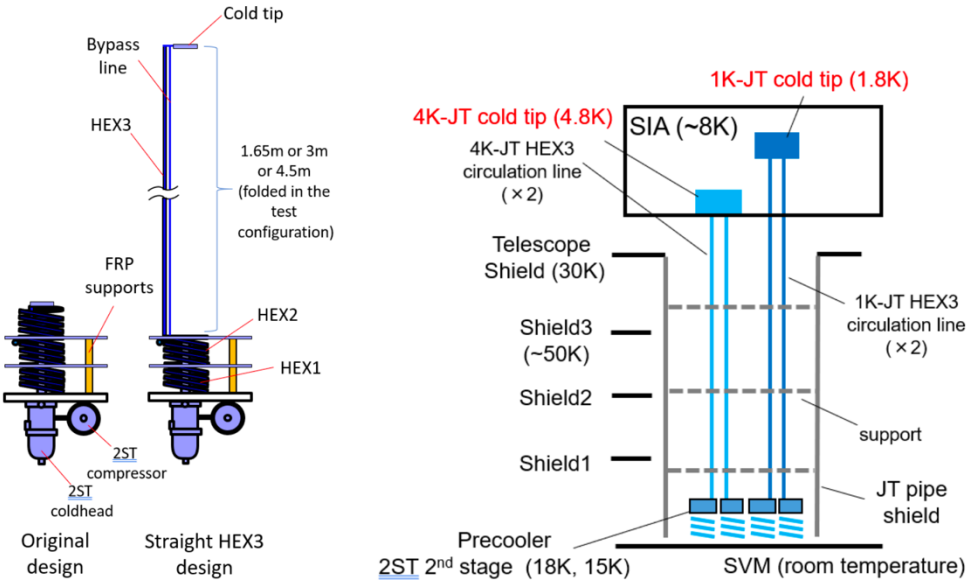

Figure 4-22: Schematic drawing of the JT cooler with HEX3 design

Cooler	Heat input	JT cold tip	2ST second stage	JT driving power
4K-JT (4.5 m)	40 mW	4.4 K	18.6 K	64 W
4K-JT (3 m)	40 mW	4.48 K	17.8 K	71 W
1K-JT (4.5m, ^{4}He)	12.5 mW	2.5 K	15.4 K	58 W
1K-JT (3m, ^{4}He)	12.5 mW	2.46 K	15.0 K	52 W

Table 4-25: Main test results of the straight HEX3 demonstration test model

Required lifetime of mechanical coolers

Currently, the required lifetime of mechanical coolers is 5 years, while it was 3 years in the payload module conceptual study until 2018. To meet the lifetime requirement, the upgrade of the 2ST compressor is desired, while the lifetime tests of the mechanical cooler engineering models are being performed.

The cooling performance degradation of the mechanical coolers is mainly caused by impurities in the working gas and the mechanical wear of the moving parts, and a lifetime verification is needed in the engineering model development. Then, the JT cooler can satisfy the lifetime requirement without any design change, because JT coolers can be designed with the lifetime of 5 years as the specification. Additionally, the 4K-JT lifetime test model has already achieved 5 years continuous operation with about half of the total cooling power (22 mW) which is almost same cooling power in nominal operation of SPICA MCS.

On the other hand, the 2ST lifetime is the most critical for the 5 years operation, because the current 2ST cooler, which has the heritage of Hitomi / SXS, has been developed with a specified lifetime of 3 years. One of the major concerns of

the 2ST cooler lifetime is the performance change of the compressor due to the wear of the clearance seal between the pistons and cylinders. As a demonstration to solve the problem, the linear ball bearing was replaced with flexure bearing supports and the upgraded 2ST compressor test model obtained the same cooling performance to the original 2ST cooler. However, another possible concern, the clearance seal wear in the displacer must be also considered. This is still under study and the strategy to solve the problem, if needed, with the displacer is to be studied in the next phase.

Higher cooling power for 1K-JT stage

In recent study of the FPIA thermal design, the cooling power requirements on the 1K-JT cooler is more demanding than current specification of the cooler. Since the 1K-JT coolers have already been completed the engineering development and the lifetime test is being continued, several possibilities to increase the 1K-JT cooling power without changing the hardware of the mechanical coolers proposed in Table 4-26 are discussed.

Most reliable solution is to operate the compressor and the coldhead of the 2ST cooler at lower interface temperature on the cooler plate. When the interface temperature is 15 K lower, the 2ST 2nd stage temperature becomes 2.2K lower with same cooling power. Then, the 1K-JT cooling power can be 3.3 mW higher with lower precooling temperature. Table 3 shows the summary to solve the item. Of course, the thermal design to provide lower interface temperature on the cooler plate must be also needed.

	Original design	1K-JT for SPICA
1K-JT cooling power	10mW at 1.7K	13.3mW at 1.7K
Precooling temperature (2ST 2nd stage)	15K as a maximum	12.8K as a maximum
1K-JT nominal driving power (EOL)	72W	72W
2ST nominal driving power (EOL)	75W	75W
Operating temperature of 1K-JT compressors	0 degC to +30 degC	0 degC to +30 degC
Operating temperature of 2ST compressors and coldheads	-70 degC to +30 degC	-70 degC to +15 degC

Table 4-26: Summary of the 1K-JT cooler parameters proposed for the nominal case at EOL

It has to be noted that this increase of cooling power of 13.3 mW for the 1K-JT is guaranteed for the nominal case but not for the contingency case. In the case of the one-cooler failure, a cooling power of 12.0 mW is expected.

The 1K-JT driver electronics development

The 1K-JT driver electronics has no flight heritage, while the driver electronics for the 2ST and the 4K-JT coolers have flight heritages of the Hitomi observatory. Though the main concept of the driver electronics for the 1K-JT is the same as the electronics for the 4K-JT coolers, several parameters, particularly the number of driving channels, are different from those for the 4K-JT coolers. Hence, the 1K-JT driver electronics is still at low TRL and is needed to be developed in the early phase of SPICA.

The most primary one is the design to drive the 4 compressors of the 1K-JT coolers. Since the number of boards increases, the mass and volume of the electronics box is larger than the box for the 4K-JT cooler electronics. Additionally, the number of driving channels are 8 for operating the two pistons independently in each compressor for the active vibration reduction control. The thermomechanical design with much number of driving channels must be also considered. The second issue is to design for the primary power of 28 V. Thirdly, the inlet pressure to be measured for the 1K-JT is about 7 kPa, which is about 1/15 of the inlet pressure designed in the 4K-JT. In the study, the electrical circuit is assumed to be almost the same design as that for the 4K-JT coolers. The drive frequency is 52 Hz, while it can be changed between 40 and 60 Hz.

In the Bread Board Model (BBM) development, all the 4 boards have already been fabricated, and the electrical functional test using the Electrical Ground Support Equipment (EGSE) is planned.

4.6.4 Integration and Test

This section describes the element and Observatory level Assembly, Integration and Test (AIT) program for the SPICA baseline concept. The test flow implemented at each level of assembly is discussed as well as the separation of thermal vacuum testing between the hot and cold zones of the Observatory. The SPICA element level AIT consists mainly of the PLM and the SVM. All the instruments are delivered to system AIT fully qualified and calibrated. The summary level AIT flow is shown in Figure 4-23. Each of these phases is further detailed in the subsequent sections below.

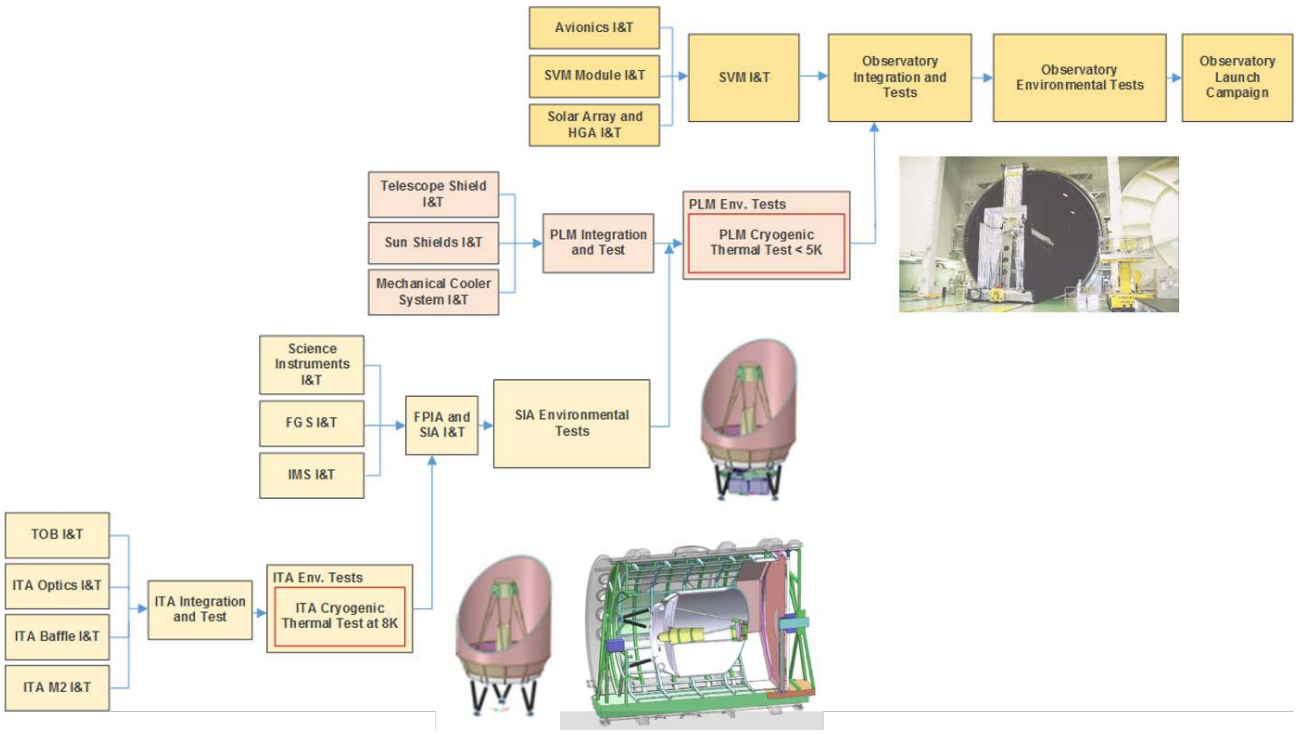

Figure 4-23: SPICA Observatory integration and test flow

Science Instrument Assembly Integration and Test

All telescope optical components, Primary Mirror (PM), Secondary Mirror (SM) are individually tested, including transmittance, surface roughness, wave front errors, polarization and coefficients of thermal expansion. PM mechanism and its electronics are qualified at unit level prior to telescope integration.

Ground testing at the ITA and FPIA element level is designed to:

- Verify telescope alignment at ambient temperature: Alignment of PM relative to TOB, SM relative to PM, telescope focus position, field curvature and WFE.
- Verify SM refocus mechanism and electronics compatibility with the harness and SVM systems. M2M functional and performance verification during thermal test.
- Characterize alignment, wavefront and thermal performances at operational temperature.
- Characterize wavefront performance and defocus stability for model validation
- Correlate PM refocus mechanism tilt and translation correction to M2M level test results
- Verify science instruments alignment with the ISM structure
- Verify science instruments compatibility with the cryoharness system, CDH, PCDU, FSW
- Verify science instruments compatibility with the FGS
- Characterize FPIA thermal performance stability for model validation
- Correlate science instruments and FGS performance in FPIA to instrument-level test results
- Verify workmanship for flight environment down to 8 K and measure mass properties

In order to conduct the telescope alignment and to establish a reference for the cool-down test, the infrared telescope wavefront error (WFE) will be measured at ambient conditions. The effect of gravity on the alignment performance needs to be mitigated. For this test, the optical axis of the telescope will be aligned orthogonally to the gravity vector. The preferred approach is to set the telescope axis horizontal to minimise mirror deformations under gravity, and to perform +/-1g measurements by 180° rotation of the ITA as illustrated in Figure 4-24. A stitching system is combined with a Hartmann measurement. The stitching system will deliver a full pupil characterization of the telescope while the Hartmann measurement will deliver relative WFE variation.

The WFE at ambient is to be measured and optimized through the hereunder scheme:

1. The WFE for a perfectly aligned telescope at ambient is predicted by analysis. It includes the Surface Figure Error (SFE) map of the optical components measured by the supplier, and the estimated gravity effect in horizontal configuration.
2. Before optical alignment, a full pupil measurement is done by the stitching method. It provides the initial WFE before alignment. The difference between the predictions and the measured value is due to the optical misalignment.
3. The Hartmann reference test is con: ducted, i.e. the sub pupil mirrors image at the focal plane level is characterized.
4. The unitary motions of the secondary mirror are performed. After each motion, a Hartmann measurement is made. The movement of the spots at focal plane level between reference and new measurement delivers the variation of WFE for each unitary motion.
5. Thanks to the previously acquired WFE sensitivity to secondary mirror unitary motions, the secondary mirror movement to be done to align the telescope is computed, based on differential WFE previously measured. The secondary mirror is aligned thanks to this computation
6. A Hartmann measurement is performed to validate the relative WFE variation
7. A stitching measurement is performed to validate the optical alignment.

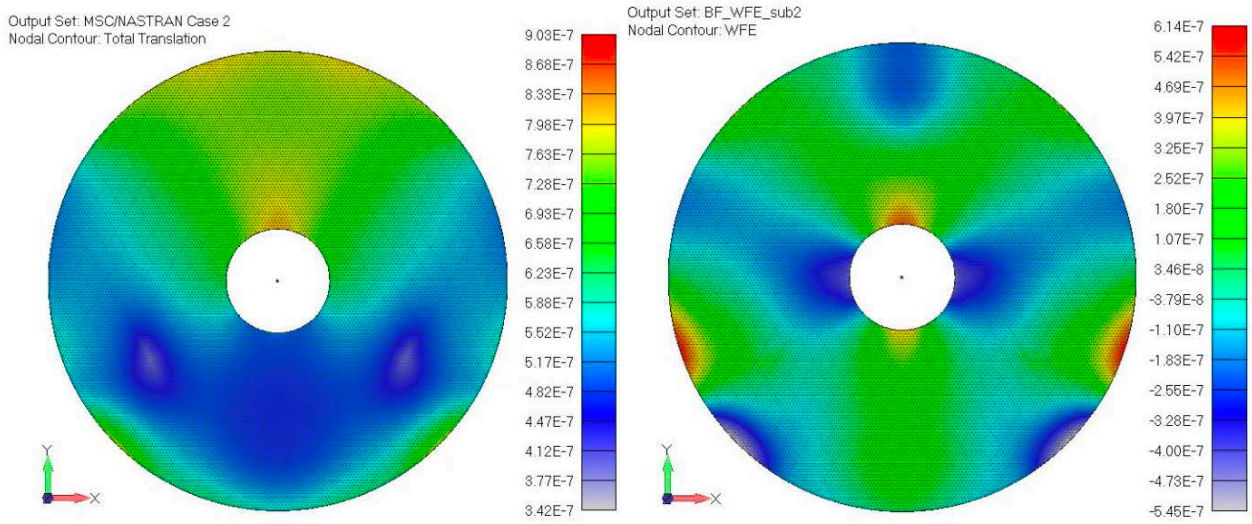

Figure 4-24: Total translation and WFE total with best focus correction in meter

The test will be complemented still at ambient condition by the measurement of the focal point location relative to ITA mechanical reference frame and the characterization of the focal plane curvature.

The measurement of telescope WFE will be repeated at the operational temperature of 8 K. Testing at the actual operational temperature will permit an experimentally verified evaluation of the ITA behaviour which is not exclusively reliant on extrapolation, and which therefore lowers the overall risk for in-flight performance predictions. The

preliminary discussions with the Centre Spatial de Liège (CSL) confirmed the validity of the proposed approach at the cost of a small increase in the cool-down duration, as thermal capacity is very low below 50K. The verification of ITA WFE performance at 8 K is considered paramount and will considerably reduce risk on PLM integration and test activities. The allocated error budget for the WFE error measurement at 8 K is 150nm rms. The thermal shrouds surrounding the ITA will be cooled to 20K. The ITA will be cooled to 8K using dedicated GSE thermal straps connected to a He liquefier.

The Hartmann measurement technique is the selected baseline for the test at operational conditions. It has the main advantages of having a low development risk (Herschel telescope heritage), and can deliver quick measurements. Nonetheless, it will only deliver partial WFE measurement, where the telescope full aperture is only sub-sampled at low spatial frequency. Moreover, material behaviour from 293 K to 8 K is not fully mastered and a rather high uncertainty could affect the capacity of the Hartmann system to measure the infrared telescope performances, especially if there are unanticipated crygenicaly induced mid and high spatial frequency error components. As an option, a stitching measurement method has also been investigated, as a possible backup option. Stitching is in any case baselined for the full aperture ambient tests.

The focus axial location will be characterized at 8 K during the TVAC campaign. Its principle is identical to the measurement at ambient. It relies on actuation of the M2M in order to find the minimum focus location. The Hartmann approach is preferred for measuring the defocus at 8 K. Indeed, a significant bias on focus location could be induced by the bending of the Autocollimation (AC) flat(s), due to cool-down and thermal gradient effects.

In parallel to the ITA sequence, CFIs are integrated and aligned on the FPIA, before coupling and alignment with ITA. The challenge is to obtain from the CFI teams their alignment cosines at ambient which can ensure the correct alignment at operational temperature. The need for a dedicated thermal vacuum test to verify SIA optical alignment at operational temperature has not been identified in Phase A. The SIA AIT flow follows the final test sequence, including electrical, functional and mechanical tests, before delivery for integration on the PLM.

No end-to-end validation of the SIA or ITA polarisation performance is currently anticipated. The polarisation performance will be validated by analysis and model correlation with measurements on samples coated alongside the telescope mirrors. Through these sensitivity analyses, it shall be demonstrated that the ITA Mueller matrix is within the range allocated for the B-BOP instrument.

The polarization knowledge error induced by ITA is not expected to be critical either. However, it shall be noted that the two following points were not studied during phase A:

- The impact of polarized straylight could contribute to the polarization error budget.
- The polarization in PSF side lobes could introduce a bias in the measurements

ITA and FPIA PFM assemblies are subsequently delivered to PLM level AIV. ITA PFM model is considered fully qualified before delivery. The SPICA SIA model philosophy supports an efficient development approach including:

- The SIA mechanical and thermal models to be delivered to PLM authority for early verification and validation of the interfaces.
- For such purposes, the mechanical model is comprised of a metallic dummy structure assembly representative of the SIA in mass, mechanical interfaces, center of gravity and first Eigen mode frequency. Based on the lessons learned from previous programmes like Euclid, this has the major advantage of decoupling telescope and PLM developments. The SIA thermal model is a dummy load with representative thermal capacitance and conductive interfaces with CRYO. It would comprise an external baffle and thermal hardware for supporting test at PLM level. A full SIA STM is therefore not considered necessary due to the proposed technical definition and the associated flight heritage. This approach has the major advantage to reduce the number of SiC structures to be manufactured and procured, with no STM required in the development. This has direct heritage from and is similar to the GAIA PLM development. Mechanical qualification is done on then on the SM which is subsequently refurbished as PFM with other flight items.
- The M2M engineering model (EM) and structural model. It allows incremental risk mitigation and performance verification that secure the flight model performance and delivery schedule.

- The SIA PFM model is used for the assembly design qualification. But the final thermal vacuum test is performed after integration with PLM module. The full qualification is therefore established at PLM level.

PLM Integration and Test

The PLM AIV flow includes the integration of SIA with CRYO, and the verification of CRYO itself and its interfaces with SIA and SVM. The most important objective of PLM AIV campaigns is to demonstrate the cryogenic performance of PLM, including the compliance of the cooling chain with the specifications. The main objectives of PLM verification programme are therefore:

1. Verify the cryogenic thermal design of PLM including TIRCS and MCS: Firstly, it will be demonstrated that the cooling of the Telescope Shield from warm temperature to the required temperature (30K) is feasible by the combination of active cooling of 2ST coolers and passive cooling by the Outer/Inner Sunshields and SVM Shields in Thermal Insulation and Radiative Cooling System (TIRCS). The Telescope Shield provides the thermal interface boundary condition for SIA. However, the tests alone do not directly verify that SIA is cooled down to the specified temperature. It will be then be demonstrated by analysis with correlated thermal models that the cooling performance meet specification in order to operate SIA below 8 K. Secondly, it will be demonstrated that SIA can be cooled down from warm temperature to the specified temperature by the combination of active cooling by 2ST and 4K-JT coolers and passive cooling by the sunshields and SVM shields in TIRCS. Due to the limited capability of the test facilities, the achievable temperature of SIA in the test campaign is different (higher) from that required in orbit. Therefore, SIA temperature achieved in orbit will be again verified by the analysis combining the test results and the thermal mathematical model. The cooling performance of the 1K-JT and 4K-JT coolers is also evaluated.
2. Verify the functions of Focal Plane Instruments (FPIs) on the PLM at cryogenic temperature: The performance of FPI shall be tested at each FPI and the FPIA levels. Only limited performance evaluations are expected to be made in this test with the constraints of much higher background conditions and possibly higher temperatures of detectors than those in orbit. The mutual electrical interference among the FPIs is to be checked during this test campaign.

Ground testing at the PLM element level is more generally designed to:

- Verify ITA and FPIA alignment with the PLM structure
- Verify FPIA compatibility with the cryoharness system, CDH, PCDU, FSW.
- Verify CRYO compatibility with the cryoharness system, CDH, PCDU, FSW.
- Verify PLM design performance relative to EMC
- Verify the workmanship of ITA and FPIA at cryogenic operational temperature
- Verify TIRCS thermal performance below 70 K
- Verify PLM thermal performance at cryogenic operational temperature
- Characterize duration of the cool-down and decontamination sequences
- Verify SIs and FGS heat loads and thermal performance verification at cryogenic operational temperature
- Verify compatibility of PLM performance with instrument operations at cryogenic operational temperature (i.e. annealing, recycling)
- Characterize PLM mechanical and thermal performance stability for model validation
- Correlate instrument performance and FGS in PLM to instrument-level test results
- Verify TSM and HDRM mechanisms compatibility with the harness system, CDH, PCDU, FSW
- Verify TIRCS deployment
- Verify workmanship for flight environment and measure mass properties

In both STM and PFM campaigns, the tests are performed under gravity condition. Therefore, the truss separation mechanism, which does not provide sufficient structural stiffness is replaced by an MGSE supporting component. For the thermal test campaigns, one of the critical issues is the control of the possible radiation heat leak in the test chamber. JAXA plan to reduce radiative heat leaks with dedicated GSE double-foldable shields enclosing the PLM. Although the Tsukuba Chamber is the baseline test facility for SPICA, the testability at CSL in Belgium has been investigated by JAXA as a possible backup option. A preliminary thermal model analysis of the CSL chamber showed that the maximum heat loads to the 2ST cryocooler for TS is 320 mW and those to the 4K-JT cryocooler for SIA is about 45 mW. It was then concluded that the excess heat loads could be control to levels that do not affect significantly the test results.

A full aperture optical test cannot be performed, because a star simulator inside the Tsukuba chamber with a 2.5-m diameter collimated beam is unrealistically large. However, an optical test can be performed based on an autocollimation flat mirror with sub-aperture size and photometric measurements made with SMI instrument. It would permit characterization of the optical alignment between ITA and FPIA after integration, and would be performed by operations of SMI instruments during the cryogenic test. SMI would integrate an infrared light source on an area of 1'x12' at either end of the SMI/LR slit mirror which is on the focal plane. No impact on in-orbit SMI observations is foreseen since direct light from the source illuminates the dark region of SMI camera, which is not nominally used for science observations. However, the wires coming from the infrared light source should be cut before launch to avoid an additional heat load. The radiation from this infrared light source will go out through ITA and will be reflected back via the autocollimation flat mirror in front of the telescope. The flat mirror with cryogenic actuators should have a diameter of about 30 cm. To monitor the alignment with the telescope optical axis during a cooling down, a target mirror will be put on ITA. The optical configuration will make an auto-collimation. Two images will be obtained simultaneously by direct and returned light of the light source by SMI instrument. The returned light path will be adjustable by the focus and tip-tilt functions of the telescope secondary mirror.

The PLM verification approach includes an STM and PFM development models. PLM FM model is subsequently delivered to Observatory level AIV, as a flight qualified element.

SVM and Observatory Integration and Test

A standard PFM approach is proposed for SVM verification. The avionics and PLM warm units Engineering Models would be validated on the avionics validation bench. The central software requirements are also derived at System level and verified on high fidelity simulators (NSVF) and validated with hardware in the loop on AVM. The AVM integrates all EM/EQM electrical hardware (including PLM warm units) on to representative test bench. Integration, SPT, ISST, mission scenario test sequences are developed here ready for use on the Observatory FM. Platform interfaces with the payload are also exercised. Central Software is validated in a hardware environment and FDIR behaviour is exercised. AOCS closed loop reference tests and the important FGS behaviour are tested. Advanced Conducted emission tests are also performed as early risk mitigation. The PLM PFM model is integrated under the responsibility of the Prime contractor, in collaboration with the PLM team. The Observatory is subject to functional testing as part of the system level activities to ensure the integrity of the payload. Some key activities include alignment and stability and EMC compatibility. The Observatory FM would then go through final validation campaign

Ground testing at the Observatory level is designed to:

- Verify PLM alignment with the SVM structure
- Verify PLM compatibility with the cryoharness system, CDH, PCDU, FSW.
- Verify SVM design performance relative to EMC
- Verify thermal performance at non-cryogenic operational temperature for model correlation
- Verify HGA and solar array deployment
- Verify workmanship for flight environment and measure mass properties
- Verify Observatory compatibility with the ground segment

4.7 Mission Operations

4.7.1 Overview

The SPICA mission would be divided into 5 operational phases: Launch and Early Operations, Transfer and Commissioning, Instrument Performance Verification and Science Demonstration, Nominal and Extended Science Operations, and Decommissioning Operations.

Launch and Early Operations Phase (LEOP)

The Launch and Early Operations Phase (LEOP) includes the activation of the spacecraft and acquisition of the transfer orbit (including the first spacecraft orbit correction manoeuvre TCM#1). The LEOP phase ends with the spacecraft in a safe attitude and nominal communications with ground.

Transfer and Commissioning Phase

The transfer phase lasts from end of LEOP (i.e. after the first trajectory correction manoeuvre TCM#1) until arrival at the science operational orbit. The phase is governed by tracking and manoeuvre coverage needs. The Transfer Phase duration is no more than 30 days. The inaccuracies in the TCM#1 will be corrected on trajectory control manoeuvres at day 5 (TCM#2) and day 20 (TCM#3).

The commissioning phase starts just after TCM#1 success confirmation. During this phase the main activity consists in switching the PLM to its operational mode. A decontamination phase is first performed, where the telescope is heated to eliminate volatiles that have condensed on the optical surfaces during AIT and launch campaign. The duration and monitoring of this phase are still to be defined, for both frequency of monitoring and data to be downloaded and analysed. Then the cooling of the SIA starts for a duration of about 120 days. The first phase of the cooling is purely passive until the telescope has reached a certain temperature level. At this stage the cryocoolers are switched on to complete the cool down phase to the operational temperature. The commissioning phase ends when the instruments activities are complete.

Instrument Performance Verification and Science Demonstration Phase

With the start of the Performance Verification Phase, SOC normally takes over the interface to the MOC and submits the operations requests based on a pre-defined Performance Verification Plan. During Performance Verification (PV) phase the spacecraft, payload and science instruments should operate nominally and the received science data is pipeline processed. PV phase is dominated by verifying science performance requirements, validating the established calibration plan and validating the ground processing. At the end of PV the mission must show readiness to enter Nominal Science Operations Phase with high confidence that the mission end-of-life scientific objectives are being met. The end of PV phase will also include a Science Demonstration Phase in order to show science readiness.

Nominal and Extended Science Operations Phases

The field of regard (FoR) is the region of the sky in which observations can be conducted safely at any time. For SPICA, the FoR is a large annulus that moves with the position of the Sun. The FoR, as is shown in Figure 4-25, allows one to observe targets from 85° to 115° of the Sun. Most astronomical targets are observable for two periods separated by 6 months during each year. The length of the observing window varies with ecliptic latitude, and targets within 5° of the ecliptic poles are visible continuously.

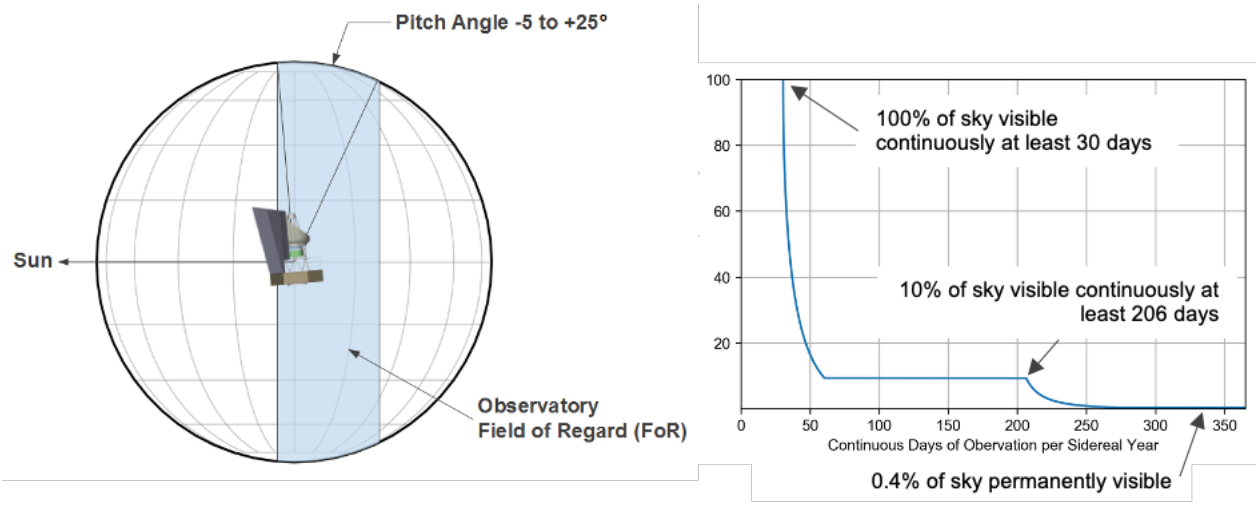

Figure 4-25: The mission Field of Regard (FoR) allows SPICA to observe within -5° to +25°

The sunshield for SPICA will permit to observe 25% of the celestial sphere at any time, which is compliant with the FoR specification. This relatively large FoR is required to provide the scheduling flexibility to allow SPICA to conduct an

efficient scientific program and simplifies orbit station keeping design since it permits a wide range of Sun orientations for thruster firing.

Based on a preliminary science reference mission derived from Herschel operations, the SPICA observing efficiency after commissioning phase is about 35%. For SPICA, observing efficiency is the time science photons are being collected divided by the mission elapsed time. Time not spent collecting science photons is termed overhead. Overhead includes all the observatory and Science Instrument (SI) operations that take place when the instrument detectors are not specifically collecting science photons. For the purposes of this effort, calibration observations are considered overhead. The mission overheads include:

- Instrument overhead
  The instrument overhead includes activities like internal instrument calibration, set-up and read out detectors, coolers re-cycling, mechanism movements and target acquisitions. The instrument engineering allocation is essentially driven by the recycling of SAFARI and B-BOP sub kelvin coolers. The re-cycling phase could occur during data transfer. The average engineering overhead in the table below has been calculated based on preliminary science mission profile and overhead of individual instrument. SMI contribution includes 5% allocation for calibration operations, while SAFARI and B-BOP overheads exclude respectively 10% and 6% of external calibration which could be performed in parallel of other operations.

	Duty Cycle	Overheads	Total
SMI	35.0%	23.0%	8.1%
SAFARI	48.0%	25.0%	12.0%
BBOP	17.0%	21.6%	3.7%
Instruments Overhead (Baseline)			23.7%

  The internal slews, including settling time and FGS acquisition, correspond to dithers or small FoV movement inside a target visit, also referenced as small angle manoeuvre. Note that the movement could be internal to the instrument or executed by an Observatory slew. In absence of detailed instrument operation plan a conservative overhead of about 20% has been provisioned.
- Observatory overhead
  The large slews correspond to spacecraft reorientation between two separated targets. As specified in [RD16], a 90° slew takes about 15 minutes, including settling time and FGS reacquisition. The science operation scheduling system may be optimized to minimize slew duration. The efficiency calculation assumed the following slew manoeuvres allocation in phase A:
  - 3500 occurrences of 90.0 degrees slews per year
  - 4000 occurrences of 10.0 degrees slews per year
  - 9000 occurrences of 5.0 arcmin slews per year

  It has been established based on a hypothetical science programme, which has been derived from Herschel operational data and SPICA preliminary science operation simulations.
  The observatory overhead includes also the momentum dumping and orbit maintenance operations
- Ground contributions to science observation inefficiencies.

	Amplitude (deg)	Yearly Occurrence	Duration (min)	Total (hr)	SPICA Baseline	SPICA Baseline
Overheads						
Science Instruments					**46.3%**	**30.0%**
Internal Slews, including Settling Time					20.0%	3.7%
Engineering Overhead (i.e. Recycling and Annealing)					23.7%	23.7%
Contingencies (e.g. SEUs)					2.6%	2.6%
Observatory					**15.7%**	**15.7%**
Large Slews, 90.0 degrees	90.0	3500	11.8	685.4	**7.8%**	**7.8%**
Large Slews, 10.0 degrees	10.0	4000	6.7	445.7	**5.1%**	**5.1%**
Large Slews, 5.0 arcmin	0.1	9000	0.5	74.0	**0.8%**	**0.8%**
Total Large Slews, including Settling Time					13.7%	13.7%
Data Transfer					0.0%	0.0%
Station Keeping					0.0%	0.0%
Momentum Management					0.1%	0.1%
Contingencies (e.g. SEUs, Safe Mode)					1.8%	1.8%
Ground Systems					**1.0%**	**1.0%**
System Overhead Margin					**10.0%**	**10.0%**
Cumulated Overhead					73.0%	56.7%
Efficiency						
Cumulated Efficiency					27.0%	43.3%
Efficiency, Parallel Operations					**34.9%**	**51.2%**
Requirements					50.0%	50.0%
Efficiency Margin					**-15.1%**	**1.2%**

Table 4-27: SPICA operational efficiency

The science observation scenario (i.e. small and large slews distribution) and instrument engineering (i.e. recycling and annealing) dominates the overhead budget. The Observatory science operations could not be consolidated in phase A. It is expected that optimization of the observing efficiency, in particular by considering parallel operations, would permit to reduce significantly the overheads.

Decommissioning Phase

The decommissioning phase shall end no later than 3 months after the completion of the operational phase. The de-commissioning phase will consist in a transfer of SPICA into a heliocentric graveyard orbit.

Ground System

The SPICA ground segment (Figure 4-26) provides the means and resources with which to manage and control the mission via telecommands, to receive and process the telemetry from the satellite, and to produce, disseminate and archive the generated products. It is composed of the Mission Operations Centre (MOC), Science Operations Centre (SOC), Science Data Centres (SDCs) and Instrument Control Centres (ICCs). The ground stations, together with the MOC, build the Operations Ground Segment (OGS), while the joint SOC and the three ICCs comprise the Science Ground Segment (SGS).

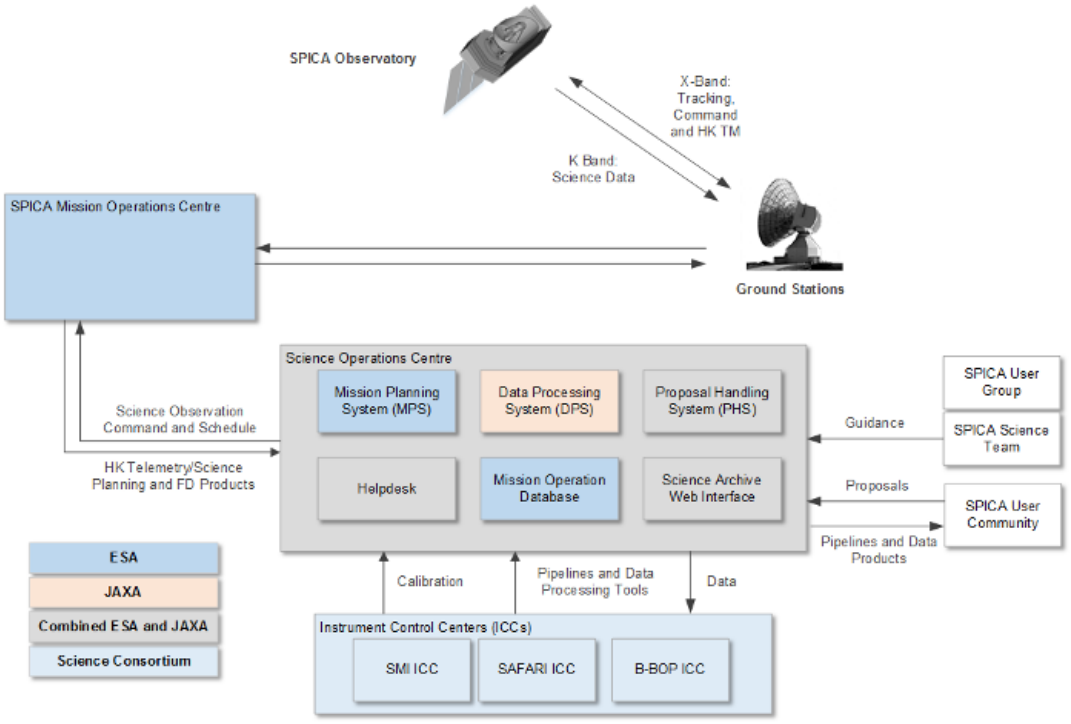

Figure 4-26: SPICA Ground Segment architecture

The mission operations are in large part similar to previous ESA astrophysics missions, including Herschel, Gaia and Euclid. The Operations Ground Segment (OGS) provides all components for the monitoring and control of the SPICA Observatory. It would use well established mission operations components and includes:

- The Ground Stations, Communications Network, ESTRACK control centre
- The Mission Operations Centre
- The Mission Data Systems
  - Mission Control system
  - Mission Planning System
  - Flight Dynamics System
  - Satellite simulator
  - Operations Preparation Tools,
- Computer Infrastructure for Mission Control System, Simulator.

ESA is responsible for the ground segment preparation, operations and maintenance, covering;

- Mission platform operations preparation, planning and execution
- Mission payload operations preparation, planning (using inputs from SOC) and execution
- Spacecraft monitoring and performance analysis
- Payload health monitoring
- Mission data distribution and archiving.

The mission operation is conducted by ESA, fully reliant on ESA/ESOC infrastructure. Use of JAXA ground stations could be considered but would depend on the ground station compatibility with X and K-band technologies baseline for the Observatory communication subsystem.

4.7.2 Mission Operations

Mission Operations Centre (MOC)

The MOC is responsible for the operations of the SPICA spacecraft, for monitoring and ensuring the spacecraft safety and health, including the payload, for provision of flight dynamics support including determination and control of the satellite's orbit and attitude, and intervention in case of anomalies. The MOC is responsible for the handling of the TM/TC for both the SPICA spacecraft and payload. The telemetry, tracking and command subsystem of the SPICA mission is to be compatible with the ESA ground segment and the ESA tracking station network (ESTRACK). The MOC is responsible for the ground station bookings, for collecting the SPICA raw telemetry science and auxiliary data and for making it available to the SOC for further processing. The responsibility for the design, implementation, and operation of the MOC rests with ESA/ESOC.

Space to Ground Interface
For the ground communications design the use of ESA's tracking station network (ESTRACK) of 35 metres antenna ground stations, with X-band for uplink and K-band for science data downlink, is foreseen. The possibility exists, however, that due to heavy oversubscription of the ESTRACK antennas, one or more JAXA ground stations would be also needed to complement ESTRACK. The Observatory would be equipped with an X-band Low Gain Antenna (LGA) and a K-band High-Gain Antenna (HGA) for science data downlink.

The ground contacts, or Daily Telecommunication Periods (DTCPs), are currently planned to last between 4 and 7 hours per day, corresponding to the expected average data rate of about 450 Gbit/day. From an operational point of view, priority will be given to the use of the ESTRACK antennas in New Norcia and Malargüe, since the Observatory is on the night side Lagrange point and thus operations from ESOC centre could take place during daytime hours.

The assumed transport protocol for the science data is file based, the CCSDS File Delivery Protocol (CFDP), which seems to become a standard for future missions. Under this assumption the mass memory organization will be file-based as well. This will be an advantage for the SGS as well over the traditional packet-based transport by having self-consistent sets of data and avoiding problems with both the packet reconstruction and packet losses.

4.7.3 Science Operations

Science Operations Centre (SOC)
The SPICA Science Ground Segment shall consist of the Science Operations Centre (SOC), Science Data Centre (SDC) in coordination with JAXA and the Payload Consortium ICC. The Science Ground Segment is responsible for:

- The planning of scientific calibration, the engineering observations and the construction of an optimised scheduled
- The issue of External Request
- The issue and support of observing Announcements of Opportunity, to be accommodated within the MOC Mission Planning cycle (which shall not result in Target of Opportunities
- The quick look analysis development, implementation and operations, performed in partnership with the ICCs
- The delivery and maintenance of a scientific analysis software system to the community, this includes the necessary calibration information. This task is performed in partnership with the ICCs
- The development, implementation and operation of the data processing pipelines to produce validated data products. This task is performed in partnership with the ICC.
- The support to scientific user community
- The delivery of the scientific results to the community through the SPICA Science Archive
- The development, implementation and operation of the long-term SPICA Science Archive
- The provision of low-level, ancillary and housekeeping data to the ICCs.

The SOC responsibilities for the science operations would be split between ESA and JAXA, while ESA will retain responsibility for the coordination of the system engineering aspects of the complete SGS. ESAC provides the data archives for all ESA scientific missions, and a dedicated team, the ESAC Science Data Centre (ESDC) ensures the same level of quality and tailoring to the mission needs for the archives together with added value tools for the general scientific community.

Instrument Control Centres (ICCs)

The Instrument Control Centres (ICCs) are assumed to represent the instrument consortium teams with respect to their contributions to the SGS tasks and activities. The ICCs are distributed over a number of institutes, with activities to be performed mostly under national funds. Although there should be close interaction and collaboration between ESA staff and ICC staff on a daily basis, a single point interface is foreseen between each ICC and ESA with regard to formal reporting and decision making: the ICC Manager. On the SOC side the interface point is the SOC Development Manager or the SOC Operations Manager (in development and operations, respectively).

During operations, the ICCs are responsible for instrument calibration and for providing the instrument data processing pipelines. They are also expected to provide the instrument operation procedures and define the observing modes, monitor the health of their instrument and deal with potential contingencies.

5 INSTRUMENT DESCRIPTIONS

5.1 Mid-infrared Imager and Spectrometer (SMI)

Instrument Description

SMI is an instrument dedicated to mid-IR spectroscopy in a wavelength range from 10 to 36 μm. SMI has three spectroscopic channels for low-resolution spectroscopy (LR), mid-resolution spectroscopy (MR), and high-resolution spectroscopy (HR), and one imaging channel at 34 μm (CAM). Key functions of the spectroscopic channels are high-speed dust-band mapping with LR, high-sensitivity multi-purpose spectral mapping with MR, and high-resolution molecular-gas spectroscopy with HR. SMI/LR is a multi-slit prism spectrometer of a wide field-of-view with 4 long slits of 10' in length and a spectral resolution of R = 50—150, operating in combination with a 10' x 12' slit viewer camera (CAM) to determine the positions of the slits on the sky. SMI/LR has a very high continuum sensitivity (~25 μJy in 1 hr, 5σ) with fine spatial sampling (0.7" / pixel), and thus has a high-efficiency spectral mapping capability. SMI/MR is a grating spectrometer with a long slit of 1' in length, high line sensitivity (~2.8 × 10-20 W/m2 in 1 hr, 5σ), and moderately high spectral resolution (R = 1300– 2300). SMI/HR is an immersion grating spectrometer with very high line sensitivity (~1 × 10-20 W/m2 in 1 hr, 5σ), and high spectral resolution (R~30000). The design of SMI/LR with CAM is based on wide-area surveys in a telescope step-scan mode to produce a spectral map of ~10' × 12' area as a minimum field unit, whereas SMI/MR and HR are operated in combination with a beam-steering mirror and shared fore-optics to perform spectral mapping (or dithering) of a relatively small (~1'× 1') area.

Scientifically, as one of the most outstanding features of SMI is that LR enables us to study spectral bands due to dust grains such as polycyclic aromatic hydrocarbons (PAHs) from an extremely large number of star-forming galaxies at redshifts from 0.5 up to 7, and silicate grains from many planet-forming debris disks with high mid-IR luminosities down to our solar system level. As by-products, the SMI/LR spectral surveys provide broad-band images with CAM (R~5, the central wave-length of 34 μm), which are also important as legacy data sets since the 30–40 μm region is an unexplored gap between the Spitzer 24-μm and the Herschel 70-μm surveys. Another important feature is that HR enables us to perform velocity-resolved studies of fundamental molecular gases (H_2, H_2O, CO) like those in the innermost regions of protoplanetary disks and in the energetic out-flow of active galactic nuclei. Complementarily to these specific functions of LR and HR functions, MR provides more versatile spectroscopic functions, for example, such as follow-up spectroscopy of targets detected by SMI/LR to study dust bands and gas lines in more detail. Hence SMI, combined with the far-IR instruments (SAFARI, B-BOP), can not only unravel the evolutionary histories of star-forming galaxies, active galactic nuclei, and planetary systems, but also comprehensively elucidate material enrichment in space from the very early universe to the present planet formation.

A conceptual design study for SMI has been performed and have found a feasible solution satisfying the scientific requirements with relatively high technology readiness levels and practically available technical resources. SMI has been designed with three spectroscopic channels—LR (high mapping speed), MR (high sensitivity), and HR (high resolution) —and one imaging channel, CAM. CAM can work as a slit viewer for LR. Table 5-1 summarizes the SMI/LR, CAM, MR and HR specifications obtained as a result of the conceptual design study.

Parameter	LR	CAM Slit viewer for SMI/LR	MR	HR
Band centre - µm	27	34	27	15
Wavelength - µm	17-36	34	18-36	10-18[a]
Spectral resolution R	60-160[b]	5	1400-2600[b]	29000[c]
(diffuse source)	(20-100)		(800)	
Field of view	600" x 3.7"	600" x 720"	60" x 3.7"	4" x 1.7"
	4 slits		1 slit	1 slit
Band centre FWHM	2.7"	3.5"	2.7"	2"
Pixel scale	0.7" x 0.7"	0.7" x 0.7"	0.7"	0.7"
Detector 1K x 1K	Si:Sb	Si:Sb	Si:Sb	Si:As
Point source sensitivity (5σ/1h)[d]				
Continuum - µJy	21[e]	11	180[e]	800[e]
Line – 10^{-20} W/m^2 [f]	4		1.7	0.6
Survey peed – arcmin^2/h [g]	~41	~5700	~3.2	
Diffuse source sensitivity (5σ/1h)[d] [h]				
Continuum – MJy/sr	0.07	0.04		
Line – 10^{-10} W/m^2/sr			0.7	0.6
Saturation limit - Jy	~10	~0.6	~600	~10000

(a) Continuous coverage up to 18.1 µm + partial coverage for H_2O 18.66 µm.
(b) $\lambda/\delta\lambda$ = 150 (SMI/LR) and 1300 (MR) at λ=36µm.
(c) Designed for λ20 µm diffraction limited PSF.
(d) Sensitivity estimated with Fowler-16 sampling for SMI/LR and /CAM (0.5Hz), and with ramp curve sampling for /MR (0.5 Hz) and /HR (1Hz sampling).
(e) Continuum sensitivity rescaled with R=50, R=1300, and R=25000 for SMI/LR, /MR and /HR, respectively, with a scaling factor of $(R_{cont}/R)^{0.5}$.
(f) Sensitivity for an unresolved line.
(g) Survey speed for the 5σ detection of a point source with the continuum flux of 100µJy for SMI/LR at λ=30µm (CAM at 34µm) and the line flux of $3x10^{-19}$ W/m^2 for MR at λ = 28µm, both in the low background case with overheads of readout time included (32 sec/frame for SMI/LR and /CAM due to Fowler-16 sampling).
(h) Sensitivity for a diffuse source in a 4"x 4" (SMI/LR, /MR) or 2"x2" area (/HR).
(i) Background levels are assumed to be 80 MJy/sr (High) and 15 MJy/sr (Low) at 25µm.

Table 5-1: SMI specifications fact sheet of the "current best estimate" case

Figure 5-1 shows an overview of the SMI optical layouts, with LR&CAM on the right side and MR and HR on the left side. About 20 mirrors in total are critically required for each channel to achieve the adequate optical performance.

For both LR and CAM which share the fore-optics, incident light from the telescope (F/5.4) is relayed and focused on a 300 tilted slit mirror without magnification. The shutter is installed in the pupil of the fore-optics with a beam size of ϕ 30 mm. In the LR rear-optics, the light passed through the slit is collimated and focused on the Si:Sb detector (1K × 1K pixels, 18 µm pitch) with F/1.9. A KRS-5 prism is installed in the pupil to disperse the light. The CAM optics pick-up light which is reflected on the slit mirror, then refocus it on the Si:Sb detector with F/1.9. A 34-µm band-pass filter is installed in the pseudo-pupil in the CAM rear-optics.

HR and MR share the fore-optics to relay the incident light without magnification. BSM which is placed at the pupil of the fore-optics enables fast mapping without telescope maneuvers. In the MR rear-optics, the light is collimated twice, with pupils for a low-pass filter and a grating (m=6—11), and a cross-disperser (m=1). There is also a slit between the two relay-optics. The light is then focused on the Si:Sb detector at F/2.2. HR has three collimator optics to install a low-

pass filter, an immersion grating (CdZnTe, m=81—153), and a cross-disperser (m=1). A slit is inserted between the 1st two relay optics. Then, the light is focused on the Si:As detector (1K × 1K pixels, 25 μm pitch) at F/1.9. The HR optical design is based on the reflective optics of aluminum-alloy free-form mirrors with 6th order polynomial.

In the SMI optics, all optical components except for the HR immersion grating, LR prism, and optical filters, are free of chromatic aberration. All the mirrors are made of aluminum alloy, the same material used for the structure of SMI, so that the optical misalignment at cryogenic temperatures due to CTE mismatches can be avoided. We have confirmed that free-form mirrors made of aluminum alloy can be fabricated with the surface figure error of 12 nm RMS and the roughness of 10 nm Ra by introducing the latest ultra-high-precision machining technology.

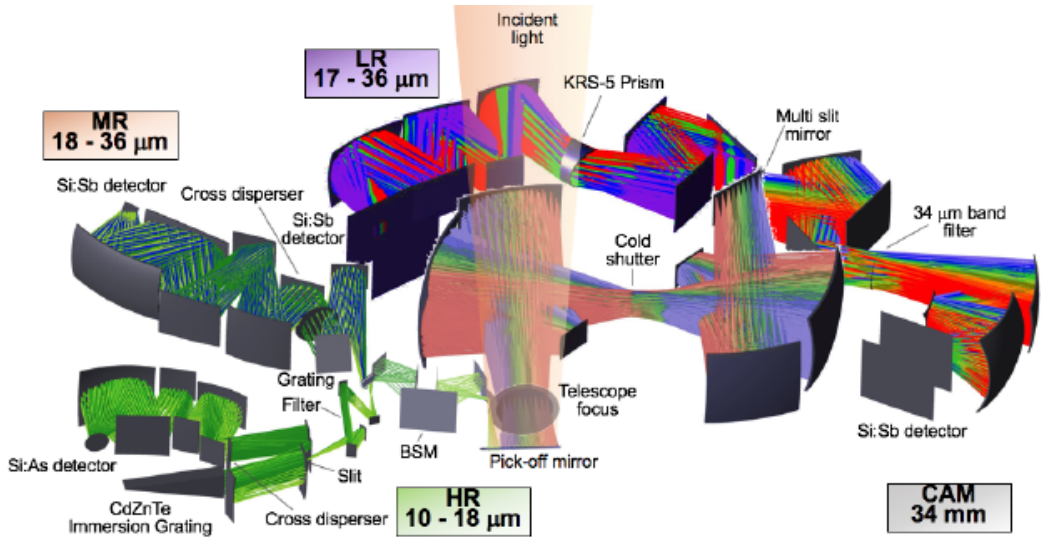

Figure 5-1: Optical layouts designed for SMI/LR with CAM (right) and for SMI/MR&HR (left). Color-coding of rays is based on angular positions in the fields-of view.

The SMI product tree is presented in Figure 5-2.

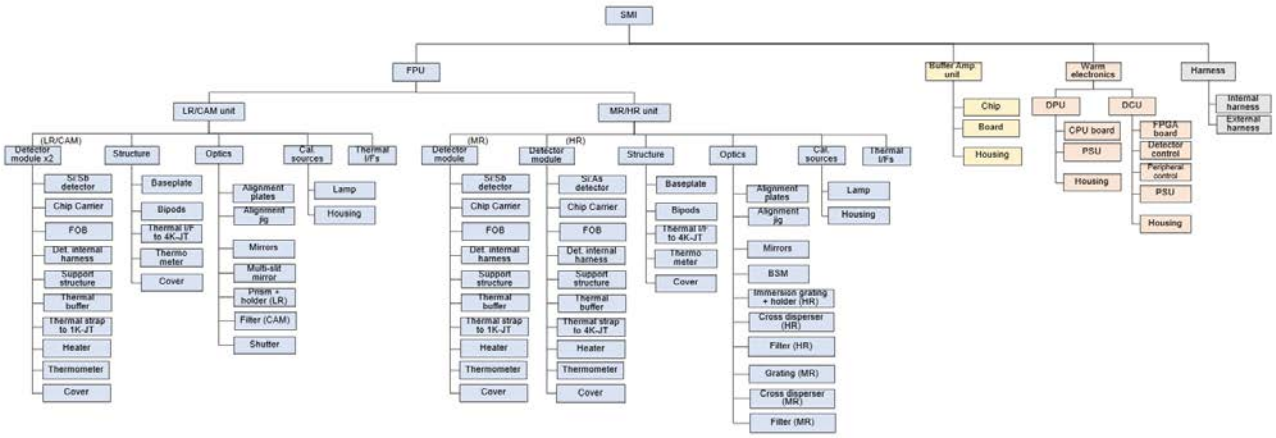

Figure 5-2: SMI product tree (ground-based support and test equipment not represented).

Observing modes

SMI has the following five operation modes: (1) Power Off, (2) Stand-by, (3) Calibration, (4) Observation, and (5) Annealing as shown in Table 5-2. The annealing mode is the SMI-specific operation mode.

Operation mode	Description
Off	There is no primary power supplied to SMI.
Stand-by	SMI is switched on, but the detectors are in low-power mode; no output signal and a small amount of heat generation. This operation mode provides housekeeping data only. SMI is set to be this mode when one of the other instruments (SAFARI or B-BOP) executes observations.
Calibration	An internal calibration is performed by using calibration lamps and the cold shutter. SMI provides science and housekeeping data.
Observation	SMI performs observations and provides science and housekeeping data.
Annealing	SMI detectors are annealed by increasing the detector temperature for a specified duration time to mitigate the effects of cosmic-ray hitting.

Table 5-2: SMI operation modes

SMI observation modes have the following four nominal and one optional observation templates, called as "Astronomical Observation Template (AOT)".

- SMI Stare mode spectroscopy: This mode is used for targeted spectroscopic observations of point-like sources with SMI/LR, MR and HR. For MR and HR, dithering or mapping of a small area can be performed by using BSM. The longest exposure time per frame is 600 sec for all channels.
- SMI/LR and CAM Survey mode (Stare-step mode): This survey mode (stare-step mode) is applied to perform slit scanning spectroscopic observations with SMI/LR to produce a spectral map of 10 x 12 arcmin area (one field unit) and CAM to produce a imaging map of the same area with 95 telescope stepwise scans by a step of 1.9 arcsec, i.e., half the slit width.
- SMI/MR Staring-step (mapping) mode spectroscopy: The mode is applied for SMI/MR spectral mapping with a 60 arcsec-long slit for extended targets such as nearby galaxies.
- SMI Scanning-mode Spectroscopy (optional): This mode performs slit-scanning spectroscopy with MR (TBD) for large area mapping up to 40 arcmin in the scan length by continuous slow-scans combined with the motion of BSM

SMI observation campaign is assumed to lasts typically for 2–3 days (Figure 5-3). Each campaign consists of one annealing operation, dark current measurements, multiple science observations, and calibration observations. The campaign starts with the annealing operation which takes 2–3 hours. During the telescope manoeuvre operation, dark measurements for LR and CAM channels are performed using the cold shutter with several different exposures, while those for MR and HR channels are not. If dark measurements of MR and HR channels are required for a special purpose, additional observations of a dark sky region will be performed. The measured dark current data will be applied to the science observation data taken in the same observation campaign for the data reduction. In the beginning of each science observation, detector performance is monitored by operating calibration lamps. Between science observations, calibration observations, especially wavelength and absolute flux calibrations, would be regularly performed with the frequency of (TBC) per campaign.

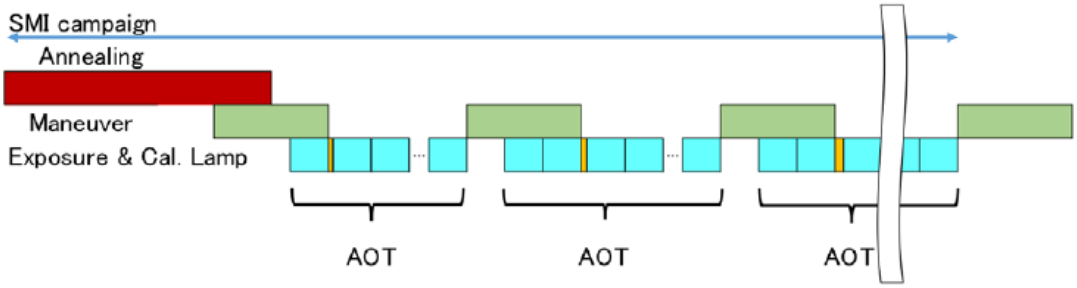

Figure 5-3: Overview of operation sequence in the SMI campaign. Red and green, cyan and yellow boxes denote the annealing operation, manoeuvre operation, science observation, and calibration observation, respectively.

Detectors

The SMI detector system is composed of sensor chip arrays (SCA), detector modules, buffer amplifiers, and driving electronics as shown in

Figure 5-4. Photon signals from celestial objects are detected by the Si:Sb/Si:As BIB detectors and converted to electrons. The electron is integrated by a capacitor in a unit cell (pixel) of the read-out-integrated circuit (ROIC) and the number of elec-trons is converted to voltage by the capacitor. The unit cell is equipped with a source follower, and the integrated signal can be read non-destructively (source follower per detector architecture). The output of each pixel is selected by the row and column scanners in ROIC and connected to the output of SCA, through two stages of source followers with impedance conversion (in the unit cell and at the output). The voltage signal from SCA is buffered by the buffer amplifier at the mid-T stage (SVM shield 1, ~180 K is assumed) to drive the analog signal through the long wire harness to the warm electronics. On the warm electronics at ~300 K, the analog signal is amplified, and then converted to the digital signal. Detector operation and simple image calculations (addition and subtraction) are carried out by the detector control unit (DCU). The digital data are compressed and sent to the satellite service module (SVM) through the data processing unit (DPU). The detector module provides thermo-mechanical I/F to the SMI structure.

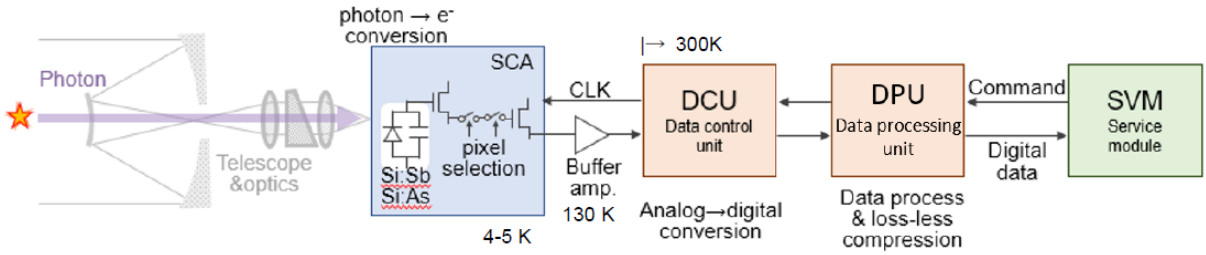

Figure 5-4: Functional diagram of the SMI detector system and its signal chain

SMI adopts three Si:Sb 1024 x 1024 (18 µm/pixel) array detectors for SMI/LR, MR and CAM, and one Si:As 1024 x 1024 (25 µm/pixel) array for SMI/HR made by a US company. The specifications of the detectors and quantum efficiencies of Si:As and Si:Sb detectors are summarized in Figure 5-5. The specifications of the Si:As array are taken from the literature on the arrays developed for JWST/MIRI, while those of the Si:Sb array are based on the latest information obtained from DRS. The detectors (at least Si:As) would be expected to be procured within the framework of international partnership (with Taiwan/ASIAA and US/JPL). In the current plan, ASIAA is responsible for the Si:As procurement and the collaboration in the low-noise ROIC development (described below).We also have a backup plan to adopt Si:As arrays, in which case the readout noise and dark current are expected to be degraded to 100 e and 0.2 e/s, respectively. This means that the degradation in sensitivity is by a factor of 1.25. To avoid the science impacts, a new low-noise ROIC is being developed. The decision should be made based on the result of the new low-noise ROIC test, which would be obtained by MSR. As can be seen in Figure 5-5, the Si:Sb detectors suffer a considerable degradation in the quantum efficiency at wavelengths longer than 35 µm. The company has proposed a solution

strategy to cope with this issue. If the quantum efficiency is successfully improved at wavelengths longer than 35 μm, not only the sensitivities of LR, MR and CAM increase accordingly, but also the spectral coverage of SMI/LR can extend to longer wavelengths accordingly, without modifying the optical design, which is significant advantage of a prism over a grating.

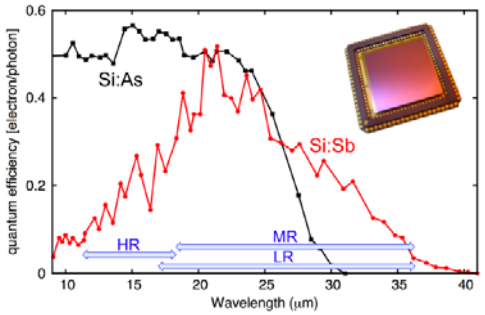

	Si:As detector array	Si:Sb detector array
Format	1024×1024	1024×1024
Pixel Pitch	25 [μm/pixel]	18 [μm/pixel]
Output	4	4
Spectral Response	4—27 μm	15—38 μm
Peak Quantum Efficiency (%)	>50	>40
Dark Current (e/s/pixel)	0.06	~0.8 [a]
Operating Temperature (K)	6.0	4.0
Power Dissipation (mW at 0.5 Hz)	1.0	1.0
Frame Time (sec)	<1	<1
Typical Response Uniformity (%)	<4	<4
Read Noise (e, CDS/Fowler-1)	~40 rms	<100 rms
Well Capacity (e)	>1×10^5	>1×10^5
Unit cell architecture	source follower per detector	source follower per detector
Channels to be used	1 array for HR	1 array for MR, LR and CAM each

a) Includes a possible contribution through the IR emission of ROIC.

Figure 5-5: a) Quantum efficiencies of Si:As (black line) and Si:Sb detectors (red line). b) Specifications of the detectors for SMI.

Interface and Resource Requirements

Information on interfaces and budgets is presented in section 5.4.

Predicted Performance and Margin

Three kinds of input-parameter sets are used for the sensitivity calculation; "current best estimate" (CBE), "nominal" (CBE+DMM), "worst-case" (CBE+DMM+SM), where SM represents the system margin which is a safety factor of 0.8 multiplied by the CBE optical throughput. The detection limits expected for SMI/LR, CAM, MR and HR in the above three inputs are shown in Figure 5-6 a), plotted as a function of wavelength in the high and low background cases. For the comparative purpose, the "nominal" line sensitivities of SMI-LR, MR and HR are shown together with those of other representative instruments in Figure 5-6 b).

The "nominal" line sensitivities are estimated to be 5.0x10^{-20} W/m^2 (λ=25μm), 2.3x10^{-20} W/m^2 (λ=25μm), and 0.8x10^{-20} W/m^2, and the continuum sensitivities are estimated to be 24 μJy (R=50), 240 μJy (R=50), and 1.1 mJy (R=25000) for LR, MR and HR, respectively. Most of the sensitivity performances specified in the Science requirements Document [RD14] are satisfied with this sensitivity with 1-hour exposure and 5 SNR. A few science cases need deeper observations. For example, deep imaging of distant galaxies requests 3 uJy at 34 microns. This observation can be realized with 20-hour exposure. These results demonstrate that SMI meets the requirements to achieve the science objectives.

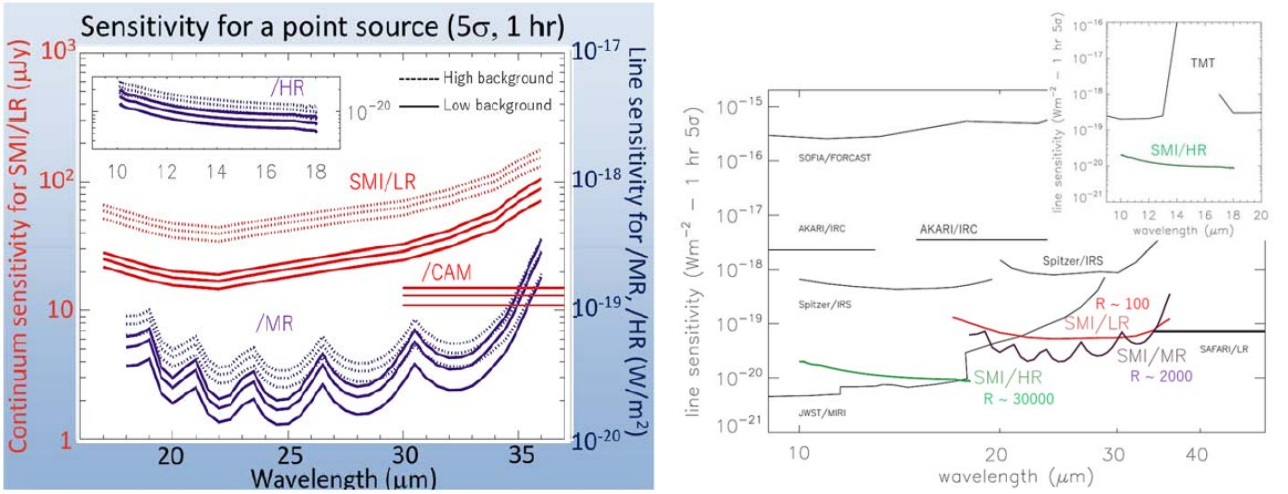

a) b)

Figure 5-6: a) Continuum sensitivity with SMI/LR and CAM (red) and line sensitivity with SMI/MR and HR (blue), both estimated for a point source (1 hr, 5σ). The LR continuum sensitivity is rescaled with R=50. Background levels are assumed to be 80 MJy/sr (high) and 15 MJy/sr (low) at 25 μm. b) "Nominal" line sensitivities of SMI/LR, MR and HR, compared with those of other instruments.

Integration, Testing and Calibration

The following verification items are considered: a) Design, b) Specifications of the fabricated parts, c) Total performance of the assembly, and d) Life time. For each SMI component (optics, detector sys-tem, mechanics, and electronics), the verification items for thermal, structural, optical, and electronics points of view are checked. Figure 5-7 shows verification flows for major development items.

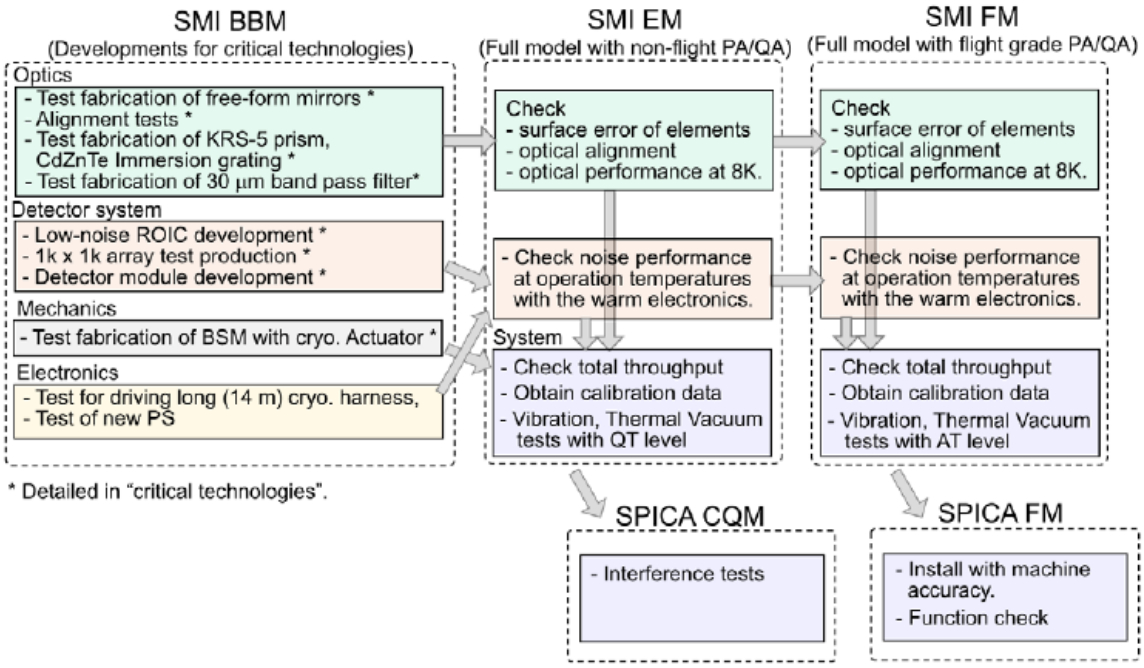

Figure 5-7: SMI verification flows

Table 5-3 shows the SMI verification matrix.

		BBM (~MSR)				BBM (~MAR)				EM						PFM					
		N.A	Similarity	Analysis	Tests	N.A	Similarity	Analysis	Tests	N.A	Similarity	Analysis	Tests	SMI CQM test	PLM QCM test	N.A	Similarity	Analysis	Tests	SMI test	PLM test
Detector	Design			○				○				○						○			
	Performance (Q.E., dark, noise)				●				○				○	○					○	○	
	Heat dissipation				●				○				○	○					○	○	
	Operability	–				–							○	○					○	○	
	Radiation tolerance		○				○				○						○				
	Life time	–				–				–							○				
	Buffer Amp. performance (gain, slew V)				●				○				○	○					○	○	
	Buffer Amp. heat dissipation				●				○				○	○					○	○	
	Module electrical design				●				○				○	○					○	○	
	Module thermal design				●				○				○	○					○	○	
	Module mechanical design				●				○				○	○					○		
Warm elec.	Design			○			○					○						○			
	Performance (noise)				●			●					●	○					○	○	
	Power dissipation				●			●					●	○					○	○	
	Life time	–				–				–							○				
	On-board software	–				–							●	○					○	○	
	Structure	–				–							●						○	○	
Optics	Design			○				○				○		○				○			
	Mirrors: surface figure accuracy				●				●				○	○					○	○	
	Mirrors: mechanical design			○				○					○	○					○	○	
	Mirrors: alignment accuracy		○						○				○	○					○	○	
	KRS5 prism: performance				○				○				○	○					○	○	
	KRS5 prism: mechanical design			○					○				○	○					○	○	
	CdZnTe IG: performance				●				○				○	○					○	○	
	CdZnTe IG: mechanical design			○					○				○	○					○	○	
	LR performance (Opt, λ/Δλ, effiiency)	–				–							○	○					○	○	
	CAM performance (Opt, λ/Δλ, effiiency)	–				–							○	○					○	○	
	MR performance (Opt, λ/Δλ, effiiency)	–				–							○	○					○	○	
	HR performance (Opt, λ/Δλ, effiiency)	–				–							○	○					○	○	
SMI as a system	Structural design			○				○					○	○					○	○	
	Thermal design			○				○					○	○					○	○	
	LR total noise performance	–				–							○	○					○	○	
	CAM total noise performance	–				–							○	○					○	○	
	MR total noise performance	–				–							○	○					○	○	
	HR total noise performance	–				–							○	○					○	○	
	EMC				●				●				○		○				○		○
	Data rate			○				○					○	○					○	○	○

● Tests with dedicated model for the purpose.

○ Tests with the FM equivalent design model.

Table 5-3: SMI verification matrix.

A summary of the SMI in-obit calibration items and plans is presented in Table 5-4.

Calibration	LR	CAM	MR	HR
Dark estimation	Opening and closing the cold shutter.		Not necessary (TBD). ON-OFF subtraction using BSM at each observation.	
Flat estimation	Observation of the Zodiacal emission.		Observing IR standard stars at multiple positions along the slits with BSM.	
Flux calibration	Observing IR standard stars. New faint standard stars need to be established with the method of Cohen standard stars' network. Filter leakage is checked by using both blue (stars) and red (asteroids) objects.			
Stability check	Calibration lamps are turned on in the beginning of each science observation. Frequent monitoring of several IR standard stars near the ecliptic poles.			
Image distortion check		Observation of a globular cluster covering the entire FoV		.
Wavelength calibration	Observation of IR standard sources.			TBD

Table 5-4: Summary of SMI in-orbit calibration items and plans.

For the calibration of the sources, SMI considers:

- Calibration lamps: Three internal calibration lamps are equipped for each detector (four detectors: LR&CAM, MR&HR). The calibration lamps illuminate the detector arrays.
- Monitoring fields (objects): For the purpose of measuring and monitoring the system overall gain, SMI observes standard celestial sources near the Ecliptic poles, such as NGC 6543.

Heritage and Enabling technologies

The main enabling technologies for SMI are summarized in Table 5-5.

Items	Elements to be developed
Si:Sb 1024 x 1024 detectors	Fabrication and test a BBM array with a BBM electronics to improve performance at the longer wavelength ends. Development of a low-noise readout integration circuit.
Optics with free-form mirrors	Performance test of the free-form mirror optics at the cryogenic temperature.
KRS-5 prism 30 μm band optical filters	Fabrication of a KRS-5 test prism and test filters to check their tolerance against the thermal stress of cooling cycles.
CdZnTe immersion grating	Development of a CdZnTe immersion grating and evaluation of its optical performance at low temperatures.
Actuator	Modification of the AKARI cryo-motors for low power consumption and high durability.
Detector module	Fabrication and testing of a BBM detector module to verify its thermal performance for a detector annealing operation.
Warm electronics	Design of software including FPGA.

Table 5-5: Main enabling technologies for SMI.

SMI back-up configuration: SMI/CAM as FGS and options to increase efficiency
This section summarises the impact at SMI level of using SMI/CAM as FGS as well as the addition of the MR/HR parallel mode proposed by SMI to increase the observing efficiency.

This SMI configuration is considered as back-up, being the MCR configuration presented above the baseline.

- SMI product tree:

The SMI product tree shown in Figure 5-2 would need to be updated with the following modifications:

For the implementation of the FGS:

- Removal of the cold shutter
- Inclusion of a redundant FPGA
- Si:Sb CAM detector moved to the 4K-JT stage
- CAM filter changed from 34 to 28 μm

For the MR/HR parallel mode observation:

- BSM exchanged by a dichroic mirror

- SMI/CAM as FGS:

In the mission consolidation review (MCR) during the ESA M5 process, it is identified that a fine guidance sensor (FGS) at focal plane is necessary to achieve the required pointing accuracy (absolute pointing knowledge error; AKE of 0.25″). Following the MCR review board recommendation, the ESA SPICA study team investigates possibility of SMI/CAM as a FGS after the MCR with help of the SMI team.

The SMI team provided two hardware solutions, 1) to replace CAM by a compact NIR camera with Si-lens optics and a Si:As detector, and 2) to use SMI/CAM as it is replacing band-pass filter. After analysis of sensitivity and reference catalogue, the ESA team concluded that SMI/CAM with a band-pass of ~28 μm satisfy required position determination accuracy (0.1″) within a period of 10 seconds.
Since it is a bus system, FGS must have higher reliability than that of mission instrument. To achieve the high reliability, two issues were investigated: 1) no mechanical moving parts, and 2) redundant detector and control electronics system.

For the first issue it was concluded that the cold shutter could be eliminated. SMI planned to use the cold shutter for the measurement of dark current of Si:Sb detector for LR and CAM. However, it was found that observing two blank sky position with different background level (at different ecliptic latitude), together with the measurement at the masked area on the detector enables SMI to achieve required dark current measurement accuracy.

For the second issue, the ESA team concluded that the quadrant of the CAM Si:Sb detector can be used as four redundant detector. The CAM Si:Sb detector is a 1024 × 1024 array detector and it consists of four 512 × 512 sub-array fabricated in a single chip. Each quadrant of the array is an independent sub-array, and SMI can operate one quadrant if other quadrant has a malfunction (see Figure 5-8).

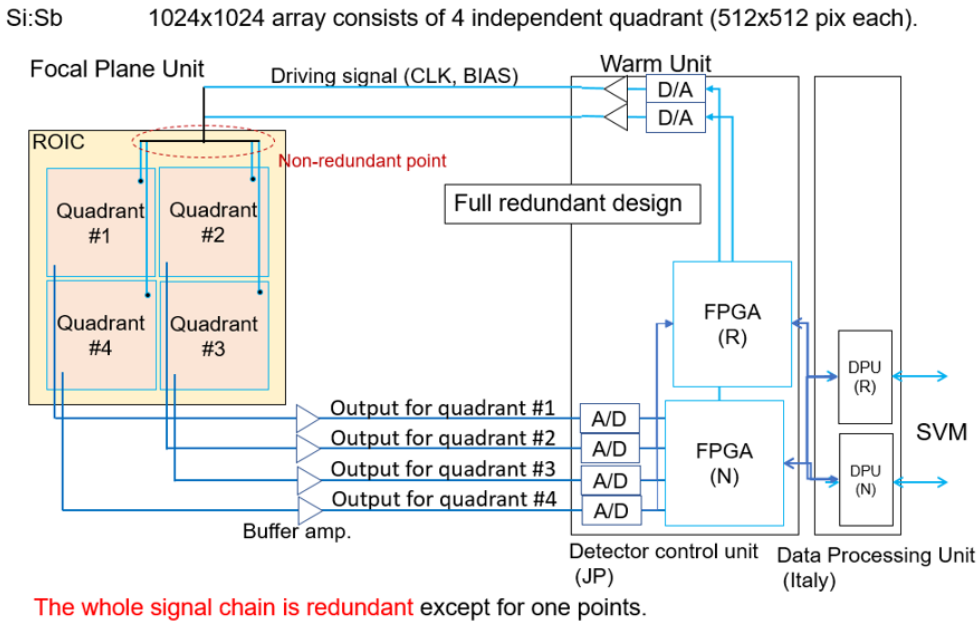

Figure 5-8: SMI/CAM architecture with redundancy for FGS.

In the current design, the four quadrant shares power supply lines and driving signal lines (22 lines). SMI would modify the warm electronics and cryo wire harness to have redundancy on that parts, and SMI expect 5% increase of parasitic heat load towards the 4K-JT stage. No significant impact on mass, power, volume budget for the system. The control electronics system handles the output signal from the four quadrant independently, and no modification is necessary for that parts.

The impact on the thermal budget is already presented in Table 4-16 (figures in brackets).
The impact on the mass budget is mainly due the implementation of the redundancy of the DCU and expected to be around 2.5kg.

- MR/HR parallel mode:

After the MCR, SMI decided not to use any cryo moving part. For SMI/MR and HR, it was decided to use a dichroic beam splitting mirror instead of the BSM to enable simultaneous observation with both MR and HR for a source to improve the observational efficiency.

Considering a nominal share in SMI observational time of (HR:MR:LR+CAM:HR+MR) = (0:0:1:1) corresponding to the case in which all HR/MR targets require both HR and MR data and the implementation of the ramp-up-sampling mode instead of the Fowler-16 sampling for the LR mode, which increases the LR data rate from 1 to 5 Mbps, the nominal Science data rate generation would be 18 Mbps (maximum) and 15 Mbps (average) (in contrast with Table 4-14).

5.2 Far-infrared Spectrometer (SAFARI)

Instrument Description
The concept of the SPICA Far Infrared Spectrometer (SAFARI) is that of a grating spectrometer to achieve a base resolution R of about 200. This is combined with a high-resolution post dispersed Fourier Transform Spectrometer to increase the resolution by a factor of 10 to 100 (depending on wavelength). A simplified version of the conceptual design can be seen in Figure 5-9, the design is simple: a 2D agile Beam Steering Mirror (BSM) selects an input beam - from the telescope, or from internal calibrators - to be directly coupled to the detectors system (the low resolution light path

LRP). Alternatively the BSM directs the input signal to a Fourier Transform Spectrometer (the high resolution light path HRP) which is subsequently coupled to the detector system through a flip-mirror.

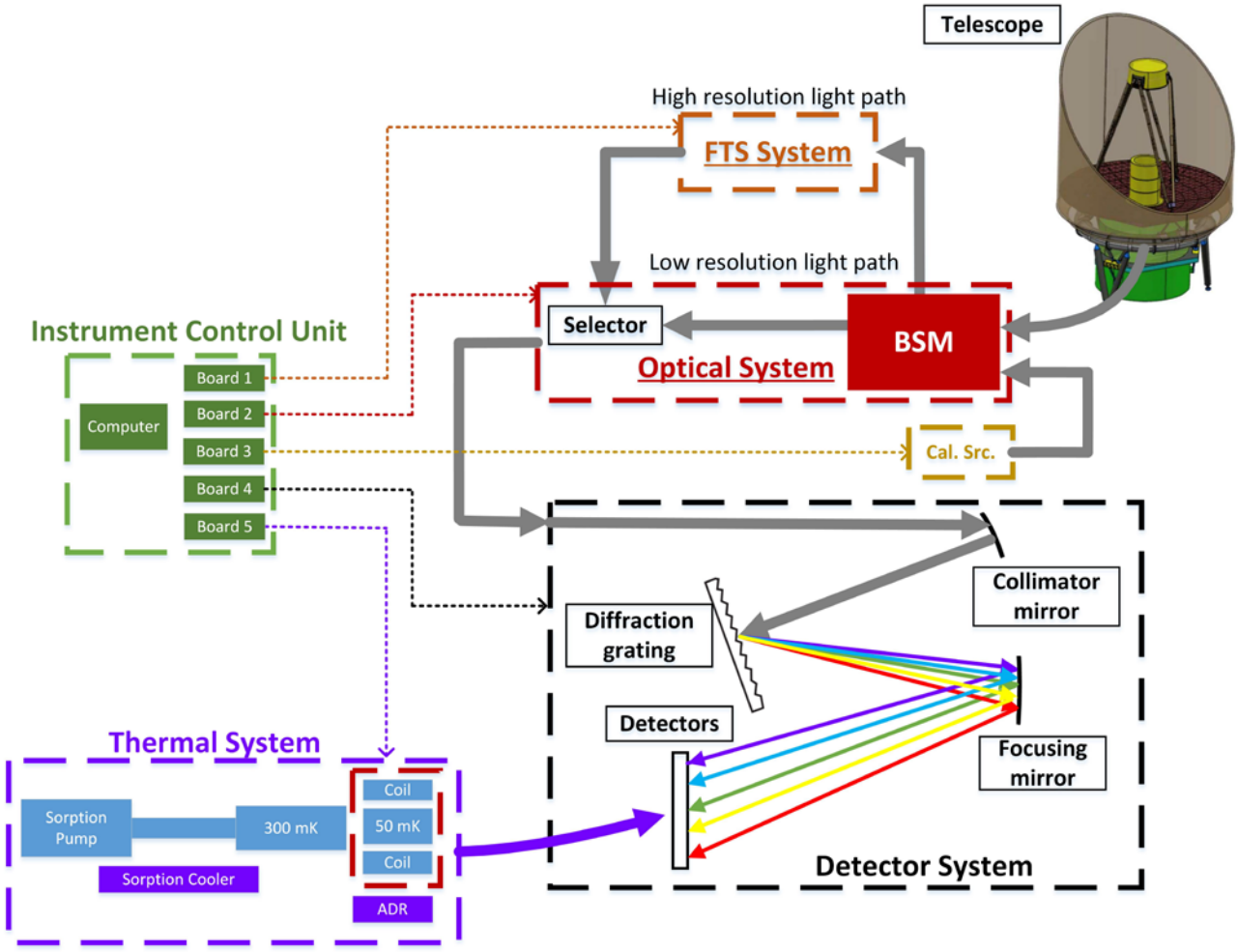

Figure 5-9: Simplified conceptual design of SAFARI. A selectable low/high resolution spectrograph/spectrometer is proposed to comply with the two different resolutions required by the science.

The LRP send the light into a spectrometer with diffraction gratings as dispersing elements. Diffraction gratings were selected, over prisms or other dispersive elements that use refraction, to minimize the loss of light in the materials due absorption and dispersion. The dispersed light will impact on straylight, while the absorbed light will impact in the temperature of the component. The gratings are designed to provide an optical resolution in the spectral axis of 250. In the HRP, the light passes first through a Fourier Transform Spectrometer, then through the grating spectrograph. This post dispersion operation increases the spectral resolution up to the range between 11000 to 1500, depending on the wavelength range (34 μm to 230 μm).
Because of the large total bandwidth and the required relative accuracy and uniformity along the whole band in the intensity and spectral measurements, it was initially decided to divide the spectral range in 4 (SAFARI 3.0). In this way, four different optimizations are possible in optical performance, mass, volume and accommodation in the available space on SPICA.

In the course of the study initially a 4-band configuration was studied for the telescope vertical topology (SAFARI 3.0). Later, driven by the retirement of the US partner and the resulting redistribution of work among consortium partners a preliminary study was started into a 3-band configuration (SAFARI 4). A further iteration was performed (SAFARI 4.2) for mass reduction. In the various redesign steps the number of detectors both in spectral and spatial domain was

reduced, which reduced both the effective instrument sensitivity and the (post-processing) effective baseline low resolution (from about R300 to R200 for SAFARI 4.2). The FTS resolution was not affected by this.

A summary of the SAFARI configuration and their main characteristics is presented in Table 5-6.

SAFARI Configuration	Reason for the change	Characteristics
2.0	First SAFARI grating configuration	4 grating modules 5 rows of 180 pixels Resolution 300
3.0	SPICA to vertical, mass reduction required.	MCR baseline configuration Front optics adapted to vertical telescope 4 grating modules 5 rows of 150 pixels Resolution 250, 20 channels
4.0	Redesign to 3 grating modules for cost reduction	Front optics equal to 3.0 3 grating modules 5 rows of 150 pixels each Resolution 235, 18 channels
4.2	Redesign for mass reduction	Baseline configuration Front optics equal to 3.0 3 grating modules 4 rows of 126 pixels each Resolution 200, 12 channels

Table 5-6: SAFARI configurations and their main characteristics

Figure 5-10 shows a block diagram of the SAFARI instrument system. The upper big blue box is the focal plane unit, which includes all the optics, detectors and cooling sub-units.

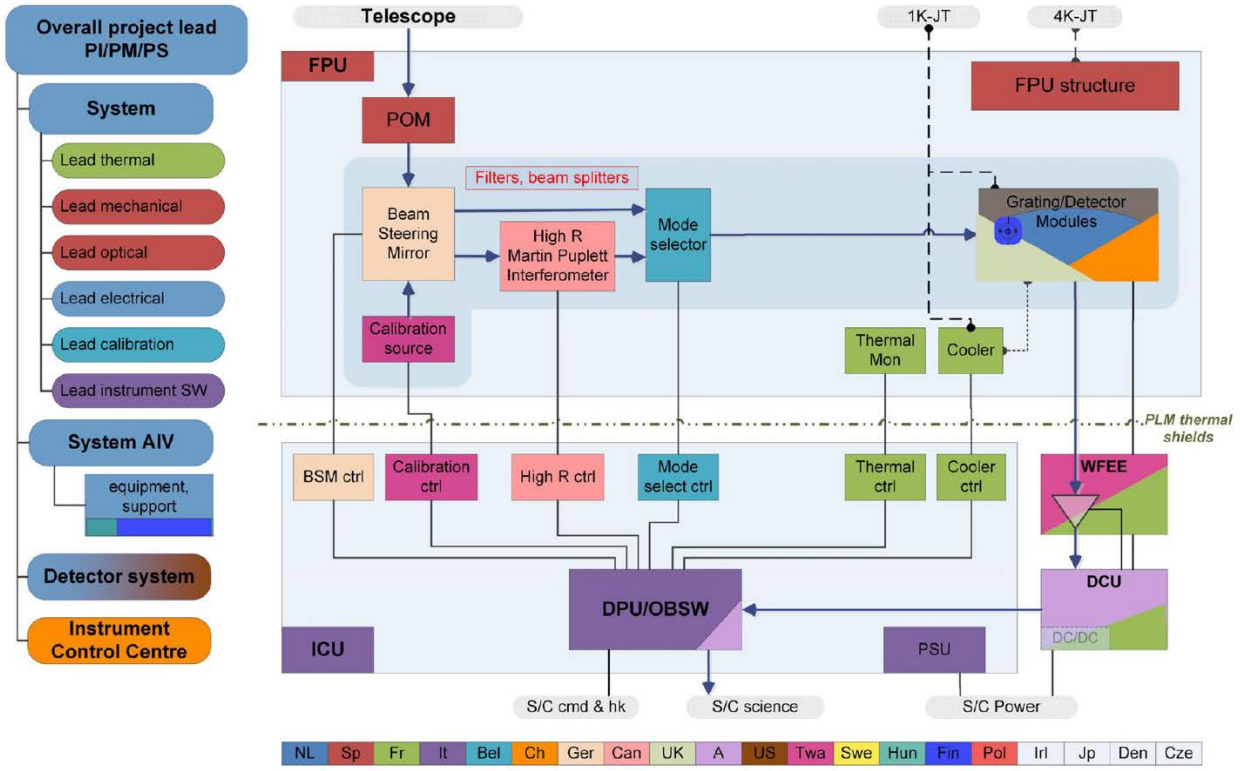

Figure 5-10: SAFARI Instrument general block diagram, the external grey round boxes represent the interfaces with the SPICA spacecraft. The colours indicated the responsibilities of the various consortium partners.

Starting from the telescope and following the light path, the infrared radiation is directed into SAFARI using a pick off mirror (POM). The radiation is filtered to allow only the wavelengths longer than 34 μm to pass and to be redirected into the instrument, it is then directed by a steering mirror (BSM) into the low- or high-resolution light paths. The BSM, with the appropriate angle, will also direct the light coming from a calibration source into the instrument.

Following the low-resolution path, the light goes into a mode selector which selects the light coming from the low- or high-resolution paths and closes the other one to avoid straylight. The mode selector is part of the Band and Mode Distributing Optics or BMDO, which uses a polarizing beam splitter to divide the total power of the radiation in two parts. Each beam will then pass through a dichroic mirror to separate the beam in 2 bands for total of 4 beams of different bands at the output. The four beams, are focused onto the slits of the grating spectrometers optimized for each of the bands. Each spectrometer is called a grating module (GM) and the four bands names are: short wavelength (SW), medium wavelength (MW), long wavelength (LW) and very-long wavelength (VLW) (SAFARI 3.0, VLW was discarded for SAFARI 4.2).

At the inputs of the GMs, there is a set of filters to form a band pass feature tuned to the specific wavelength bands of every grating module, the filter set also rejects the frequencies lower than 10 GHz. The GM bands have a slight overlap to allow cross-calibration of the resulting band sub-spectra.
All the sub-units are mounted on a structure stiff enough to maintain the positions under operational conditions and keep the components in place during launch.

The GMs utilise a few rows of ultra-sensitive TES detectors (NEP = 2×10^{-19} $W/\sqrt{Hz}$), which require an operating temperature To of about 50.0 mK; a cryocooler is required to achieve and maintain this low temperature. The dynamic range of the detectors has been estimated as at least 10000 in order to be able to detect optical powers as high as 3.45x10-15 W without saturation.

Every GM contains 5 rows of 150 Transition Edge Sensors (TES) (4 rows of 126 TES for SAFARI 4.2). The dispersed radiation is coupled into the detectors with feed horns. The optical power absorbed by a voltage biased detector will change the resistance and thus the current through the detector. This current is sensed by a Front-End SQUID amplifier. An additional amplifier, the AMP SQUID, is used to provide sufficient gain to overcome the long cable harness.

As the linear input range of the SQUID amplifier is limited, a feedback loop called Base Band Feed Back (BBFB) is used to reduce the excursion range. The detector control unit (DCU) dynamically generates the bias voltage and a feedback signal for each detector. The instrument control unit (ICU) commands and supervises all the operations and the status of the instrument. In the high-resolution light path, the only difference is that the BSM redirects the incoming beam (telescope or calibration source beam) into the Fourier transform spectrometer (FTSM).

The FTSM is a Martin-Puplett interferometer with a 3 cm mechanical stroke. The optical path has a folding factor of 8 for a total of 24 cm optical stroke. This stroke is enough to provide, combined with the GM, an intrinsic resolution between 1500 at the longest wavelengths, and 11000 at the shortest wavelengths.
The maximum scan velocity of the FTSM is constrained by the maximum detector bandwidth that can be realized at the lowest wavelength (SW band, 34 um). In order to avoid phase errors in the reconstructed spectrum and velocity jitter errors, the minimum detector bandwidth for the SW band is specified as 40Hz whereas the maximum modulation frequency is 20Hz. A single full stroke of the FTS lasts 410 seconds including the acceleration ramps.

There are harnesses to interconnect electrically all the sub-units with their respective driver. Also, thermal straps join components to operate under specific thermal requirements. Interfaces with the instrument and the spacecraft are: Mechanical, thermal, electrical power, electrical commands, electrical data science. For calibration purposes, SAFARI includes a blackbody source attached to an integrating sphere with filtered output for in band light supply only. The beam steering mirror is capable of redirecting the calibration beam into SAFARI light path.

A representation of the FPU mechanical design of SAFARI 3.0 and SAFARI 4.2 are presented in Figure 5-11 a) and b), respectively.

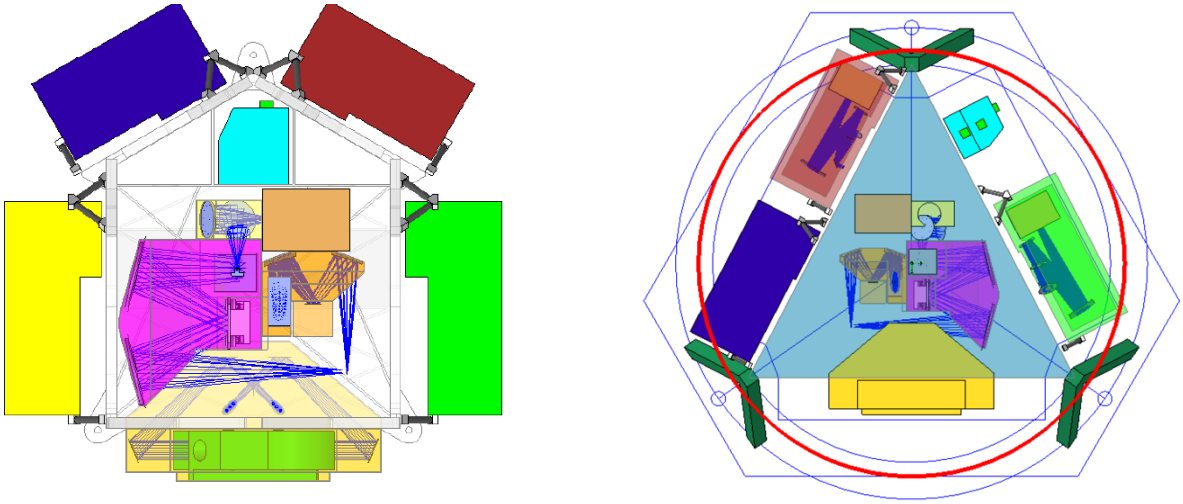

a) b)

Figure 5-11: SAFARI FPU mechanical design: a) SAFARI 3.0, b) SAFARI 4.2

Observing modes

Table 5-7 provides a summary of the SAFARI observing modes and the components of SAFARI and the telescope used.

Mode	Resolution	Modules	Components	Timing	Flux Accuracy Absolute / Relative	note
Stare - HR	High (from 1500-11,000)	FTS + Grating	CSA-on CSA-off, BSM, MS, FTS	410 s per FTS scan	10%/1%	
Stare-step LR	Low (~300)	Grating	MS, BSM, CSA-on, CSA-off	BSM at 2Hz	10%/1%	Step is performed by BSM and satellite
Stare-step HR	High (from 1500-11,000)	FTS + Grating	MS, BSM, FTS, CSA-on, CSA-off	410 s per FTS scan	10%/1%	Step is performed by BSM and satellite
Stare-step MR (TBC)	Medium from 400-3000 -	FTS + Grating	MS, BSM, FTS, CSA-on, CSA-off	110 s per FTS scan	10%/1%	Step is performed by BSM and satellite
On-The-Fly (OTF)	Low (~300)	Grating	MS, BSM, CSA-on, CSA-off	BSM at 2Hz	10%/1%	Continuous scan performed by BSM and satellite

Table 5-7: SAFARI observing modes: Systems/components used per observing mode

Detectors

The three main blocks within the SAFARI detector technology development program are:

- The linear detector arrays on "stitched" silicon wafers
- The multiplexed detector readout and control electronics,
- The grating modules and focal plane arrays that house them.

SAFARI's requirements for large linear arrays of TES detector pixels with low noise (NEP_{goal} = $2x10^{-19}$ W/√Hz) and efficient optical coupling (64% coupling to the instrument's geometrical optical throughput) are addressed by the integration of SiN-isolated TES detectors with a horn-absorber optical coupling scheme. To achieve the required number of spectral bins for the spectral sampling, the TES detectors, with a typical pitch of ~ 0.8 mm, cannot be fabricated on a single silicon wafer. Multiple wafers therefore have to be "stitched" side-by-side.

With a cooler base temperature of 50 mK, the combination of a TES with Tc = 100 mK and thermal isolation by high aspect-ratio SiN support legs, it has been demonstrated to be sufficient to reach the goal NEP of $2x10^{-19}$ W/√Hz, with a performance already demonstrated in the lab. Electro-thermal feedback in voltage-biased TES's and a low thermal mass combine to ensure that even with the high thermal isolation required to achieve the instrument's sensitivity goals, response speeds that are compatible with a fast-scan FTS can still be achieved.

The horn-absorber coupling scheme planned for SAFARI is designed to offer high optical coupling efficiency, while maintaining a low suspended thermal mass (for high speed) and high thermal isolation (for low NEP). A multi-mode pyramidal horn geometry maximizes the horns' filling fraction in the focal plane and offers the potential for high optical coupling to the instrument's multi-mode optical beam

A detail of the manufactured TES detector and stitched arrays, as well as the detailed design of the horn block and filters is presented in Figure 5-12.

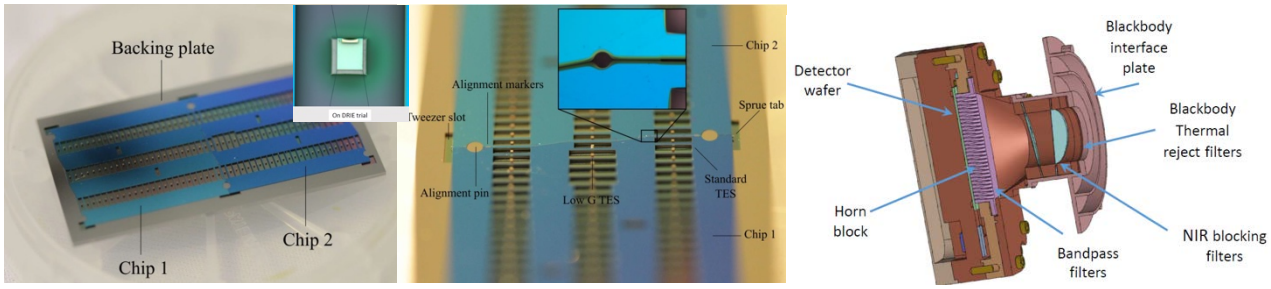

Figure 5-12: SAFARI TES detector, stitched arrays and horn block.

Interface and Resource Requirements

Information on interfaces and budgets is presented in section 5.4. For completeness, the main differences in terms of mass of the different SAFARI configurations is presented in Table 5-8.

Unit		4.2 4x126 R200 12ch		4.0 5x150, R235 18ch		3.0 5x180 R250 20ch	
Grating Modules[1]	0.5 mm mag.shield	54.6		60.6		54.4	
FPU structure	Structure + covers	48		52.0		37.7	
IOM	Mirrors, structure, BSM	3.4		3.4		3.4	
MSO	Mirrors, structure, MSM	2.1		2.1		2.1	
	FPU main sub total	+	108.1	+	118.1	+	97.6
CSO	Mirrors, structure, CS	2.31		2.31		2.31	
FTS	Mirrors, structure, FTSM	10.95		10.95		10.95	
BMDO	Optical elements, HWP, structure	4.6		4.6		4.95	
CryoCooler		6.2		6.2		5	
Other	Filters, harness, etc	6.5		6.5		6.5	
	FPU units sub total	+	30.6	+	30.6	+	29.7
Warm units	ICU	15.5		15.5		15.5	
	DCU	12.1		13.3		13.1	
	WFEE	5,4		6.3		6.5	
	Warm units sub total	+	33	+	35.1	+	35.1
	SAFARI total		171.7		183.8		162.4
	(FPU bipods)		(9.0)		(9.0)		(0)
Cryo harness	number of wires for detector system		60%		90%		100%

SAFARI [1] 4 GMs for 3.0, 3 GMs for 4.x

Table 5-8: SAFARI mass breakdown (CBE) evolution: SAFARI 3.0, 4.0 and 4.2.

Predicted Performance and Margin

The sensitivity calculation and assumptions for the SAFARI 4.1 configuration are presented in this section for two cases, the baseline and CBE. The baseline defines a set of parameters which are used as requirements for design and development of SAFARI 4.1. The Current Best Estimates (CBE) represent what it is expected SAFARI may get if all things go well, and can be considered as the goal/target. The CBE does not include margin, the baseline effectively is the CBE plus a margin.

For clarity, SAFARI 4.1 is equivalent to SAFARI 4.0 in terms of channels (18 ch), resolution (R ~ 235) and spatial pixels (5) but 144 spectral pixels per GM. The wavelength specification of the three bands is summarized in Table 5-9. These bands are applicable to SAFARI 4.0, 4.1 and 4.2.

Band	λmin (μm)	λc (μm)	λmax (μm)	Fractional BW
S	34,0	48,8	63,6	1,87
M	61,8	88,7	115,6	1,87
L	112,2	161,1	210,0	1,87

Table 5-9: SAFARI 4.0-4.1-4.2 wavelength band specification.

The results of the baseline and CBE sensitivity analysis, extended to the full wavelength bands of each sub-array, for the LR and HR mode are indicated in Figure 5-13 a) and b) respectively, where the black lines represent the baseline and the blue lines the CBE.

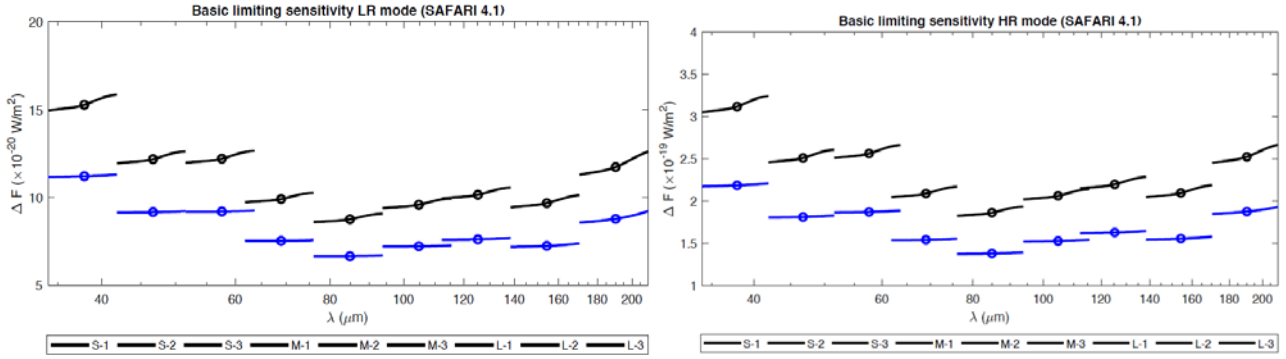

a) b)

Figure 5-13: Comparison of baseline (black) and CBE (blue) SAFARI performance: a) LR mode, b) HR mode

A comparison of the SAFARI 4 sensitivity in LR mode with respect to the M5 proposal configuration and SAFARI 3.0 is presented in Figure 5-14.

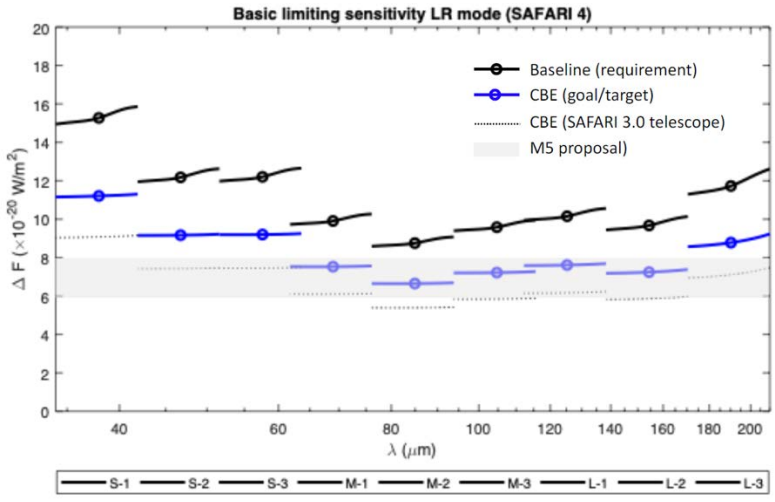

Figure 5-14: SAFARI 4 limiting sensitivity in LR mode compared to M5 proposal baseline and SAFARI 3.0 telescope assumption.

The analysis presented in this document (with the sensitivity summarized in Figure 5-14) indicates a reduction in SAFARI capabilities both in terms of sensitivity and spectral resolution (in the low resolution mode). Discussions at SST level indicated that these capability reductions would not fundamentally invalidate the SPICA/SAFARI science case. To maintain the M5 specified sensitivity SAFARI would need to target the updated CBE values. This would require further

internal iteration and consolidation within the SAFARI consortium, as we would need to deviate from the current baseline assumptions and requirements.

Integration, Testing and Calibration

A summary of the SAFARI general flow for the AIV and testing process is presented in Figure 5-15 and Table 5-10, respectively.

Model	Requirements to verify	Units	FPU	ICU	DCU	WFEE	On Board Software	FPI Warm Harness	FPI Cryo Harness
STM									
Mechanical	Static Assembly		T	T	T	T	T	T	T
	Dynamic								
Thermal	Operation Temperature		T	A	A	A	A	A	T
	Power dissipation		T	T	T	T	T	T	T
	Stability		T	A	A	A	A	A	T
	Operation cycles		T						T
DM									
Performance	Wavelength range		T	T	T	T	T	T	T
	Spectral resolution		T						
	Spatial resolution		T						
	Spatial coverage		T						
	Spatial coverage		T						
	Sensitivity		T	T	T	T	T	T	T
	Absolute intensity accuracy		T						
	Relative intensity calibration		T						
	Operation modes		T	T	T	T	T	T	T
	Signal processing/reconstruction		T					T	T
Mechanical	Static		A	A	A	A	A	A	A
	Dynamic		A	A	A	A	A	A	A
Thermal	Operation Temperature		T	T	T	T	T	T	T
	Cooling power		T						T
	Stability		T	T	T	T	T	T	T
	Operation cycles		T						T
Environmental	Electromagnetic		T	T	T	T		T	T
	Electric Fields		T	T	T	T		T	T
	Magnetic Fields		T	T	T	T		T	T
	Tempetarure Cycles (No cryo)			T	T	T	T		
QM									
Performance	Wavelength range		T						
	Spectral resolution		T						
	Spatial resolution		T						
	Spatial coverage		T						
	Spatial coverage		T						
	Sensitivity		T						
	Absolute intensity accuracy		T						
	Relative intensity calibration		T						
	Operation modes		T	T	T	T	T	T	T
	Signal processing/reconstruction		T	T	T	T	T	T	T
Mechanical	Static		T						
	Dynamic		T	T	T	T	T	T	T
Thermal	Operation Temperature		T						T
	Cooling power		T						T
	Stability		T						T
	Operation cycles		T						T
Environmental	Electromagnetic		T	T	T	T	T	T	T
	Electric Fields		T	T	T	T	T	T	T
	Magnetic Fields		T	T	T	T	T	T	T
	Tempetarure Cycles (No cryo)			T	T	T	T		
FM									
Performance	Wavelength range		T						
	Spectral resolution		T						
	Spatial resolution		T						
	Spatial coverage		T						
	Spatial coverage		T						
	Sensitivity		T						
	Absolute intensity accuracy		T						
	Relative intensity calibration		T						
	Operation modes		T	T	T	T	T	T	T
	Signal processing/reconstruction		T	T	T	T	T	T	T
Mechanical	Static		T						
	Dynamic		T	T	T	T	T	T	T
Thermal	Operation Temperature		T						T
	Cooling power		T						T
	Stability		T						T
	Operation cycles		T						T
Environmental	Electromagnetic		T	T	T	T	T	T	T
	Electric Fields		T	T	T	T	T	T	T
	Magnetic Fields		T	T	T	T	T	T	T
	Tempetarure Cycles (No cryo)			T	T	T	T		

Table 5-10: SAFARI test matrix

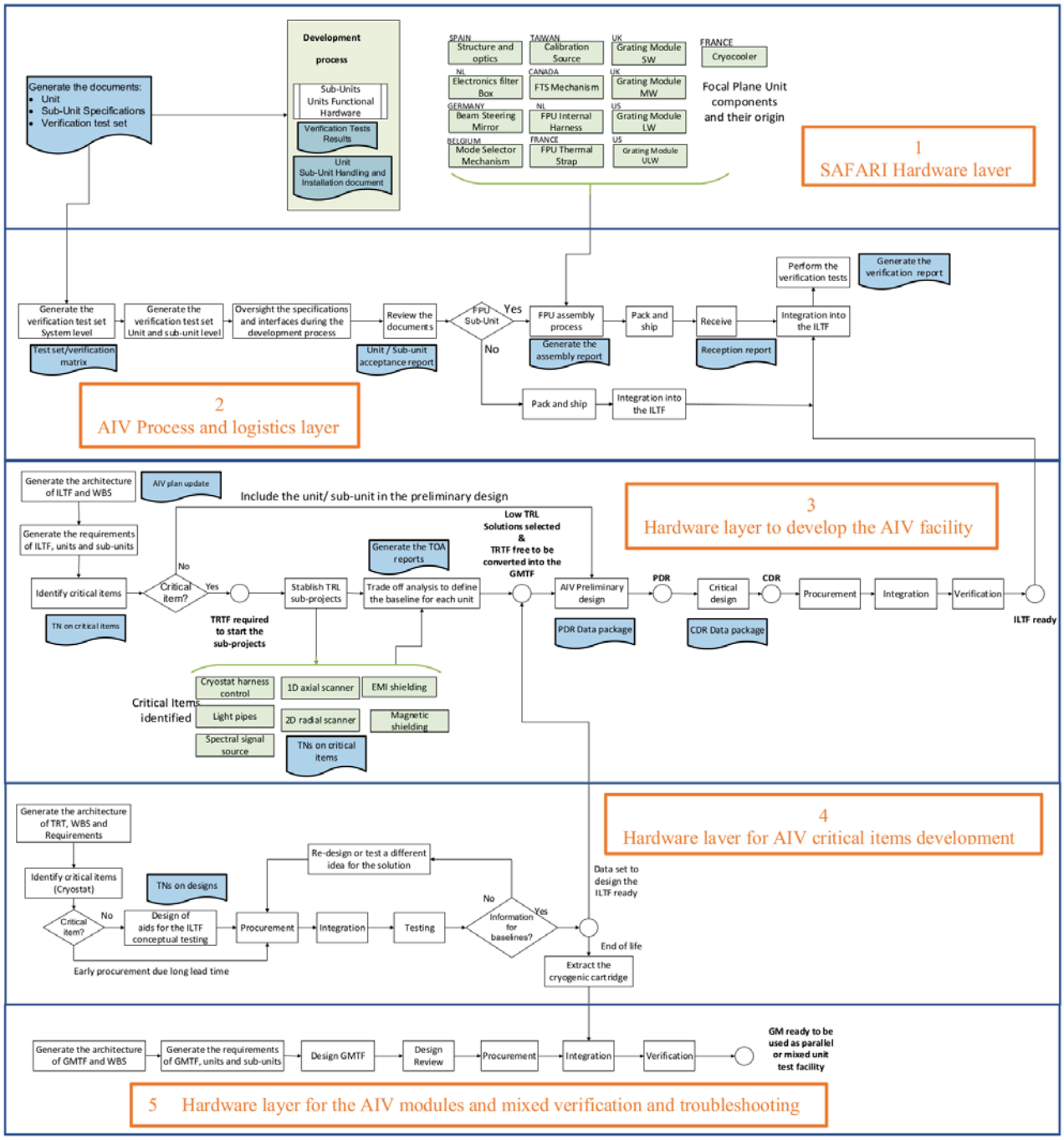

Figure 5-15: SAFARI general flow for the AIV process.

Different calibrations would be performed throughout all SPICA mission phases. Before Integration within the satellite the instrument performance shall be assessed in the laboratory which shall provide an initial calibration of key components of SAFARI:

- Wavelength coverage and resolution
- Initial absolute flux, flatfield, RSRF Focal plane geometry & Astrometry Detailed instrument PSF
- Spectral/Spatial detector responses
- Photometric band passes

For some of these components this calibration remains unchanged throughout later phases, ie. The detectors parameters:

- response,
- linearity,
- time constants,
- dynamic range,
- read noise,
- noise spectral power

Just after launch, in the very early phases of the mission, the SAFARI instrument together with the SPICA satellite would perform further tests and calibrations. This will be the first time that SAFARI is assessed and calibrated to verify its performance in full under the flight environment conditions. Some parameters are: calibration source flasher and load to determine detector time constants in flight, and wavelength calibration, performance of implemented observing modes and the determination of instrument NEP among others.

- During the mission, there will be calibration steps taken for each observation (for example, calibration source observations) and specific calibration observations to determine or monitor instrument parameters like absolution flux calibration.
- Validation wavelength (planetary nebulae, evolved stars)
- Absolute Flux calibration on sky calibrators (fiducial stars, faint asteroids) Flatfield on any extended source
- PSF with real telescope at limited detector array positions
- Monitor of detector response
  - Periodic (1/week TBD) monitor of CS LR and HR spectral features
- Calibration time scales
  - blind pixels ~15min – internal flasher
  - ~day – internal response flat, cold shutter, internal wavelength reference monitoring
  - ~week – reproducibility sky wavelength & flux sources
  - ~mission – dozens of absolute flux calibrator measurements, systematic error SQRT(n)
  - Fiducial stars
  - Faint asteroids
  - Cross-calibration with Herschel, JWST: Herschel observations of several suitable sources available already, missing sources to be observed in cross-calibration program soon.

Table 5-11 summarizes the SAFARI calibration parameters to be measured and monitored during the different mission phases.

ID	Parameter	Explanation
CP-1.	Absolute Spectral Flux	The requirement states 10% (post processing) and it depends on external calibration sources.
CP-2.	Relative spectral flux	Relative flux refers to the calibration across a spectrum. The measured flux at one wavelength relative to another wavelength should be shown within 1% (post processing) in high resolution observing modes. In low resolution observing modes, the requirement is 0.1% (post-processing).
CP-3.	Wavelength calibration	Wavelength calibration requirements are 1% (post processing) in the SAFARI Science Requirements Document for both low resolution and high-resolution modes
CP-4.	Beam steering mirror	Actuator to angles: sky to focal plane Link with detector response (TBC)
CP-5.	Spectral/Spatial Detector Response	Dependent on BSM position? Drives relative flux calibration, wavelength calibration and FTS calibration.
CP-6.	FTS zero displacement	Calibration source to determine and set. Key input to FTS wavelength calibration.
CP-7.	FTS scan speed/step size	
CP-8.	Detector Non-linearity	
CP-9.	Detector dynamic range	
CP-10.	Detector time constants	
CP-11.	Non-linearity	The CS flasher in combination with the CS broad band emitter, could be used to calibrate the non-linearity of the detectors since the time constant depends on loading.
CP-12.	Purity	
CP-13.	Cross talk matrix	The TES detectors may experience cross talk. The stable component will be corrected by applying a cross talk matrix.

Table 5-11: SAFARI Calibration parameters to be measured and monitored during different mission phases

Heritage and Enabling technologies

The main critical technologies identified for SAFARI are the following:

- Detector technology
- Detectors system and Focal Plane Array
- Sub-K cooler
- Mode selector mechanism
- Fourier Transform Spectrometer (FTS)
- Half-wave plate
- Grating modules

5.3 Far-infrared Polarimeter (B-BOP)

Instrument description

B-BOP is an imaging instrument, providing diffraction-limited imaging simultaneously in total power mode, i.e. measuring the total flux of the sky, and in a polarimetric mode, where it records signals that are linked to the linear polarised fraction and linear polarisation angle of the incoming flux. Indeed, unlike most polarimetric imagers, polarisation is not measured using an optical device that splits the incoming light according to its polarisation state. Rather B-BOP's detector arrays are composed of two types of pixels where, in each pixel, the power imbalance between two orthogonal grids of absorbers is recorded, with a rotation of 45° between the two types of pixels. Pixels are arranged in a checkerboard manner in the focal plane, and the pixel sizes are adjusted so that the spatial sampling frequency of each type of pixel is well within the Nyquist criterion. Full spatial sampling is recovered by scanning the sky.

B-BOP carries 3 imaging channels, or bands, centred at 70 μm for band 1, 200 μm for band 2 and 350 μm for band 3. Each channel has a resolving power ($R = \lambda/\Delta\lambda$) of order 2-3. The 3 channels image a common field of view of approximately 160"x160".

To operate, the B-BOP detectors need to be maintained at 50 mK. This temperature is delivered by a hybrid cryo-cooler of the same family as that used by SAFARI. The instrument itself is maintained at 2 K for the part that is closer to the detector (the bolometer focal plane and the camera optics), and at 4K for its main structure and the entrance optics.

B-BOP carries three arrays of silicon bolometers corresponding to three spectral bands centred at 70, 200 and 350 microns (1344 detectors in total). The bolometer arrays are cooled down to 50 mK and contain their own cryogenic frontend electronics which is directly integrated below the detection stage. A differential read-out scheme enables the simultaneous detection of the total intensity and the polarization level of the submillimetre light, for each individual pixel.

B-BOP consists of three main elements:

- The Focal Plane Unit (FPU) which sits on the Instruments Mounting Structure (IMS), next to the SMI and FGS (TBC) focal plane units, and on the opposite side of the SAFARI focal plane units.
- The Cold Front-End Electronics which is a relay element that serves to carry the signals from the bolometers to the electronics on the SVM.
- The Warm Electronics, on the SVM performs all the control and readout functions of the instrument.

The FPU and CFEE belong to the Payload Module (PLM), while the Warm Electronics belong to the Service Module (SVM). All these elements are connected with a cryo-harness which is the fourth "element" of the instrument. Taken together these 4 elements (FPU, CFEE, WE, and harness) form the so-called Focal Plane Instrument (FPI).

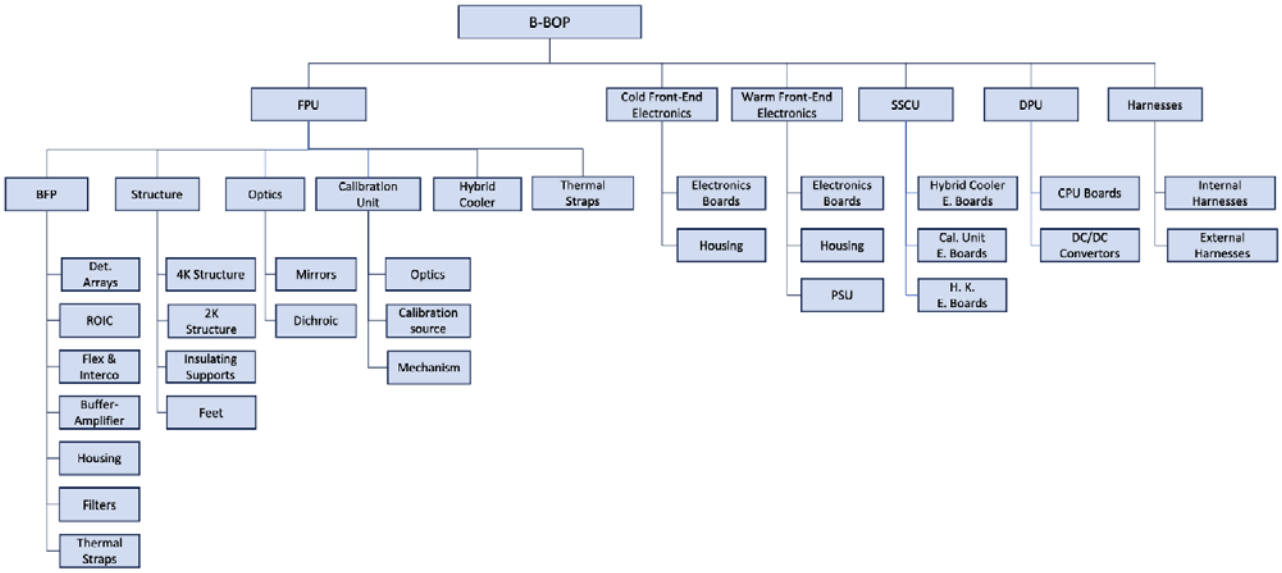

Figure 5-16: B-BOP product tree (ground-based support and test equipment not represented)

The B-BOP Bolometer Focal Plane (BFP) is shown in Figure 5-17. The light blue indicates the 50mK stage, the blue one is the 300mK box and the green envelope represents the 1.8K housing. The detectors arrays are the yellow structures at the heart of the BFP. Kevlar strings, ribbon cables between the different temperature stages and connectors are indicated.

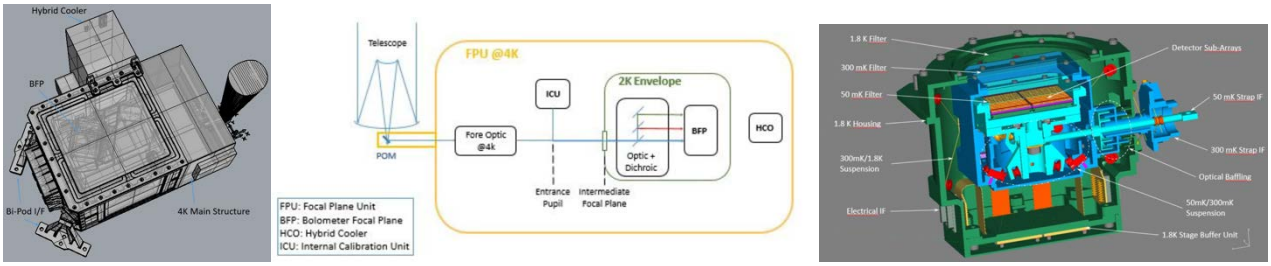

Figure 5-17: B-BOP FPU mechanical design, optical design and Bolometer Focal Plane (BFP)

Observing modes

The instrument modes for B-BOP are the following.

- Off: All elements on the PLM are off, all elements on the SVM are off. This is likely the mode in which the instrument will be during Launch and Early Operations.
- Stand-by "warm": The DPU, WFEE, SSCU on the SVM are on, the Hybrid Cryo-Cooler ready to be recycled, the CFEE is off, the detectors are not biased.
- Test "warm": In addition to Stand-by "warm", the detectors are now biased, with a setting that is compatible with the fact that their current temperature is that of the 2 K level. The CFEE is on.
- Recycling: In addition to the Stand-by "warm" mode, the SSCU executes the sequence of commands that recycles the cooler.
- Stand-by "cold": The cooler has been recycled and therefore the detectors are at their operating temperature. The DPU, WFEE and SSCU are on, and the detectors are biased with a setting that is compatible with their temperature (but may not be the operational bias setting).

- Operating: In addition to Stand-by "Cold", the detectors are now biased with a setting that is optimized for operations. Detectors are read continuously. This mode has two sub-modes:
  - Internal Calibration Sequence (ICS): The internal calibration system is operated for a predetermined calibration procedure. The actual pointing of the telescope is either irrelevant or toward an appropriate region of the sky (TBD).
  - Observing (OBS): The internal calibration system is off and the telescope is used to achieve a scientific observation or an external calibration. The observing mode parameters are entirely within the pointing system. There is no B-BOP specific operation during an observation (apart from continuously reading the detectors).

Figure 5-18 gives a likely scenario for the way the instrument can switch between modes.

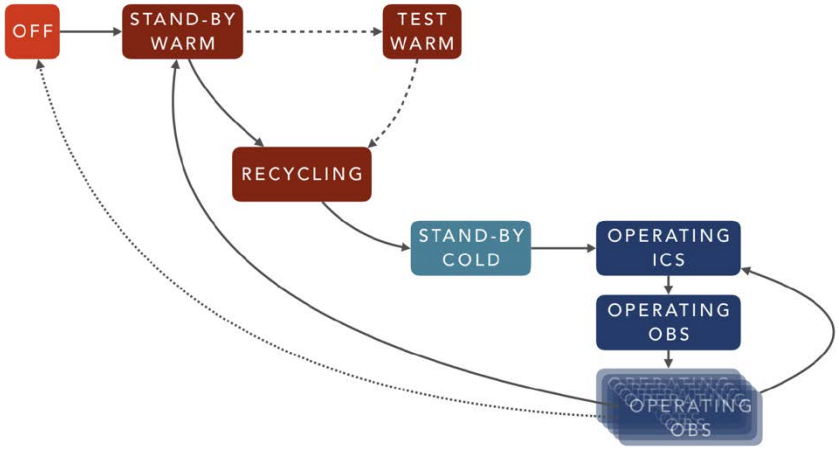

Figure 5-18: A plausible scenario linking the different modes of B-BOP

Detectors

The B-BOP detectors of each band are polarization-sensitive bolometers cooled to an operation temperature of 50mK. They use a similar principle to record signals from which the polarization properties of the incoming power can be derived.

The basic principle starts with a fully symmetrical Wheatstone bridge that is implemented in the pixel, as shown on Figure 5-19 **a)**. This electrical circuit contains fixed load resistors (Rc) which are located on each side of the pixel and thermally connected to the 50 mK bath, and variable resistors (RH and RV). The H and V refers to Horizontal and Vertical. Indeed, these variable resistors correspond to the cyan, red, blue and yellow "spirals" in the pixel (right-hand panel of
Figure 5-19 a)) which are doped silicon beams that carry a grid of either horizontal or vertical dipoles. The red and yellow spirals carry horizontal dipoles and thus each constitutes a RH resistor, while the cyan and blue spirals carry vertical dipoles and constitute the RV resistors.

Because each spiral carries dipoles oriented in a single direction, it couples to the incoming light in a way that is dependent on the polarisation fraction, p, of this light and of its polarisation angle, ψ.

On each pixel two quantities are measured, indicated on the left of
Figure 5-19 a). Vamp is linked to the total amplitude of the incoming power, while Vimb is linked to the imbalance between the power absorbed by the vertical and horizontal grids and thus is a function of p and ψ. To disambiguate the two, a second type of pixel is used with the same doped silicon spirals but where the dipoles have been rotated by 45°. So instead of measuring the imbalance of the power absorbed by a grid at 0° with respect to a grid at 90°, the imbalance of the power absorbed by a grid at +45° with respect to a grid at -45° is measured.

A detector matrix is thus made of a succession of these two types of pixels, arranged in a checkerboard manner.

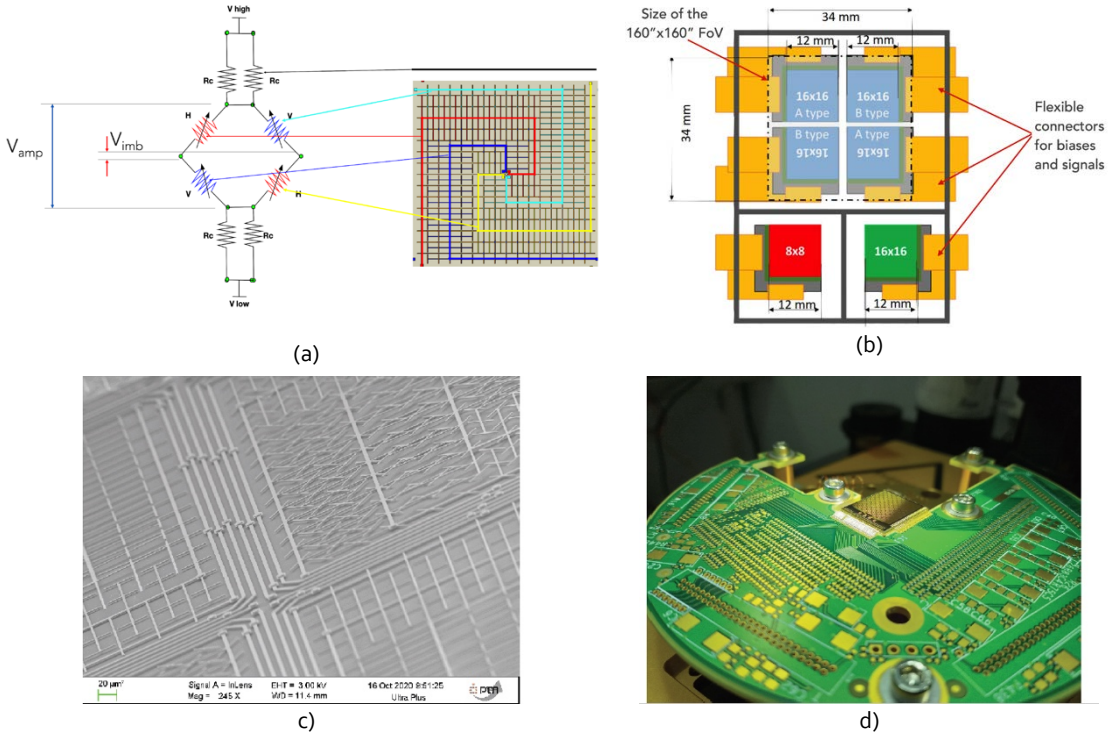

Figure 5-19: a) The principle of B-BOP's pixel (electrical circuit and physical implementation). b) Physical arrangement of the detector matrices. c) Manufactured and d) integrated detector on the test set-up for ground-based characterization.

In order to achieve the full sampling of the PSF in each band and considering that all bands have a similar field of view, the number of pixels per band is a function of the wavelength with the following implementation:

- Band 1: 4 detector matrices of 16x16 pixels each
- Band 2: 1 detector matrix of 16x16 pixels
- Band 3: 1 detector matrix of 8x8 pixels

Figure 5-19 b) presents the physical arrangement of the detector matrices on the BFP, as seen from above, looking at the detectors' sensitive side.

Interface and Resource Requirements

Information on interfaces and budgets is presented in section 5.4.

Predicted Performance and Margin

The following list describes the elements that enter in the sensitivity computation for B-BOP. Unless specified otherwise, the quantitative information given in the list below corresponds to the CBE situation.

- **Camera Optics**: this corresponds to the optical elements (mirrors and dichroic mirrors) within the camera optics at 1.8 K. A representative number of 6 components for all three bands is considered. Each optical component is attributed an emissivity of 3%, and we considered that the optical transmission of this ensemble is globally 0.5 (essentially due to the presence of the filters and dichroic mirrors).
- **Entrance Optics**: this corresponds to the mirrors of the entrance optics at 4.8 K. In the current design there are 7 optical surfaces, and as the beam is not yet separated into wavelength channels this number is the same for all three B-BOP bands. The same emissivity (3%) as for those in the camera optics is used for these mirrors, and given that

this part of the optics is made solely of mirrors, the optical transmission from the entrance optics to the detectors is effectively 1.

- **Telescope**: The telescope mirrors (M1 and M2) contribute to the background level and photon noise at the detector. Their temperature is assumed to be 8.0 K. M1 is considered as a 2.5m diameter disk with a 25% obscuration, and M2 occupies the same solid angle. Both surfaces are taken to have a 4.5% emissivity. The optical transmission applicable to the telescope is also 1 (as per the MRD, AD1, the telescope's transmission shall be better than 0.97, thus at this stage it can safely be considered that all transmission losses occur in the instrument).
- **Zodi**: The zodiacal light represented in B-BOP bands by a 265K black-body with an emissivity of 10^{-7}.
- **CIB**: The Cosmic Infrared Background (unresolved galaxies) represented in the B-BOP bands by a 30K black-body with an emissivity of $2.25\ 10^{-6}$.
- **CMB**: The Cosmological Microwave Background as a perfect 2.725K black-body.
- **Detectors**: The physical principles at work to transform the incoming radiation into a temperature elevation, and then through the readout circuit into a voltage variation induce their own contribution to the noise, and hence sensitivity. B-BOP has a top-level requirement that this contribution amounts to a detector NEP of less than 3×10^{-18} $W.Hz^{-1/2}$. Physical models of the detectors have shown that the expected performance is better than this level but this is not considered in the CBE.

The Evolution of the sensitivity parameters in the three sensitivity scenarios, CBE, Nominal and Worst-case, is presented in Table 5-12. The CBE column has the actual values used by the sensitivity estimation code, while the Nominal and Worst-Case column list the factor by which the CBE value is degraded. For all parameters except the transmission, degrading the parameter value mean multiplying it by this factor. For the transmission, it means dividing it by this factor.

	CBE	Nominal	Worst-Case
Transmission	0.5	/1.2	/1.4
Entrance Optics Temperature (K)	4.8	×1.15	×1.3
Telescope Temperature (K)	8.0	×1.1	×1.3
Telescope Emissivity (%)	4.5%	×1.1	×1.3
Detector NEP ($W.Hz^{-1/2}$)	$3\,10^{-18}$	×1.0	×1.5
Stray Light Factor	1.0	×1.1	×1.3

Table 5-12: B-BOP sensitivity parameters.

In Table 5-13 the sensitivities that result from these three scenarios/levels are compiled. One should note that they correspond to situation where everything that could have gone wrong actually has. Whether or not this is realistic is debatable but should be considered when communicating/using these numbers. Only the point source sensitivity in total power is provided for the time being, when the sensitivity scenarios are agreed mission-wide, the table may be completed with the sensitivities for extended source as well as those corresponding to the polarisation fraction measurement.

Source type	Case	70 μm	200 μm	350 μm
Point Source Sensitivity	CBE	0.11 mJy	0.37 mJy	1.29 mJy
(5σ,10 h, 1 square degree)	Nominal	0.13 mJy	0.55 mJy	2.05 mJy
	Worst-Case	0.23 mJy	1.22 mJy	4.12 mJy

Table 5-13: B-BOP Sensitivities in the CBE, Nominal and Worst-Case scenarios.

Integration, Testing and Calibration

Model/ Sub-Assemblies	Sub-Array	BFP	HCO	CU	Assembled FPU (BFP + HCO + CU + FPS)	CFEE	WFEE	SSCU	DPU
CQM									
Performances Tests • Sensitivity • NEP	 T T	 T T			 T T	T	T	T	T
Physical Properties • Mass / Dimensions • CoG / MoI		 T T	 T T	 T A	 T T	 T T	 T T	 T T	 T T
Mechanical tests • Vibrations (Sine & Random)		QL	QL	QL	QL	QL	QL	QL	QL
Thermal Tests • TV / TC • Thermal performances		QL T	QL T	QL T	QL T	QL T	QL T	QL T	QL TL
EMC tests (configuration TBD) • EMC (Radiated & Conducted) • ESD		 T Q		 T Q	 T Q	 T Q	 T Q	 T Q	 T Q
FM									
Performances Tests • Sensitivity • NEP	 T T	 T T			 T T	T	T	T	T
Physical Properties • Mass / Dimensions • CoG / MoI		 T T	 T T	 T A	 T T	 T T	 T T	 T T	 T T
Mechanical tests • Vibrations (Sine & Random)		AL	AL	AL	AL	AL	AL	AL	AL
Thermal Tests • TV / TC • Thermal performances		 T T	 T T	 T T	 T T	 AL T	 AL T	 AL T	 AL T
EMC tests (configuration TBD) • EMC (Radiated & Conducted) • ESD		 T -		 T -	 T -	 T -	 T -	 T -	 T -
• NEP	T								
DP-2									
Performance Tests • Sensitivity • NEP	 T T								
BBM									
Performances Tests • Sensitivity • NEP		 T T				T	T	T	T
DM					Deliverable for the PLM DM				
EMC tests (configuration TBD) • EMC (Radiated & Conducted) • ESD		 T T		 T T		 T T	 T T	 T T	 T T
STM		Deliverable for the PLM STM							
Physical Properties • Mass / Dimensions • CoG / MoI		 T A	 T A	 T A	 T T	 T A	 T A	 T A	 T A
Mechanical tests • Vibrations (Sine & Random)		QL (TBC)	QL (TBC)		QL	QL	QL	QL	QL
Thermo/Electrical Tests • TV					QL	QL	QL	QL	QL

I: Verified by Inspection
A: Verified by Analysis
T: Verified by Tests

QL: Qualification Level
AL: Acceptance Level
NA: Not Applicable

Table 5-14: B-BOP verification matrix

For B-BOP, calibration can mean two things:

- Performing an observation of an astronomical calibrator. In the present context, this is just another observation, similar to any science observation.

- Using the internal calibration system of B-BOP to monitor key elements of the detectors' response.
  - Less dependent on the spacecraft actual pointing (e.g. stare on a clean high-visibility field).
  - Current baseline is to schedule these short sequences during an operation cycle, with a frequency smaller than the observation frequency (i.e. less calibration sequences than observations).

B-BOP shall house an internal calibration device that should allow monitoring the variations in sensitivity to polarization fraction and angle to a level less than 1% (polarization fraction) and less than 1° (polarization angle).

Heritage and Enabling Technologies

The critical technologies needed to achieve the B-BOP performances are summarized in Table 5-15:

On the detectors

Critical technology	application	resolution
Silicon Spirals warping at cold.	Not controlled contact between sensors and cold bath.	For the current pixels the warping is simulated upwards. For the next detector generation two more nails will be added to spirals to control the backshort cavity
The 350 µm band is difficult to made in current technology	*The quarter wave cavity is too wide for the copper nails*	*A Si anti-reflection layer is added above the absorbers to cope with the new band.*
idem	idem	As backup, we build a high impedance surface prototype to replace the ¼ wave cavity.
Manufacture is a complex process (more that 150 technological steps)	*Even a very large step percentage of success cannot achieve a large yield*	*Almost each technological step is followed by a control step, in order to be able to perform corrections.*
Sensitivity to technological variation	Doping and etching can differ from one pixel to the next	Inside one pixel the four sensors must be well matched: this is ensured by the fact that spirals are interleaved and very close. Differences are foreseen at the array scale but mitigated by the differential readout.

On the detector uses.

Critical technology	application	resolution
Is the measured transfer function invertible?	The V_{tot} and $V_{unbalance}$ on Stokes pixels are not easily analytically inversible	To retrieve the 3 Stokes Parameters, we have at least 4 measures inside the Airy disc (8 potential), giving fast & unambiguous results from a calibration table.
Dynamic range usually limited with bolometers	*Four orders of magnitude required by scientific objectives.*	*The bias voltage can be set before observations to adapt to scenes intensities. Others strategies (supplementary nails, and multi doping, zones ...) have already been explored by models with good prospective. To be confirmed by real prototypes.*
Impact of inhomogeneities on operability of detector arrays	Can same detector setup be optimal as outputs	The different electronics levels are designed to adjust dynamically the offsets in order to take the best advantage from differential measurements.
Impact of external perturbations (thermal stability, particles hits...) on final performances.	*On other sensitive observatories in space, the external perturbations have hampered the data collection.*	*External global perturbations: almost wiped by differential measurement. For particles: the sensor cross-section is minimal in comparison with PACS detectors (0.5% of dead time). The single ended/differential electronic scheme can discriminate between the two branches of a same spiral*

On the optics

Critical technology	application	resolution
Impact of optical elements on polarization measurement	The mirrors, filters and dichroic mirrors can induce changes in the entering images polarization: linear or circular.	A known polarization degree and angle rotative calibration source can resolve this issue. The linear to circular issue cannot be done that way. A known retardance plate (Quarter Wave Plate) can resolve the problem. To avoid a second mechanism the QWP could be placed over a small fraction of one (200µm), or of the three spectral bands arrays.
The use of the calibration source can lead to a power limited dissipation. Can this affect the detector use?	*The dissipation induced by the source motor to set different angles of polarization could perturbate the detector stability.*	*The detector cooling is an active operation on the demagnetization stage ensuring a large decoupling between source and focal plane temperature.* *The impact on emission is small: few tenths of K for a source at 28 K.*

Table 5-15: B-BOP critical technologies

6 MISSION PERFORMANCES SUMMARY

Table 6-1 provides a summary of the key mission performances. All the main mission requirements are met with adequate reserve left over by the baseline design. The few minor non compliances summarized below have not been considered critical at that stage of the mission definition:

- The line sensitivity of SAFARI instrument around 45.0 µm, in low resolution mode at 5σ in less than 1-hour exposure is 10.7 10^{-20} Wm^2, which is marginally above the science requirement. The current best estimates have been extracted from the SAFARI 4.1 preliminary sensitivity analysis and corrected to account for the reduction of the entrance pupil diameter to 2.5 metre. The instrument baseline architecture with 144 spectral pixels per each of the three grating module bands has resulted in a small degradation of the estimated performances compare to the original proposal. The sensitivity performances relative to the different instrument configurations and observing modes are presented in section 5.2. This discrepancy would have required iteration with the SPICA Science Study Team but it appears that the reduction of the instrument capabilities would not fundamentally violate the science objectives.

- The thermal self-emission stray light from the Observatory incident into an instrument acceptance cone at the exit pupil of the telescope shall be attenuated by a factor 10^4. The requirement has been derived from the old SPICA telescope specification [RD24][RD25]. The view factor from observatory parts at surface temperatures above a given threshold that enters the instrument FoV at the telescope focal plane has not been calculated in phase A. It is not considered critical and the telescope surface emissivity at EoL meet the specification in the wavelength range.

- The polarization error induced by ITA is not expected to be critical. However, it shall be noted that the two following points were not studied during phase A. The impact of polarized straylight could contribute to the polarization error budget and the polarization in PSF side lobes could introduce a bias in the measurements.

- The SMI RMS wavefront error and 40% encircled energy radius at 20 µm are marginally non-compliant. The impact on sensitivity performances is considered negligible. The encircled energy stability over 1 hour was not determined in phase A but is not considered critical.

- The SAFARI sub-Kelvin cooler duty cycle is marginally non-compliant. The consolidation of the design and the consideration on uncertainties and margin on the 50mK and 300mK stages led to an increase of the heat loads. Applying those loads resulted on a duty cycle of 67%, which is significantly lower than the 75% specified. It affects the Observatory operational efficiency. An increase of the duty cycle can be envisaged by optimizing the sub-Kelvin coolers in accordance to the new heat loads, considering the transient heat loads during the recycling process and revisiting the resource allocations.

- The Observatory operational efficiency is significantly below 50%. The science observation scenario and instrument engineering overheads (i.e. recycling and annealing) dominates the overhead budget. The Observatory science operations could not be consolidated in phase A. It is expected that optimization of the observing efficiency, in particular by considering parallel operations, would permit to reduce drastically the overheads.

- The maximum cooldown duration, including decontamination, is about 120 days and exceeds requirement of 100 days. A preliminary transient thermal analysis was conducted to estimate the cooling time in orbit. It was assumed that FPI is made of Al with 334 kg and ITA is made of SiC and weighs 457 kg. The transient thermal analysis permitted to establish that SIA can reach 4.8 K in about 105 days. To estimate a more realistic cooling time, one must take the operational procedures into account. One critical operation is the decontamination operation to avoid telescope contamination by water vapor outgas.

Performance/Resources Parameters	Unit		Requirement Capability	Estimate Prediction	Margin
Sensitivity Parameters					
SMI Point Source Sensitivity at 34.0 μm (Tint=3600sec)	μJy	≤	15.0	11.0	27%
SMI Point Source Line Sensitivity at 27.0 μm (R=1300, Tint=3600sec)	Wm^2	≤	2.80E-20	1.98E-20	29%
SAFARI Point Source Line Sensitivity at 45.0 μm (R=250, Tint=3600sec)	Wm^2	≤	9.50E-20	1.07E-19	-13%
B-BOP Point Source Sensitivity in Stokes at 200.0 μm (Tint=5040sec)	mJy	≤	36.7	27.1	26%
ITA Effective Collecting Area	m^2	≥	4.0	4.08	2%
ITA Transmission at 35.0 μm	-	≥	0.97	0.97	0%
ITA Rejection of Stray Light at 20.0 μm, Normalized Detector Irradiance (NDI)	-	≤	6.20E-03	5.20E-04	92%
ITA Rejection of Thermal Emission	-	≤	1.00E-04	TBD	TBD
Polarization Parameters					
Fractional Linear Polarization Error	-	≤	1.0%	TBD	TBD
Polarization Angle Error	deg	≤	1.0	TBD	TBD
Image Quality Parameters					
SMI RMS Wave Front Error at 20.0 μm (Strehl Ratio ≥ 0.8)	nm	≤	1400.0	1415.0	-1%
SAFARI RMS Wave Front Error at 30.0 μm	nm	≤	2200.0	2180.0	1%
B-BOP RMS Wave Front Error at 200.0 μm	nm	≤	15000.0	15000.0	0%
40% Encircled Energy Radius at 20.0 μm	as	≤	0.9	0.97	-7%
80% Encircled Energy Radius at 20.0 μm	as	≤	6.00	5.07	18%
80% Encircled Energy Radius Stability over 1.0 hour at 20.0 μm	-	≤	5.00%	TBD	TBD
ITA RMS Wave Front Error at 20.0 μm	nm	≤	695.0	695.0	0.0%
Thermal Parameters					
Duty Cycle SAFARI ADR at 0.05 K	-	≥	75.0%	67.0%	-12%
Cryogenic Module Rejection Capacity at 1.8 K	mW	≤	10.0	10.0	0%
Cryogenic Module Heat Rejection Capacity at 4.8 K	mW	≤	30.0	28.6	5%
Cryogenic Module Heat Rejection Capacity at 30.0 K	mW	≤	320.0	310.0	3%
Pointing Parameters					
Absolute Pointing Error (APE)	mas	≤	500.0	260.0	92%
Relative Pointing Error (RPE)	mas	≤	150.0	100.0	50%
Absolute Pointing Knowledge Error (AKE)	mas	≤	250.0	205.0	22%
Observatory Resources					
Observatory Wet Mass	kg	≤	3750.0	3550.0	6%
Observatory Maximum Power Load	W	≤	3445.0	2650.0	30%
Observatory Decontamination and Cooldown Power Load	W	≤	1254.5	965.0	30%
Data and Link Parameters					
X-Band Uplink Telecommand Recovery Margin	dB	≥	3.0	4.42	32%
X-Band Downlink Telemetry Recovery Margin	dB	≥	3.0	5.70	47%
K-Band Downlink Telemetry Recovery Margin	dB	≥	5.0	5.29	5%
Observatory Storage Capacity	Gbits	≥	2850.0	1415.0	101%
Operations Parameters					
Observatory Operational Efficiency	-	≥	50.0%	35.0%	-30%
Observatory Slew Capability over 90 degrees Maneuvre	min	≤	15.0	11.75	22%
SAFARI Radiated Susceptibility in K-Band	mV/m	≤	20.0	20.0	0%
Observatory Residual Acceleration around SEL2	km/s^2	≤	2.00E-11	1.00E-11	50%
Maximum Cooling Time (Detract 80 days for Performance Verification)	days	≤	100.0	120.0	-20%

Table 6-1: SPICA mission performance budget

7 MANAGEMENT

7.1 Management Structure

The project management approach is expected tofollow the current practices of ESA science missions.

Within the Directorate of Science, the SCI-F department is in charge of the development of fast-track science missions, in addition to all future science mission definition, technology preparation, and science payload activities. Therefore, the SPICA feasibility and preliminary definition and implementation are assumed to be under the Future Missions Department responsibility, under the overall coordination of the Strategy, Planning, and Coordination Office. The Science Support Office is to support the mission implementation for all scientific aspects, including the interface with the science community and monitoring of scientific performance.

The SPICA Study Manager is charged with the overall responsibility for the management, implementation and execution of all technical and programmatic aspects of the mission definition that are under ESA's responsibility. As such he is the formal point of contact at study level for JAXA. SPICA study team in Japan is a pre-project preparatory team under the responsibility of the program director of ISAS, JAXA. The Japanese pre-project is referred below as SPICA-J. In parallel to its liaison with the ESA mission analyst, JAXA would also directly assist the Observatory Systems Engineer in the definition of launch environmental conditions and interfaces with the Launch Vehicle.

The SPICA Science Study Team (SST) is the main scientific coordination body of the mission and supports the assessment phase by performing the following tasks:

- Provide scientific oversight in the fields associated to the scientific theme of the mission
- Participate to the preparation and revision of the mission scientific requirements
- Assess the scientific aspects of the mission performance
- Assist in making any trade-offs
- Support the preparation of the scientific operation plan and calibration strategy
- Assist in setting-up scientific requirements on the Science Ground Segment
- Advise on the Science Management Scheme
- Produce the Assessment Study report ("Yellow Book")
- Act as a focus for the interests of the broad scientific community

The System Engineering Working Group (SEWG) is the main system engineering coordination body of the mission during the study phase. It is co-chaired by the SPICA Payload Manager at ESTEC and the Project Manager at JAXA. It advises the ESA Study Manager and System Engineers on a regular basis. The SEWG shall contain members of the ESA system and instrument teams. The Lead and Study Scientists are observers to the SEWG.

The SEWG shall support the mission definition in the following areas:

- The preliminary definition of interface requirements common to all instruments.
- The consolidation of the system budget report.
- The preparation of the System Engineering Plan (SEP), including the AIT overall logic, mission schedule and taking into considerations the lower level plans. The plan shall address all the technical activities necessary to specify, design, verify, operate and maintain the SPICA system.

When required, technical experts shall support the SEWG. The SEWG shall also define the implementation of specific working groups, i.e. EMC working group, including the scope, structure, timeline and membership. In addition, the industrial system contractor shall provide support to the SEWG working group by active participation to their meetings,

and provision of expertise on the spacecraft design in support to the trade off and analysis. It is expected that the working group results would be used for the definition of ICDs with instruments and ground segment.

The joint responsibilities to conduct the SPICA mission definition are defined in [RD19]. This document includes all content required by the ESA Project Management Standards. It would be updated to become the Joint Project Implementation Plan (JPIP), subject to the adoption of the SPICA mission and upon issuance of the Letter of Agreement (LoA) or the Memorandum of Understanding (MOU) between ESA and JAXA, should the mission be selected.

7.2 Responsibilities and Proposed Implementation Approach

SPICA is an ESA mission in collaboration with JAXA, and contributions from individual ESA Member States for the provision of payload elements. The SPICA system comprises the following segments and elements:

1. The SPICA observatory is composed of the Service Module (SVM) and the Payload Module (PLM). The PLM Module includes the Cryogenic Assembly (CRYO) and the Science Instrument Assembly (SIA). The SIA Assembly includes the Infrared Telescope Assembly (ITA) and the Focal-Plane Instrument Assembly (FPIA). The FPIA includes four instruments:
   - SAFARI, a far-infrared spectrometer science instrument,
   - SMI, a mid-infrared imager and spectrometer science instrument,
   - B-BOP, a far-infrared imager and polarimeter science instrument,
   - Two redundant Fine Guidance Sensors for attitude determination during Science observations.
2. The Ground Segment is composed of the Mission Operations Centre (MOC), Science Operations Centre (SOC), Science Data Centres (SDCs) and Instrument Control Centres (ICCs).
   - The Mission Operations Centre (MOC),
   - The Science Operations Centre (SOC),
   - The Science Data Centres (SDCs),
   - The Instrument Control Centres (ICCs).
3. The Launch Segment comprises the provision of the launch services, including Launch Vehicle (LV) and Launch Vehicle Adapter (LVA).

ESA is responsible for the overall mission management. This includes the present industrial activity for mission design and in later phases, procurement of the Spacecraft through industrial contracts, but also the management of the Ground Segment and Operations Phases, as well as shared Science Operations in coordination with the Japan Aerospace Exploration Agency (JAXA). JAXA would contribute science instrument, payload hardware, launch vehicle service, ground system and operational support. JAXA would also be expected to contribute the management of the science data centre, as well as the science operations in coordination with ESA. ESA decided to take charge of the complete SIA system design in the Phase A, in close coordination with JAXA.
The scientific instrument(s), including verification and delivery of flight model hardware and software, and scientific operations and calibration in-flight, would be developed by nationally funded instrument teams and would be provided to the industrial Contractors through ESA as customer furnished items during the Implementation Phase.

The instrument and payload studies shall be planned to run in parallel with the industrial studies. The instrument and payload requirements, design and interface information shall be planned to be fed by ESA into the industrial studies at pre-planned milestones. The definition of the SAFARI instrument would be carried out by a consortium of institutes and companies. The Netherlands Institute for Space Research (SRON) would be responsible for the activities. The Atomic Energy Commission (CEA) from France would lead the management and system engineering team that is responsible for the definition of the B-BOP instrument.

Figure 7-1 illustrates the possible roles and responsibilities of the organizations contributing to the mission. Based on consolidation of the mission and Observatory concepts in phase A, the physical accommodation and functional interface of the following mission components have deviated from the definition in Figure below:

- The Mechanical Cryocoolers System (MCS) is installed on two separate panels, which will be integrated in SVM module.
- The FGS is considered fully integrated in SMI for completion of phase A.

Finally, SOC architecture and share of responsibilities has been iterated during Phase A by the Science Ground Segment Working Group (SGSWG). The respective responsibilities are detailed in [RD17].

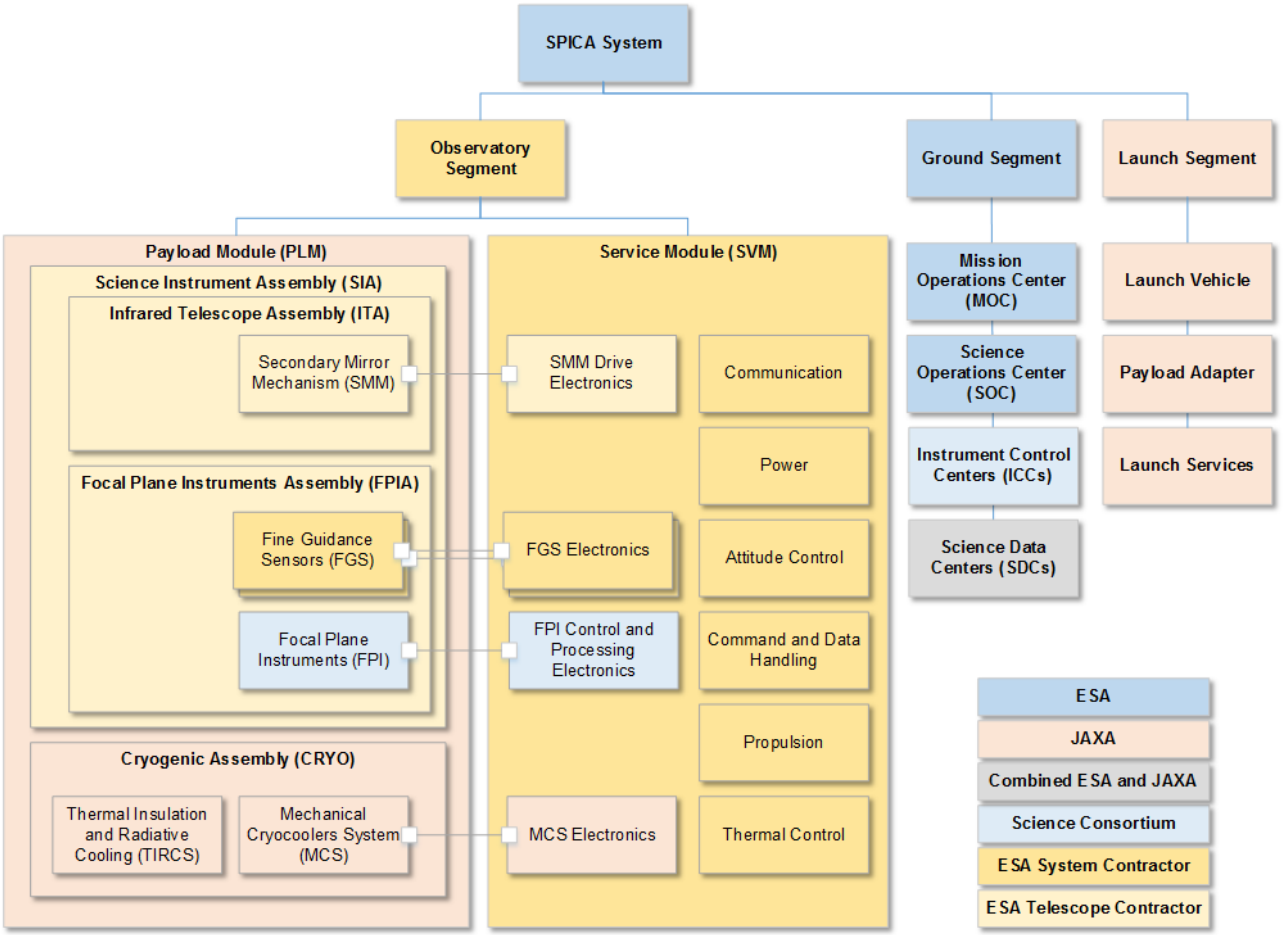

Figure 7-1: SPICA mission elements

7.3 Risk Management

ESA will implement a comprehensive risk management plan according to its established procedures as documented in ESA ECSS Standards, i.e. ECSS-M-ST-80C. Risks will be reported with management and schedule reports, at reviews and will be discussed during management team meetings and teleconferences. In parallel, JAXA will perform risk management according to its established internal procedures. Risks will be reported with management and schedule reports, at reviews and will be discussed during management team meetings.

The top risk items in this section are based on the SPICA baseline mission concept design. Risks shall be assessed in terms of their probability relative to their likelihood of occurrence and possible impact on time, cost and performance where:

1. Cost impact is measured as the M€ deviation against cost targets
2. Schedule impact is measured in calendar days against the schedule critical path

3. Performance impact is measured against technical specification and is evaluated in percentage of the targeted performance.

Schedule and Performance impacts will be translated into financial impacts.

Severity	Very Low	Low	Medium	High	Very High
Cost Increase	< 20k€	< 200k€	< 1M€	< 5M€	≥ 5M€
Schedule Impact	< 2 days	< 1 week	< 1 month	< 6 months	≥ 6 months
Performance Impact	Requirement not achieved but does not affect the mission	Requirement not achieved but the impact on mission is negligible	Requirement not achieved with degraded mission as impact	Requirement not achieved with a significant impact on the mission	Requirement not achieved with a catastrophic impact on, or loss of, the mission

Probability	Very Low	Low	Medium	High	Very High
Probability of Occurrence	P < 0.1%	P < 1%	P < 10%	P < 50%	P ≥ 50%
	Would materialize under absolute worst case assumptions	Would materialize under pessimistic assumptions	Could possibly materialize	Would not materialize under optimistic assumptions only	Will materialize almost certain

Table 7-1: Preliminary risk scoring scheme

An overall risk assessment was performed based on the preliminary scoring scheme defined in Table 7-1, and a risk rank was assigned according to the standard scale. Figure 7-2 shows the risk ranks in a 5x5 risk matrix. All SPICA top risks are yellow and considered acceptable, with the possible exception of ITA primary mirror procurement on the development schedule critical path.

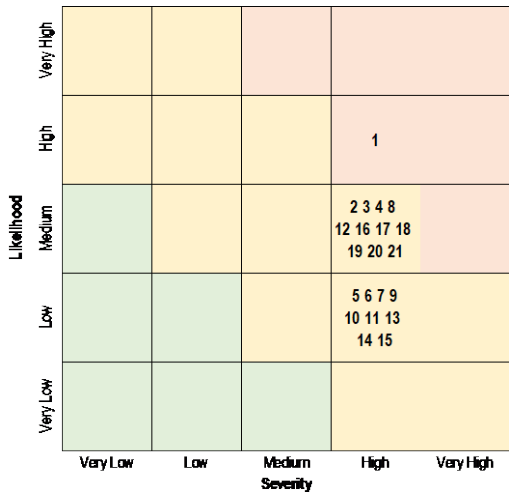

Figure 7-2: SPICA Risks Matrix

Risk	Risk Definition	Like.	Sever.	Index	Risk Assessment	Risk Mitigation	Element
1	ITA primary mirror development not compatible with Phase B2CD overall schedule	High	High	3	If manufacturing steps are not properly controlled and delayed (i.e. segments, blank assembly, proof test, polishing, coating), mission development schedule will be impacted	- Consolidate polisher capability on large mirror breadboard - Anticipate M1 development before kickoff phase B2CD - Focus advanced M&P activities on M1 perimeter	PLM/SIA
2	SIA qualified material and processes not available in due time, or not with expected properties	Medium	High	5	If qualification of material and processes is failed or longer than expected, late redesign and/or use of back-up solutions will impact development plan. Microvibration from FPI difficult to damp at source level, affecting LoS stability.	- Assess availability M&P qualification chambers. - Identify existing facilities or laboratories able to characterize material properties at 8K. - Secure material and processes baseline, released ahead of B/CD phase kick-off. - Ensure design for manufacturing feasibility on baffle. - Maintain, as far as possible, design compatibility with potential alternatives	PLM/SIA
3	ITA optical performance difficult to validate at 8K	Medium	High	5	If test facilities are not compatible with low cryogenics verification, it will impact correlation of thermal model and test schedule.	- Consolidate existing test capability in Centre Spatial de Liège (CSL) - Converge on thermal validation strategy in phase B1 - Maintain overall schedule margin in validation campaign	PLM/SIA
4	ITA M2M design feasibility not guaranteed	Medium	High	5	If M2M scaling up to 600mm M2 and 8K operation is beyond current technology coverage, it will impact procurement schedule. If HDRM needed on M2M as outcome of structural sine analysis, it will impact of launch locking system on mass, electrical I/Fs, reliability, and validation	- Assess Lessons Learned from on going M2M TDA - Assess actual acceleration levels on M2M from system mechanical analysis, to avoid useless over-sizing Implement techno BB or EQM for de-risking tests to reach TRL 5/6 for B2CD KO.	PLM/SIA
5	SIA major manufacturing problem on SiC parts	Low	High	6	If major manufacturing problem occur on M1 and Torus, which are Long Lead Items (LLIs), it will affect critical path and impact mission schedule. Spare approach is a major topic to derisk the manufacturing and having a back-up in case of anomaly	Consider procurement of spares for LLI: Torus elementary segment in spare for each kind of segments, M1 blank in spare, M2 blank in spare	PLM/SIA
6	SIA could be not enough robust to sun illumination	Low	High	6	If SIA design is not compatible with direct solar illumination during launch and transfer to orbit, it will lead to higher mass to increase robustness and could impact the stray light performances.	Implement locally a thicker baffle skin to face sun illumination due to spin during launch phase.	PLM/SIA
7	Cooling time of cryogenic system	Low	High	6	If time for cryogenic system to cool from the room temperature to the operational temperature is not compliant, it will extend in-orbit commissioning phase and affect mission performance .	- Evaluate the cooling time by performing transient cooling analysis of the whole PLM based on thermal properties of the materials to reduce the uncertainty of the estimate of cooling time. - Optimize the thermal design to reduce the cooling time (e.g. change of materials with small heat capacity).	PLM/CRYO
8	Cryocooler performances	Medium	High	5	If cryocoolers fail to provide required environment for telescope and instruments, then science will be severely impacted, resulting in diminished science	- Allocate sufficient margin in the thermal budget to respond the change of the FPI heat dissipation at later stages. - Modify the operation plan of the FPIs so that the peak heat load is to be mitigated to the allocation. - Adopt an incremental verification approach to allow for early risk mitigation.	PLM/CRYO
9	Passive cooling performances	Low	High	6	If the uncertainty of the design of thermal insulating and radiative cooling system is too large, including structural performance, it will affect the feasibility of the system and development schedule. If the performance of MLI does not meet the thermal requirements at TRL6 by MAR, it will affect schedule and system performances	- Mitigate the influence of the TIRCS design uncertainty by allocating sufficient margins - Make systematic measurements of thermal properties of the materials to reduce the uncertainty of the TIRCS design, - Conduct full thermal evaluation test at STM level. - Decide a concrete design of the thermal shields with a reliable connection between the main truss and the shields so that the thermal and structural requirements can be met. To carry out BBM demonstration of the design. - Decide the detailed requirements for MLI and to construct its baseline design by MSR. To evaluate a partial BBM by MAR. Consider alternatively a PLM design by using standard MLIs.	PLM/CRYO
10	Pipe shield and thermal strap performance	Low	High	6	If the structural and thermal interface conditions cannot meet their specification, it will affect the thermal and stability performances.	- Decide the detailed design of the piping shield and thermal straps of the cryocooler and evaluate it with a BBM. - Review the design of the whole PLM so that the piping shield which meets the interface requirements from the cryocooler can be established.	PLM/CRYO

Risk	Risk Definition	Like.	Sever.	Index	Risk Assessment	Risk Mitigation	Element
11	PLM module separation and Sun Shields deployment	Low	High	6	If sun shields fail to deploy, tehn cryocooler may not be able to cool telescope and instrument to operationa tempearture, resulting in pa partial or complete loss of the mission. If the truss separation mechanisms (TSM) does not have the required performance at TRL6 by MAR, it will impact the structural and thermal perfromances, including possible degradation of in-orbit performance due to failure of the separation.	- Decide the detailed design of the separation mechanism of the truss and sun shields deployment, and to evaluate a BBM. - For the separation and deployment mechanisms, high-reliability and flight-proven parts shall be adopted.	PLM/CRYO
12	Lifetime verification of mechanical cryocooler	Medium	High	5	If the lifetime of mechanical cryocoolers does not satisfy the mission requirements of five years.	Conduct lifetime evaluation test for 2ST cryocoolers with an improved design. The 4K-JT cooler has already passed the 5-year long life test. The life-time test for the 1K-JT cooler is on-going. At the time of March 2019, a successful operation of 3.2 years is confirmed.	PLM/CRYO
13	1K-JT cooler driver	Low	High	6	If development of 1K mechanical cryocooler could not meet requirements at TRL6 by MAR, it will impact mission schedule and science.	- Make a demonstration of the operation of the 1K cryocooler with a BBM 1K driver electronics, which is to be developed at an early stage for the requirements specific for the 1K cryocooler. - Consider possibility to use the two sets of drive electronics for the 4K-JT coolers for one set of the 1K-JT cooler. In this case the mass of the drive electronics is expected to be increased, because the number of the driving channels for 1 K-JT coolers is higher than those of the 4K coolers.	PLM/CRYO
14	Pointing performance and FGS	Low	High	6	If definition of interface between FGS and AOCS is incorrect, pointing performance and development schedule could be impacted.	- Ensure adequacy and commun understanding of FGS specification between prime contractor and instrument teams. - Request early testing of FGS by instruemmt to demonstrate performance early in programme. - Perform FGS integration test early (and off the critical path) on the AVM to mitigate any missing or incorrect requirements.	SVM
15	Microvibration	Low	High	6	If cryocooler mechanical disturbance levels or transmission through the structure at cryogenic temperature are higher than anticipated, the mission and science may be impacted.	- Implement isolation systems for RW and cryocoolers. Minimize impact of the mechanical disturbance early in the development of cryocoolers. - Characterize material behavior at cryogenics temperature - Consolidate cryocooler microvibration levels and uncertainty	SVM
16	Mission element interfaces	Medium	High	4	If complexity of interfaces and programme organization is not correctly controled, the development schedule could be impacted.	- Ensure that all stakeholders share a common understanding of the interface requirements. - Converge on the technical, schedule and validation aspects of the different mission interfaces. - Foresee at prime level sufficient margins and/or prepare back-up solutions for these interfaces - Foresee solid management of interfaces in coordination with PLM authority	SVM
17	SMI immersion grating	Medium	High	5	If immersion grating cannot meet requirements at TRL 6 by MAR, then science may be impacted.	Demonstrate the optical performance of a small sample at an early stage and replace the immersion grating with a normal grating, if necessary.	SMI
18	Mid-infrared detectors	Medium	High	5	If mid-IR Si:Sb detectors cannot meet sensitivity and thermal requirements at TRL 6 by MAR, then mission will be delayed or science may be impacted.	Demonstrate performance of the detector module which will be fabricated and tested by MAR in order to achieve TRL 5 (TBC).	SMI
19	Far-infrared detectors	Medium	High	5	If far-IR detectors cannot meet sensitivity and thermal requirements at TRL 6 by MAR, then mission will be delayed or science may be impacted.	Prepare detector system development plan. Demonstrate performance of the detector system on DM which would be subject to pre-qualification test campaign in order to achieve in order to achieve requirements at TRL 6 by MAR.	SAFARI
20	Far-infrared polarimetric detectors	Medium	High	5	If mid-IR detectors cannot meet sensitivity and thermal requirements at TRL 6 by MAR, then mission will be delayed or science may be impacted.	Demonstrate performance of the detector system on DM which would be subject to pre-qualification test campaign in order to achieve in order to achieve requirements at TRL 6 by MAR.	B-BOP
21	SAFARI mechanisms	Medium	High	5	If SAFARI mechanisms fail, then instrument functionality will be impaired resulting in reduced science return.	Prepare Fourier Transform Spectrometer (FTS) development and verification plan by MCR. Demonstrate performance of the BSM and FTS mechanisms on DM which would be subject to pre-qualification test campaign in order to achieve in order to achieve requirements at TRL 6 by MAR.	SAFARI

Table 7-2: SPICA top risks register

7.4 Preliminary Mission Development Schedule

The schedule of SPICA has been thoroughly analysed (according to a Phase A level) and dependencies between all mission element developments have been identified. The preliminary master schedule been analysed as presented in Figure 7-3, based on the following assumptions:

- A targeted launch in 2032
- M1 mirror design and manufacturing staring already at KO of B1
- A schedule reserve of six months, under full ESA control, is requested between the FAR and the start of the launch campaign. A three-month duration has been assumed for the launch campaign leading to a FAR review in Q4 2031. This is also the delivery date of the fully integrated and flight accepted spacecraft.
- A provision of project main milestone logic and phase duration, partly imposed by ESA, which would lead to phase B2, C and D durations of respectively 18, 24 and 34 months:

Mission Adoption Review (MAR)	Q2 2024
Phase B2CD Kick-Off	Q1 2025
System Requirements Review (SRR)	Q3 2025
System Preliminary Design Review (PDR)	Q3 2026
System Critical Design Review (CDR)	Q3 2028

The overall project critical path is through the delivery of the science instruments and infrared telescope (ITA). Starting from the ITA need date, and considering the long delivery time of the M1 mirror, the design and manufacturing of primary mirror would need in principle to be anticipated at the beginning of ESA KO B1 milestone, that means middle of 2022, positioned 18 months before MAR milestone. However, it shall be noted that procurement and manufacturing of the critical (and significant) components before mission adoption within the science programme is not a confirmed assumption. Further this would mean that specifications and interfaces would need to be frozen at the beginning of ESA Phase B1 for the M1, one month later for the torus, and few months later for the rest of the telescope. With the more reasonable assumption to start M1 procurement/manufacturing after MAR the launch date would shift to 2034/35.

The ITA schedule includes about 12 months industrial margin after ITA AIT and before SIA AIT in order to increase flexibility and absorb ITA AIT potential problems and CFIs delivery delays. The SVM schedule is adapted to the payload schedule. The aim is to reduce the cost by delaying the start of system activities to catch up with the instrument in time for the mating and system-level testing. This leaves just a little over one year for the PFM AIT activities before the scheduled flight acceptance and system qualification review. This compressed timeline is driven by the payload schedule, the targeted launch date and the requirements on ESA margins in the schedule and is judged as critical. A time spam of at least 18 ideally 24 months would reduce risks for delays in this phase. This should be considered in a future consolidation of key dates at project level.

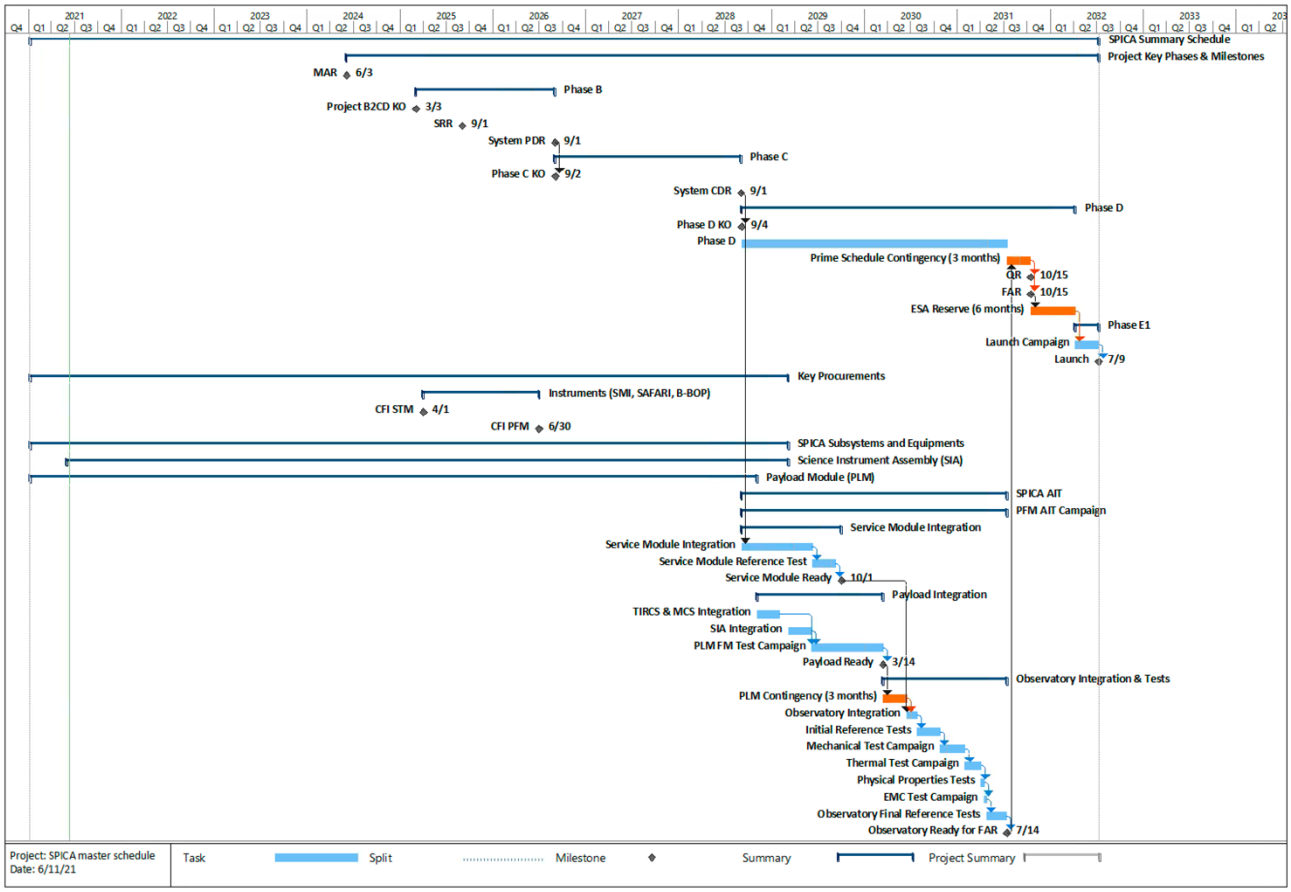

Figure 7-3: SPICA implementation master schedule

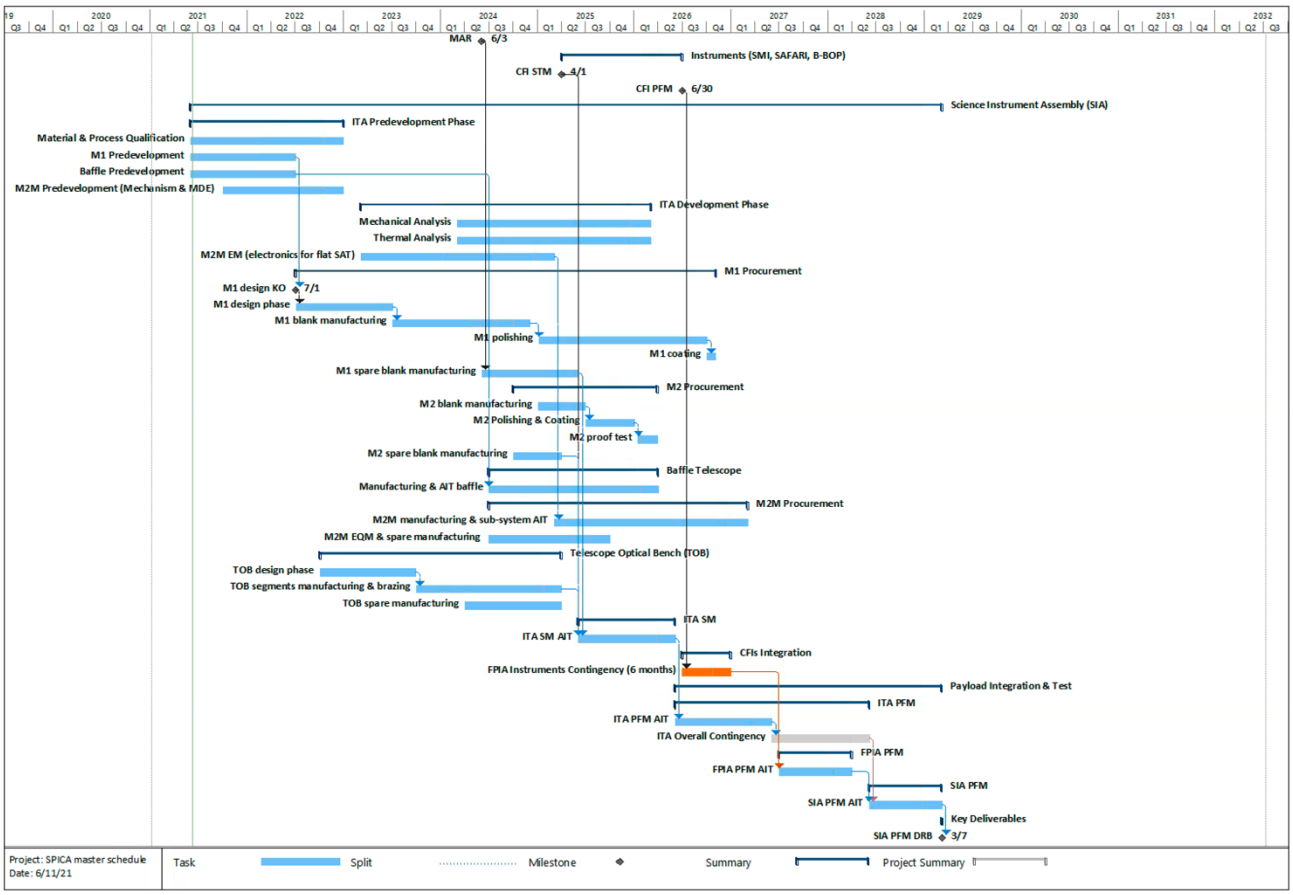

Figure 7-4: SIA development schedule

8 REFERENCES

[RD1] SPICA: Unveiling the obscured Universe. A proposal presented to ESA on behalf of the international SPICA consortium in response to ESA's call for M5 mission proposals.

[RD2] SAFARI Science Requirements. Doc no SRON-SAF-SP-2018-001. Issue 0.55

[RD3] SPICA - a large cryogenic infrared space telescope Unveiling the obscured Universe, Roelfsema et al. PASA 35, e030 (2018)

[RD4] Galaxy evolution studies with the SPace IR telescope for Cosmology and Astrophysics (SPICA): the power of IR spectroscopy Spinoglio et al. PASA, 34, e057 (2017)

[RD5] SPICA and the chemical evolution of galaxies: the rise of metals and dust Fernández-Ontiveros et al. PASA, 34, e053 (2017)

[RD6] Feedback and feeding in the context of galaxy evolution with SPICA: direct characterisation of molecular outflows and inflows Gonzalez-Alfonso et al. PASA, 34, e054 (2017)

[RD7] Tracing the evolution of dust obscured star-formation and accretion back to the reionisation epoch with SPICA Gruppioni et al. PASA, 34, e055 (2017)

[RD8] Unbiased large spectroscopic surveys of galaxies selected by SPICA using dust bands Kaneda et al. PASA, 34, e059 (2017)

[RD9] Probing the baryon cycle of galaxies with SPICA mid- and far-infrared observations van der Tak et al. PASA, 35, e002 (2018)

[RD10] Probing the high-redshift universe with SPICA: toward the epoch of reionization and beyond Egami et al. PASA, 35, e048 (2018)

[RD11] Probing the cold magnetized Universe with SPICA/POL André et al., PASA 36, e029 (2019)

[RD12] Mid-IR cosmological spectrophotometric surveys from space: Measuring AGN and star formation at the Cosmic Noon with a SPICA-like mission Spinoglio et al. PASA (2021) in press

[RD13] The formation of planetary systems with SPICA Kamp et al. submitted to PASA

[RD14] SPICA Science Requirements Document, SPICA-EST-SCI-RS-001, v1.2-final, 15/01/2021

[RD15] Justification for the SPICA Science Requirements Document SPICA SST, SPICA-EST-SCI-RS-002, 15/01/2021

[RD16] SPICA Mission Requirements Document (MRD), ESA-SPICA-EST-SYS-RS-001, Issue 1.4

[RD17] SPICA Science Operations Assumptions Document (SOAD), SPICA-ESAC-SOC-AD-00, Issue 0.13

[RD18] SPICA Mission Operations Assumptions Document (MOAD), SPICA-ESOC-MIS-AD-001, Issue 1.0

[RD19] SPICA Joint Study Management Plan (JSMP), SPICA-EST-MAN-PL-001, Issue 1.0

[RD20] Goran L. Pilbratt, " Herschel mission: status and observing opportunities", Proceedings Volume 5487, Optical, Infrared, and Millimeter Space Telescopes; (2004) https://doi.org/10.1117/12.562382

[RD21] Fischer, J., Klaassen, T., Hovenier, N., Jakrob, G., Poglitsch, A., Sternberg, O., "Cryogenic far-infrared laser absorptivity measurements of the Herschel Space Observatory telescope mirror coatings", APPLIED OPTICS, Vol. 43(19), (2004).

[RD22] Sakon, I., Kaneda, H., Oyabu, S., Ishihara, D., Wada, T., Fujishiro, N., and SMI consortium, "Sensitivity Estimates for the SPICA Mid-Infrared Instrument (SMI)", Proc. SPIE 9904, Space Telescopes and Instrumentation 2016: Optical, Infrared, and Millimeter Wave, 99043V; (29 July 2016); doi: 10.1117/12.2232402.

[RD23] SPICA Experiment Interface Document Part A (EID-A), ESA-SPI-EST-PL-IF-001, Issue 1.2

[RD24] SPICA 2013 View Factors Introduction, SPICA-EST-SIA-HO-001

[RD25] SPICA 2013 View Factors impact on SAFARI, ESA-SPI-SRON-SIA-HO-001

9 LIST OF ACRONYMS

Acronym	Definition
AD	Applicable Document
AI	Action Item
AIV	Assembly, Integration and Verification
AIT	Assembly, Integration and Testing
AOCS	Attitude, Orbit and Control Subsystem
CaC	Cost at Completion
CAD	Computer Aided Design
CATIA	Computer Aided Three-dimensional Interactive Application
CDF	Concurrent Design Facility
CFI	Customer Furnished Items
CReMA	Consolidated Report on Mission Analysis
CV	Cosmic Vision
DOORS	Dynamic Object-Oriented Requirements System
ECSS	European Cooperation for Space Standardisations
EFM	ESTRACK Facilities Manual
EID	Experiment Interface Document
ESA	European Space Agency
ESAC	European Space Astronomy Center
ESARAD	ESATAN Radiative module
ESATAN	ESA Thermal Analysis Modelling
ESOC	European Space Operations Centre
ESTEC	European Space Technology Center
ESTRACK	ESA Tracking Stations
FDIR	Fault Detection, Isolation and Recovery
FEM	Finite Element Model
FGS	Fine Guidance Sensor
FP	Final Presentation
GMM	Geometrical Mathematical Model
GSP	General Study Programme
ICD	Interface Control Document
ICC	Instrument Control Centre
IR	Intermediate Review
ISO	International Organization for Standardization
ITA	Infrared Telescope Assembly
ITT	Invitation To Tender
KO	Kick-Off
LLI	Long Lead Items
LV	Launch Vehicle

MAG	Mission Analysis Guidelines
MAR	Mission Adoption Review
MCR	Mission Consolidation Review
MIRD	Mission Implementation Requirement Document
MOC	Mission Operations Centre
MRD	Mission Requirements Document
MSR	Mission Selection Review
NA	Not Applicable
NASTRAN	NASA Structure Analysis
OIRD	Operation Interface Requirement Document
PA	Product Assurance
PM	Progress Meeting
PDD	Payload Definition Document
PSF	Point Spread Function
PV	Performance Verification
QA	Quality Assurance
RD	Reference Document
RID	Review Item Discrepancy
RFI	Request For Information
RMP	Reference Mission Programme
SC	Spacecraft
SEL2	Sun-Earth Lagrange Second Point
SIA	Science Instrument Assembly
SOC	Science Operations Centre
SRD	Systems Requirements Document
SMM	Structural Mathematical Model
SPICA	Space Infrared Telescope for Cosmology and Astrophysics
SSAC	Space Science Advisory Committee
SST	Science Study Team
SVM	Service Module
SW	Software
TBC	To Be Confirmed
TBD	To be Determined
TDA	Technology Development Activity
TMM	Thermal Mathematical Model
TRL	Technology Reference Level
TT&C	Telemetry, Tracking and Command
UM	User Manual
WFE	Wave Front Error